POLSKA AKADEMIA NAUK
KOMITET FIZYKI

# ACTA PHYSICA POLONICA

KWARTALNIK

Vol. XII — Fasc. 3—4

WARSZAWA 1953

*Volumen XII (1953) — Fasciculus 3—4*



## *Содержание*

# AN INTEGRATING APPARATUS FOR THE SCHRÖDINGER EQUATION

By K. Antonowicz

Physics Department, Nicholas Copernicus University, Toruń

*(received January 1, 1953)*

An integrating apparatus for the Schrödinger equation has been constructed based on an analogy between the equation of motion of a magnetic needle and the one-dimensional Schrödinger equation. The apparatus was checked with a harmonic oscillator as example. Eigenfunctions were obtained and by comparison with those given by theory were shown to be in agreement within an error of 1 per cent only.

At one of the first Conferences of Polish Physicists after World War II, a construction scheme of an integrating instrument for Schrödinger's equation based on the aforementioned analogy was discussed by Professor A. Jabłoński. The idea of the apparatus is, in short, as follows: the motion of a magnetic needle in a homogeneous field of varying intensity $H$ is described by the equation

$$B\frac{d^2\alpha}{dt^2} + mH\sin\alpha = 0, \tag{1}$$

where $B$ is the moment of inertia of the needle and $m$ its magnetic moment. For small angles $\alpha$, (1) takes the form

$$B\frac{d^2\alpha}{dt^2} + mH\alpha = 0, \tag{2}$$

similar to that of Schrödinger's equation. To make this point clearer, we put

$$H = H_0 - H(t), \tag{3}$$

$H_0$ being a constant, and inserting (3) into (2), we get

$$\frac{d^2\alpha}{dt^2} + \frac{m}{B}[H_0 - H(t)]\,\alpha = 0. \tag{4}$$

Equation (4) has the form of the one-dimensional, time-independent Schrödinger equation:

$$\frac{d^2\psi}{dx^2} + \frac{2\mu}{\hbar}[E - U(x)]\,\psi = 0. \tag{5}$$

The corresponding quantities in Eqs. (4) and (5) are

$$\alpha \sim \psi,$$

$$t \sim x, \qquad H_0 \sim E,$$
$$m/B \sim 2\mu/\hbar^2, \qquad H(t) \sim U(x)$$

Thus the problem consists in constructing an apparatus in which a magnetic needle executes small oscillations in a homogeneous magnetic field with given time-dependence, the damping of the oscillatory motion of the needle being so small that it may be altogether neglected; the variation of the magnetic field with time has to be the same as that of $U(x)$ with $x$ in the wave-mechanical problem in question.

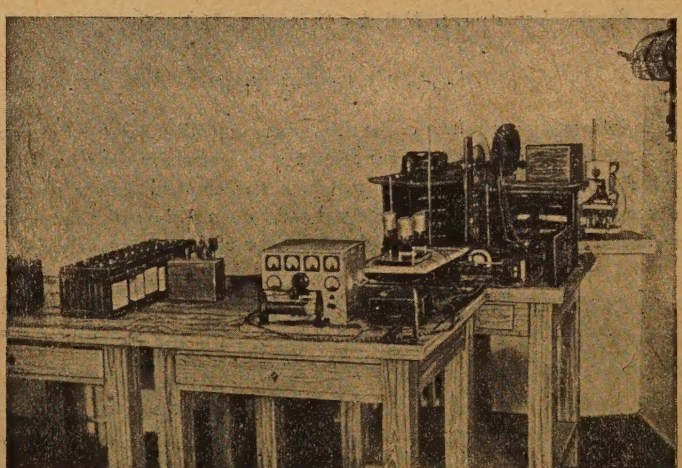

Fig. 1. General View of the Apparatus

In order to solve a problem by means of our apparatus it is necessary to pick out from among all the possible $\alpha(t)$ the ones satisfying the same conditions as those satisfied by the function $\psi$. These conditions are fulfilled only for certain values of $H_0$, which represent thus the eigenvalues of our problem. In many problems $\psi(x)$ must become zero at infinity, which would correspond in our apparatus to $\alpha(t)$ disappearing for $t = \pm\infty$. This condition cannot, of course, be strictly realized, it suffices, however, in practice when $\alpha(t)$ disappears for sufficiently great values of $t$.

In our apparatus (block-diagram Fig. 2) the magnetic needle $A$ is suspended on a cocon thread, its moment of inertia being increased by the addition of a lead disc. A small mirror is rigidly fastened to the needle. The displacement of the needle is recorded on photographic paper placed on a drum $T$ in a camera similar in construction to that of the Moll microphotometer. The rigidity of the cocon thread and the weight of the moving part have been so chosen as to make the whole system as insensitive to external shocks as possible. The constant and the varying magnetic fields are produced by two coils of the Helmholtz type which produce a homogeneous magnetic field over a considerable space. The light beam reflected from a mirror rigidly fastened to the needle

falls on the photographic paper on the drum which rotates at constant speed. As a source of light ($B$) a linear filament of an incandescent lamp is used. The system of lenses $O$ and the cylindrical lens $C$ are so chosen as to have the motion of the light spot observable on the slit of the drum chamber, and at the same time have it focussed on the photographic paper. The drum is driven by the motor $M$ fed by a separate battery of accumulators to ensure constant speed of revo-

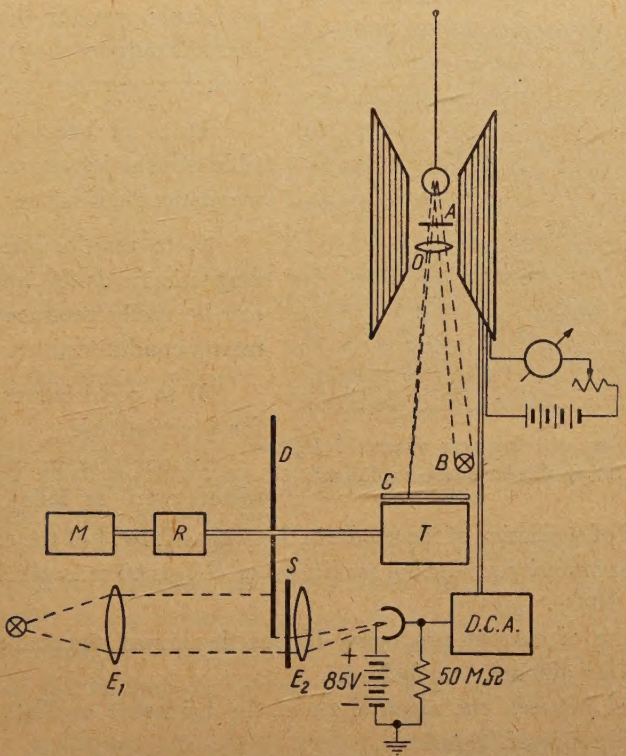


Fig. 2. Bloc diagram of the apparatus. $A$–magnetic needle, $O$–system of lenses, $C$–cylindrycal lens, $B$–linear light source, $M$–motor, $R$–worm gear reduction box, $D$–disc, $S$–slit, $E$–lenses, $T$–drum, $DCA$ — D.C. Amplifier

lution. The motor speed is reduced by a worm gear box $R$. On the drum axis, in the front of the slit $S$, a rotating disc is placed by which the slit $S$ is partially or completely screened. The disc edge is cut in such a way that the length of the unscreened portion of the slit is at every instant proportional to the ordinate of the potential curve of the problem considered. The point light source placed in the focus of the lens $E$ provides a parallel light beam falling on the slit. The light which passes through the slit $S$ is focussed again on the photocell by a lens $E_2$. The photocurrent is amplified by a D. C. amplifier which supplies current to one of the windings of the coil. This current produces the magnetic field $H(t)$. The second winding of the coil is fed by a D.C. current and produces the magnetic field $H_0$. The fields $H_0$ and $H(t)$ have opposite directions. The coil axis is parallel to the mag-

netic field of the earth. The coils and a fixed holder of the cocon thread are placed on an appropriate stage with a micrometric screw by means of which the coils can be rotated with respect to the magnetic field of the earth and the point of suspension of the cocon thread adjusted so as to have the needle set parallel to that field.

In principle, the parameters of the equation of motion of the needle, i.e. the moment of inertia, the magnetic moment, and the motor speed, may be chosen arbitrarily, yet for the apparatus to serve its purpose they must be chosen in such a way as:

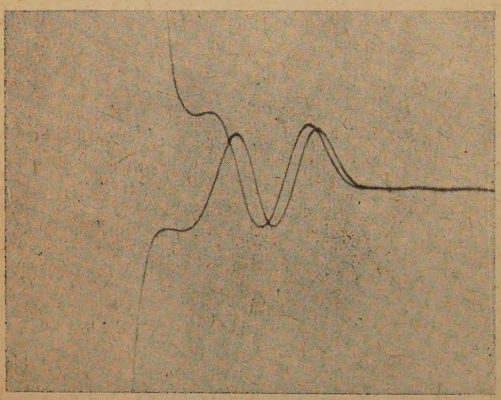

Fig. 3. Two curves $\alpha(t)$ for near values of $H_0$ which do not satisfy the boundary conditions

1) to ensure the smallest possible sensitivity to mechanical and magnetic disturbances,

2) to require intensities of the magnetic fields $H_0$ and $H(t)$ which can be easily produced under laboratory conditions,

3) to yield curves good enough for practical use.

In our measurements the parameters were as follows:

1) Period of oscillation of the needle in the magnetic field of the earth $\sim 30$ sec.

2) Current intensity producing maximum of $H(t)$ is 60 mA, which corresponds to $H(t)_{max} = 10$ Oe.

3) Intensity of current producing $H_0$ for the lowest eigenvalue of the harmonic oscillator = 80 mA (see below).

4) Interval between the eigenvalues of the harmonic oscillator corresponds to current difference of 20 mA.

5) Time of one revolution of the drum 3 minutes.

The problem of the harmonic oscillator has been chosen as an example to test the apparatus.

The eigenfunctions and eigenvalues may be easily found by the following procedure: the needle having been brought to rest, we wait till the slit begins to become unscreened by the revolving disc, then the field $H(t)$ is switched on; $H(t)$ has now a great value, and $H_0 - H(t)$ has the opposite direction to that of the magnetic moment of the needle. The equilibrium of the needle becomes unstable and the needle begins to move. The number of zeros of the curve is the quantum number to which the eigenvalue $H_0$ corresponds. Fig. 3 shows two curves, neither of which representing an eigenfunction, the eigenvalue of the function with two nodes lying beyond doubt somewhere between the two values of $H_0$ corresponding to these curves.

The amplitudes of the curves depend on the moment in which the $H(t)$ field is switched on. This moment is experimentally chosen so as to obtain curves

with amplitudes fitted to the size of the drum. An accurate control check of the amplitudes cannot be achieved, hence only unnormalized eigenfunctions have been obtained. The eigenfunction to be found may be better and better approximated by varying successively $H_0$.

Fig. 4 shows the eigenfunction for the lowest eigenvalue of the harmonic oscillator. The boundary conditions are now satisfied. The curve flies off to infinity on the left hand side because the needle after having been stopped is again in an unstable equilibrium. Although after tracing the whole curve the further behaviour of the needle is of no interest to us, yet it may be profitable to switch off the power supply to the coil after the needle has come to rest; then, according to the adjustment of the eigenvalue, we get a sine curve of smaller or greater amplitude. Fig. 5 is an exam le of such a curve. For determining the eigenvalues the apparatus is very sensitive, because even slight deviations from the true eigenvalue give sine curves of considerable amplitudes after switching off the field. The eigenfunctions for the three lowest eigenvalues of the harmonic oscillator are shown in Fig. 6.

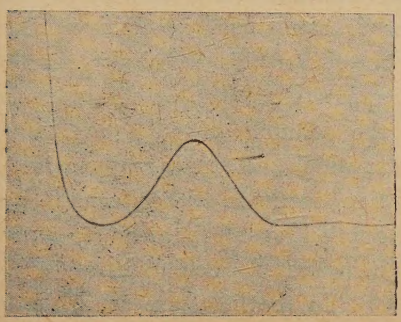

Fig. 4. Eigenfunction for the lowest eigenvalue of the harmonic oscillator

From these curves it may be seen that the needle still swings more or less appreciably after switching off the external field. This fact may account for some deviation of the values of $H$ from the actual eigenvalues. Nevertheless the theoretically computed points (indicated by crosses) are in good agreement with the obtained curves over their whole length with the exception of one extremity.

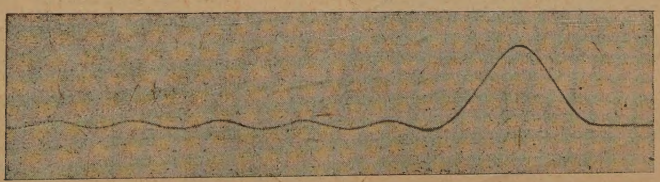

Fig. 5. A curve obtained under the same conditions as in Fig. 4

The errors of the curves do not exceed 1 per cent. A more accurate evaluation of the errors has not been tried as it turned out that the factor chiefly responsible for the errors lies in the inaccurate construction of the potential curves. The error caused by damping of the motion of the needle is negligible, consecutive amplitudes differing by less than 0,1 per cent. The needle once set in motion and left to itself in the magnetic field of the earth still oscillates appreciably after a lapse of three hours. Thus a special method of stopping it had to be invented. It has been found that damping by induced currents is quite inefficient. On the other hand, the needle must be stopped quickly

to make quick succesive trials possible. It appeared that this may be done without difficulty by switching the constant magnetic field $H_0$ on and off at suitably chosen instants: when the needle passes the equillibrium position the magnetic field $H_0$ is switched on, and when it reaches its maximum deviation the field is switched off; by repeating this procedure several times the needle can be stopped dead.

These preliminary results lead us to the conviction that great accuracy in solving the Schrödinger equation for particular problems can be achieved by means of this relatively simple apparatus. What we aimed at is the solution of such problems to which the existing approximation methods either cannot be applied at all or lead to very complicated calculations.

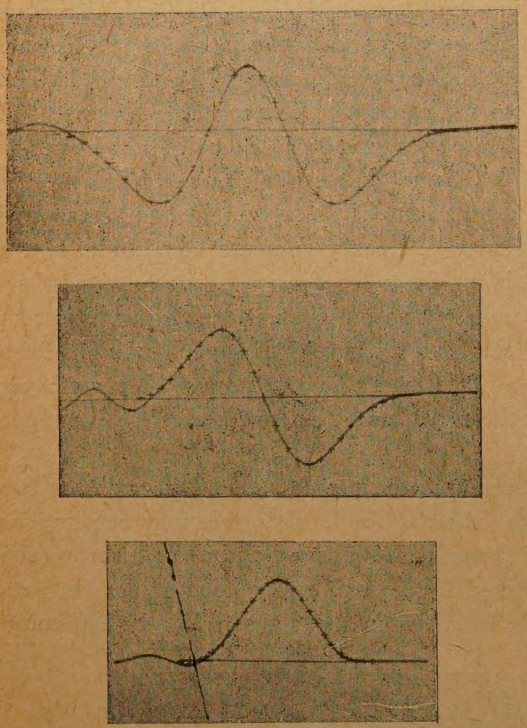

Fig. 6. Continuous curves obtained by means of the apparatus. Theoretically computed points are marked with crosses

In the literature available to him, the author has found no report on the construction of an integrating apparatus for Schrödinger's equation based on a similar idea, except a short remark in Kamke's well-known textbook (1943, p. 181) that Bullard and Moon (1931) had put forward an idea of a magnetic device for the solutions of the equation $y'' = f(x)y$. Garwin (1950) maintains that an apparatus exploiting the motion of a magnetic needle in a magnetic field may be constructed, but thinks it to give only very inaccurate results; thus he has constructed an instrument on different principles. Coolidge, James et al. of the Massachusetts Institute of Technology (1938, 1939) have constructed an apparatus called "Differential Analyzer". A number of problems has been solved by means of this instrument which is much more expensive than the one described here. Therefore, the construction of a cheaper instrument seemed worth while.

The author wishes to express his deepest gratitude to Professor A. Jabłoński for his kind encouragement and constant guidance throughout the work, to his co-worker M. Rytel for assistance in this work and to the mechanician of the Department Mr B. Markowski for the execution of the mechanical parts. of the apparatus.

## КРАТКОЕ СОДЕРЖАНИЕ

К. Антонович, *Прибор для интегрирования уравнения Шредингера.*

Был построен прибор для интегрирования уравнениа Шредингера, основанный на подобии этого уравнения с уравнением движения магнитной иглы в магнитном поле.

Магнитное поле создаётся двумя системами катушек (Гельмгольца), один из которых питается постоянным током, другой же током, сила которого меняется со временем таким же образом, как в пространстве изменяется потенциальная кривая рассматриваемой проблемы. Луч света отражённый от зеркала, прикреплённого к магнитной игле, падает на светочувствительную бумагу, намотанную на барабан вращающийся с постоянной скоростью, и рисует на нём кривую. Можно так подобрать силу постоянного тока чтобы эта кривая исполняла краевые условия, тогда сила постоянного тока пропорциональна собственному значению уравнения, кривая же представляет собственную функцию (ненормированную).

Действие аппарата было проверено на примере гармонического осциллатора. Были получены собственные функции, которые не отличаются от теоретически высчитанных более чем на 1%.


## REFERENCES


Coolidge A. S., Coolidge H.M., and Vernon E.L., *Phys. Rev.*, **54**, 726 (1938).
Coolidge A.S. and James H.M., *J. Chem. Phys.*, **6**, 730 (1938).
Garwin R.L., *Rev. Sci. Instrum.*, **21**, 411 (1950).
James H.M. and Coolidge A.S., *Phys. Rev.*, **55**, 184 (1939).
Kamke M., *Differentialgleichungen. Lösungsmethoden und Lösungen* (1943).
Kamke M., *Proc. Camb. Phil. Soc.*, **27**, 546 (1931).

# EFFECT OF ELECTRIC FIELD ON THE DIELECTRIC CONSTANT OF FERROELECTRIC TITANATES*

By A. Piekara and Z. Pajak

Physical Laboratory I, Institute of Technology, Gdańsk

*(received January 12, 1953)*

The dielectric constant of polycrystalline barium- and barium-strontium titanates was measured as a function of temperature, time, AC-measuring field, and DC- and AC. biasing fields. In particular the relation between the dielectric constant and the DC-biasing field was investigated. Curves of the dielectric constant as a function of the DC-biasing field for quasistatic states both below and above the Curie point were obtained. The effect of prepolarization of the sample on the measured time changes of the dielectric constant below the Curie point was observed. This "prepolarization-effect" manifested itself in different values of the dielectric constant corresponding to different directions of the applied fields.

I. Introduction. Titanates of alkali-earth metals below the Curie point show well-known ferroelectric properties. The exceptionally high dielectric constant of these compounds reveals a strong temperature dependence and rises to a maximum at the temperature of the Curie point. At this point spontaneous polarization, dielectric hysteresis, and the domain structure of crystals disappear. Accordingly, a polymorphic transition from a tetragonal to a cubic crystal structure takes place. Some anomalies in the behaviour of the dielectric constant *vs* temperature were described in our previous paper (1952). In the present work the effect of an electric field on the dielectric constant of polycrystalline barium and barium-strontium titanates was investigated.

II. Method of measurements. The bridge method was used for the dielectric constant determination. The scheme of the circuit arrangement is shown in Fig. 1. The Sullivan bridge was supplied by an acoustic frequency oscillator *AFO*, the frequency being from 0 to 20 kc/s and the measuring field from 0 to 28 V/cm. The voltage drop on the resistor $R = 3\text{k}\Omega$ was amplified with the amplifiers $A1$ and $A2$ and applied to the loud-speaker *LS*. In the cases when an AC-biasing field was applied (the frequency being 50 c/s) the low-frequency filter $F$ was included between the amplifiers. The condenser $C_x$ (with the sample) was connected in series with a blocking condenser, the capacity $C$ being 0,25 $\mu$F resp. 0,05 $\mu$F. Owing to $C \gg C_x$ the measured capacity $C_m = CC_x/(C + C_x) \approx C_x$. The external field

* Results presented at a scientific session of Institute of Technology, Gdańsk, June 1951 and at a meeting of the 14-th Conference of Polish Physicists, Poznań, December 7—10, 1952.

was applied to the condenser $C$ through the resistor $R_1 = 6\text{k}\Omega$ in the case of an AC-bias and through the resistors $R_1$ and $R_2 = 30\,\text{k}\Omega$ when a DC-bias was applied. After exposure to the field, the condenser $C$ was discharged through the resistor $R_1$. The

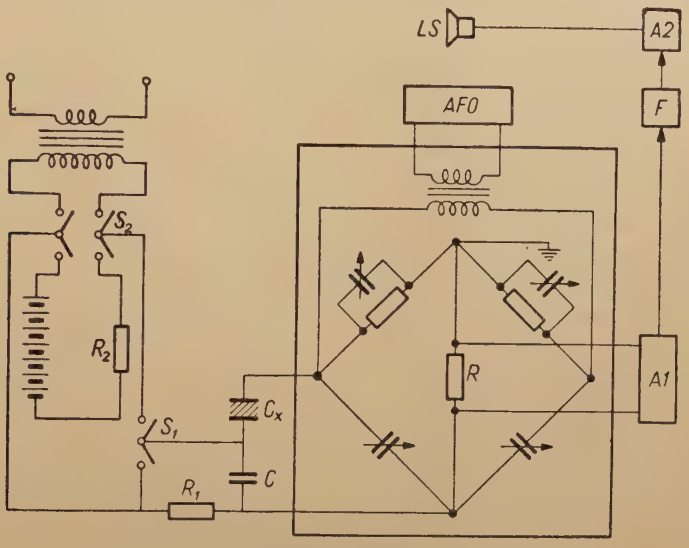


Fig. 1. Diagram of the circuit arrangement

high tension producing the biasing field was measured with an electrostatic voltmeter and the low measuring AC-tension with a valve voltmeter. The sample was placed in a small vessel which is shown in Fig. 2. The copper wires $A$, $B$ were soldered to silver electrodes made by a thermogenic method (Partington *et al.* 1949). The measuring vessel was provided with an accurate thermometer $T$ and three thermocouples 1, 2, 3. It was heated in a Hoeppler ultrathermostat or in a special electric furnace. The temperature was maintained to an accuracy of 0,1° C and measured by the thermocouples to an accuracy of 0,05°C.

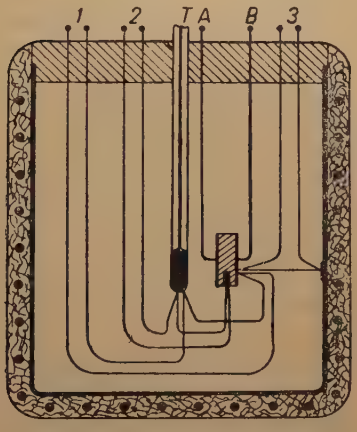


Fig. 2. The measuring vessel

$BaTiO_3$ ceramics and compositions of 78,6% $BaTiO_3$ + 21,4% $SrTiO_3$ (by weight) were prepared by the Inorganic Chemistry Institute of the University, Wrocław.[1]

III. Results of measurements. The AC-measuring field of frequency 1, 2, resp. 5 kc/sec was used for the dielectric constant measurements. The Curie point of barium titanate lies at *c.* 127°C and of barium-strontium titanate at *c.*

[1] The authors are greatly indebted for the supply of these specimens to Professor W. Trzebiatowski and Dr J. Wojciechowska.

56°C. The measurements were performed between 20°C and 150°C for barium titanate and between 20°C and 75°C for barium-strontium titanate. The time changes of the dielectric constant were observed as quickly as possible after having applied or removed the biasing field, *i.e.* in some seconds, and were carefully measured during several hours without changing the measuring conditions (temperature, field, etc.). Fields up to 7 kV/cm for the DC-bias and up to 6 kV/cm for the AC-bias were used.

1. Temperature dependence of the dielectric constant. The dielectric constant *vs* temperature was measured, and known curves were obtained. Nevertheless, in the vicinity of the Curie temperature, an anomaly known as the thermal pseudohysteresis of the dielectric constant was observed. This latter was described in our previous paper, and was also observed by Roj (1951).

2. Time dependence of the dielectric constant. The dielectric constant of the barium titanate varies in general with time. The sample maintained at constant temperature during several days shows the dielectric constant to be almost independent of time. Thus it may be said that the sample is thermally balanced. The establishment of *thermal equilibrium* requires a longer time period when cooling than when heating. In the latter case the time period is rather short and equilibrium is reached very rapidly. The dielectric constant in its unbalanced state has different values at the temperature in question depending on the thermal history of the sample. The value measured at a definite temperature is higher when this temperature is established by cooling than by heating. In the first case it decreases with time to the value of the equilibrium state, which is almost equal to that of the dielectric constant measured when heating. The influence of the thermal history on the dielectric constant of the sample is noticeable after a lapse of many haurs. It may be said that the sample has a *thermal memory*, which is, however, a memory of higher temperatures only.

The value of the dielectric constant of the sample of barium titanate in thermal equilibrium depends also on the external field and changes, *e.g.*, after the application or removal of the biasing field. The thermally balanced sample maintained at a constant external field for a longer period of time shows again the dielectric constant to be almost independent of time and it may be said in analogy to thermal equilibrium that the sample is now in *electrical equilibrium.* There is also a remarkable influence of the electric history on the dielectric constant of barium titanate and similarly it may be said that the sample has an *electric memory* (see § III.4 below).

3. Dependence of the dielectric constant on the measuring field. Measurement of the dielectric constant as a function of the measuring AC-field, the frequency being 5 kc/s at temperatures below and above the Curie point, were carried out. Fig. 3 shows two curves obtained for barium-strontium titanate at temperatures below (curve I) and above (curve II) the Curie point. The succession of the measured points is shown in the figure. It may be seen that the first and the last measurement although taken at different times are in good agreement with as good an accuracy as the measuring method allows, showing that

the sample was thermally balanced during the measurements. The experiments show an increase of the dielectric constant with the AC-measuring field both above and below the Curie point. This increase is much greater below the Curie point

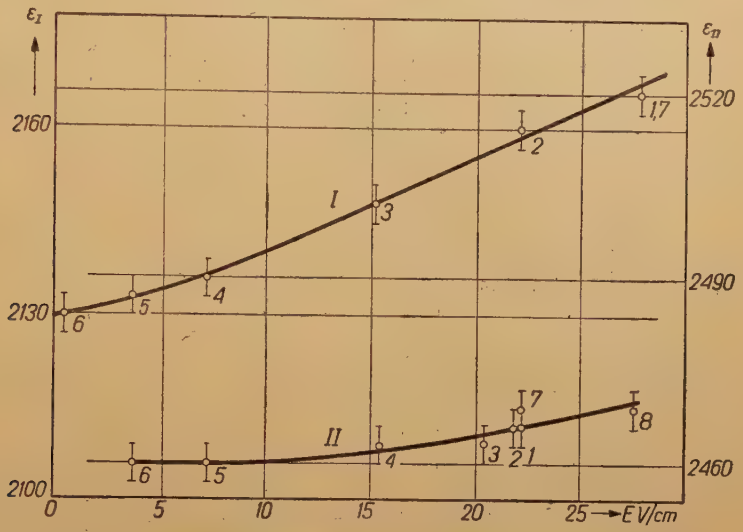


Fig. 3. Dielectric constant as a function of the measuring AC-field below (curve I at 45° C) and above (curve II at 66° C) the Curie point

and amounts to 2 per cent when the AC-field is risen from 0 to 28 V/cm. On the other hand it amounts only to 0,4 per cent above the Curie point for the same change of the field.

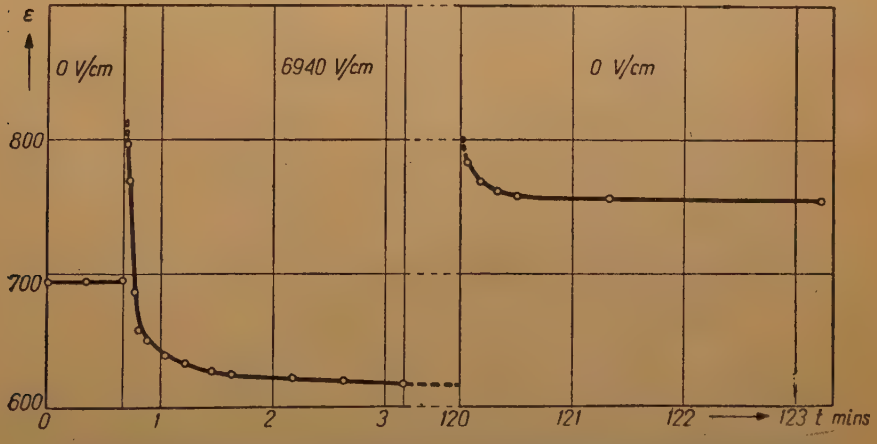


Fig. 4. Time dependence of the dielectric constant below the Curie point at 20°C

4. Dependence of the dielectric constant on the DC-biasing field. After having applied or removed the biasing field the dielectric constant of ferroelectric titanates, atlhough thermally balanced becomes now electrically

unbalanced and changes its value with time. These time changes were first investigated by Partington *et al.* (1949). Our measurements are in good agreement

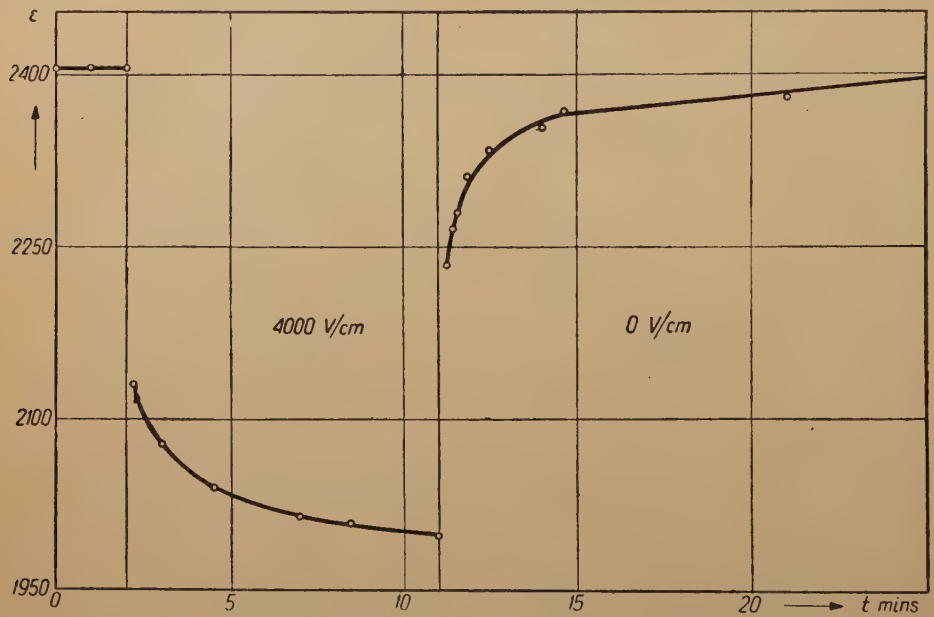


Fig. 5. Time dependence of the dielectric constant above the Curie point, at 66°C

with Partington's results. Fig. 4 shows the time changes observed for barium titanate both after the application and removal of a 6940 V/cm DC-bias, below the

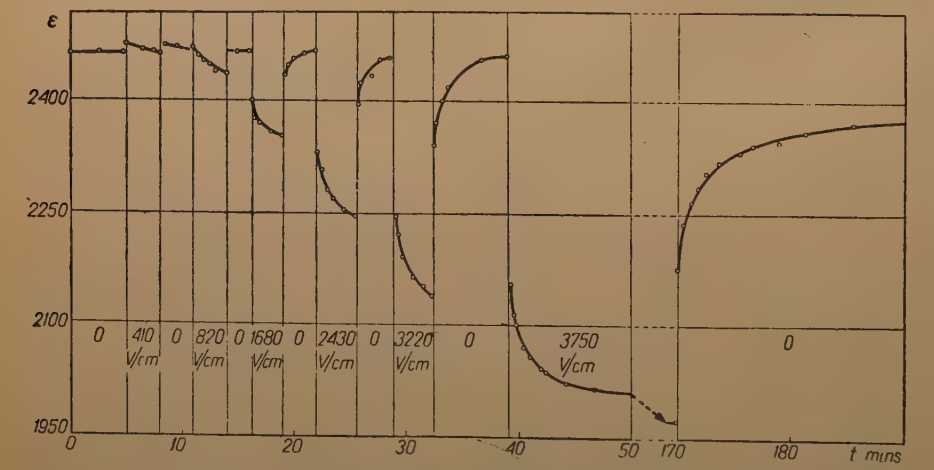


Fig. 6. Time dependence of the dielectric constant after the application and removal of various DC-bias, above the Curie point at 66°C

Curie point. Fig. 5 shows the time changes of the dielectric constant observed for barium-strontium titanate both after the application and removal of a 4000 V/cm DC-bias, above the Curie point. A temporary increase of the dielectric constant

below the Curie point is caused by applying the DC-bias to the sample. In turn a slow decrease of the dielectric constant takes place. In the course of many hours

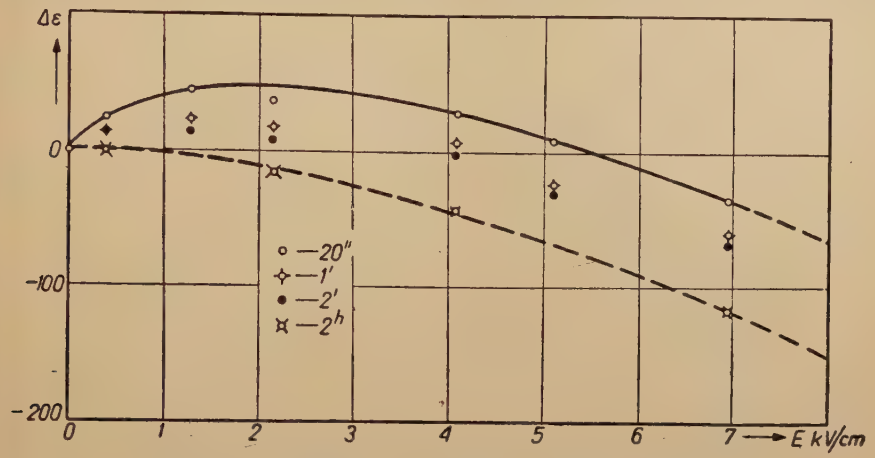


Fig. 7. The change of the dielectric constant as a function of the DC-field below the Curie point at 20°C

the dielectric constant falls to a value lower than the initial one. After the removal of the field similar changes of the dielectric constant may be observed, thereby causing the dielectric constant to fall slowly to the initial value.

After the application of the external field above the Curie point only a decrease of the dielectric constant can be observed. After the removal of the field the dielectric constant shows a slow increase to its initial value.

In order to obtain a relation between the dielectric constant and the DC-bias, a series of time measurements of the dielectric constant was made using various tensions below and above the Curie point. Fig. 6 shows the results obtained for barium-strontium titanate above the Curie point. It may be seen that the effect under observation increases with the external field. Figs. 7 and 8 show the increase $\Delta\varepsilon$ of the dielectric constant as a function of the DC-field. Fig. 7 refers to the sample of barium titanate below the Curie point and Fig. 8 to the barium-strontium titanate above the Curie point. Measurements carried out after the same time

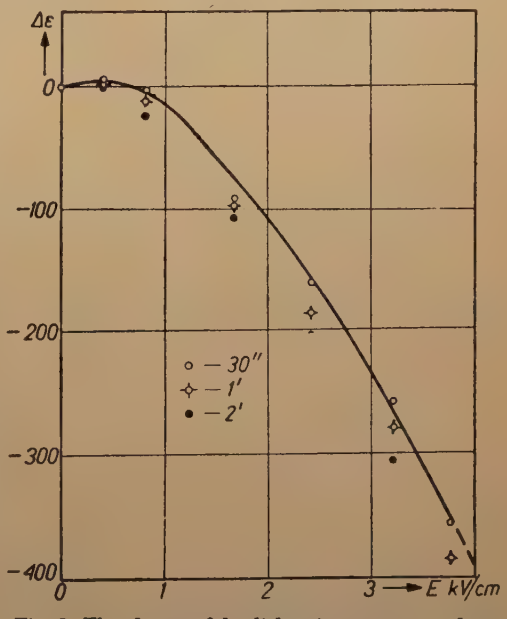


Fig. 8. The change of the dielectric constant as a function of the DC-field above the Curie point at 66C°

of application of the biasing field are denoted in the diagrams in the same manner. The dotted curve in Fig. 7 shows the increase of the dielectric constant measured about 2 hours after the application of the field, *i. e.* in an electrically partially balanced (quasistatic) state. The increase $\Delta\varepsilon$ of the dielectric constant changes its positive sign to a negative one at a certain value of the DC-bias, when the measurements were made shortly after the application of the field. Thus the sample was electrically unbalanced.

The increase $\Delta\varepsilon$ of the dielectric constant changes its sign at a field strength depending on the time period after which the measurements were made. This change of sign takes place, *e.g.*, for barium titanate below the Curie point at about 5,5 kV/cm, when measuring the increase of the dielectric constant 20 seconds after the application of the external field (Fig. 7). The increase measured about 2 hours after the bias application is, however, only negative and its value rises with the DC-bias field both below and above the Curie point. For barium-strontium titanate above the Curie point the corresponding value of the biasing field which causes the change of sign of $\Delta\varepsilon$ amounts to *c.* 750 V/cm when measuring the increase 30 seconds after the application of the field. The increase $\Delta\varepsilon$ is negative only when the change is measured 2 minutes after the application of the DC-bias.

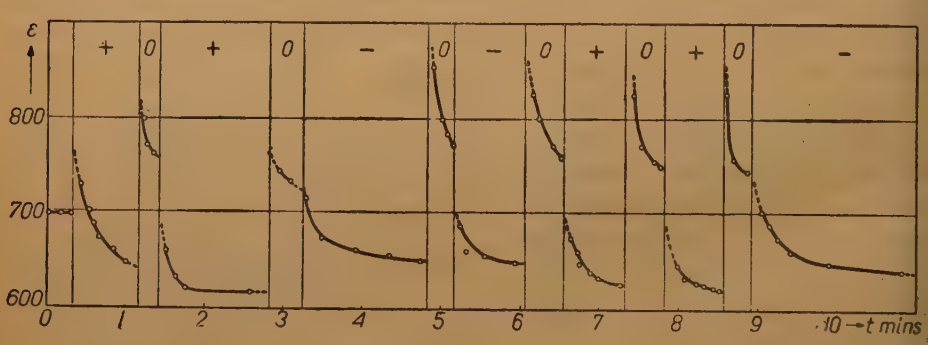


**Fig. 9. Time dependence of the dielectric constant of prepolarized barium titanate after application or removal of the bias (6940 V/cm) at 21°C**

The influence of the prepolarization of the sample on the measured time changes of the dielectric constant below the Curie point was next observed. The measurements were carried out in isothermic conditions. A DC-biasing field was repeatedly applied to and removed from the sample for a number of days, the direction of the field being always the same (plus). The time changes of the dielectric constant observed after the application of a reverse field (minus direction) appear somewhat different from the case of the plus direction. The curves in Fig. 9 show greater values of the dielectric constant after the application of the reverse field (minus) than after the application of the field agreeing with the initial prepolarizing bias (plus). In Fig. 10 are shown the results of measurements carried out immediately after those of Fig. 9. In this case the dielectric constant of the sample was measured using successively both directions of the biasing field. Here,

as in Fig. 9, it may be observed that the values of the dielectric constant are lower after the application of the bias with the direction of the prepolarizing field (plus) than with the reverse direction. It may be said that the sample "becomes accustomed" to the plus-direction of the prepolarizing field. This "prepolarization-

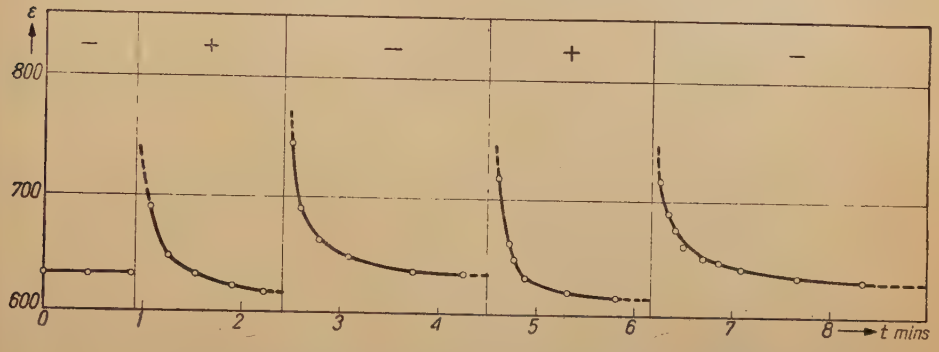


Fig. 10. Time dependence of the dielectric constant of prepolarized barium titanate after alternate application of the DC-bias in both directions at 20°C

effect" can be obtained through long hours of prepolarization. It manifests itself in the tending of the dielectric constant in the course of time to a lower value in the case of a field in the direction of prepolarization than in the case of the same field

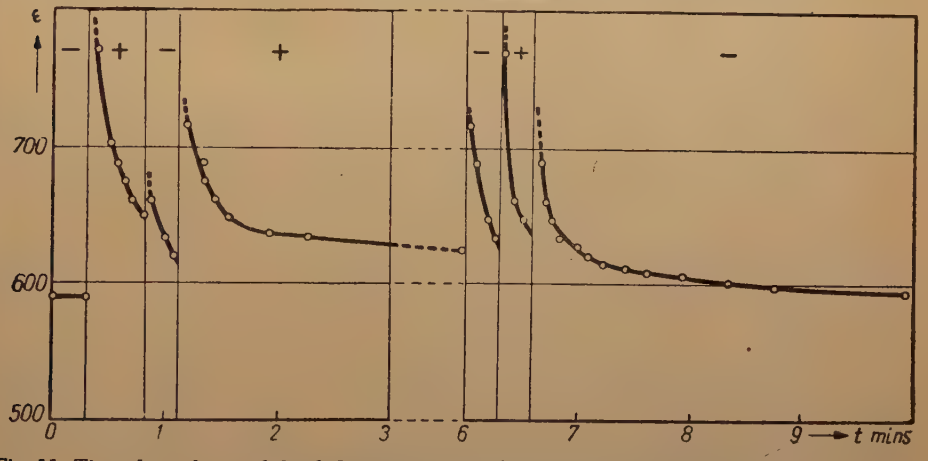


Fig. 11. Time dependence of the dielectric constant of prepolarized barium titanate after application of differently directed fields of equal strength at 20°C

in the reverse direction. Fig. 11 shows curves for the same sample, prepolarized by an 18 hour application of the „minus-field", the biasing voltage being $E = 6940$ V/cm. A "plus-field" and a "minus-field" were alternately applied; one can see the expected differences in the time changes of the dielectric constant, which tends now to lower values after application of the "minus-field". The differences between the values of the dielectric constants of this sample in the unprepolarized and prepolarized states are clearly visible in Fig. 12 and amount to *c.* 14 per cent

when measured 2 minutes after the application of the field. The application for some minutes of a strong AC-field to the prepolarized sample has no influence on the prepolarization-effect and is of no consequence for the time changes of the

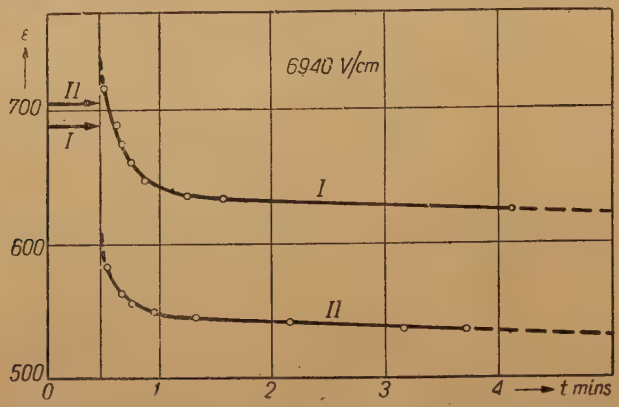


Fig. 12. Time dependence of the dielectric constant of the unprepolarized (curve I) and prepolarized (curve II) barium titanate after application of the field at 20°C

dielectric constant. The prepolarization-effect can be wiped out by a longer application of a strong DC-field with the reverse direction to that of prepolarization.

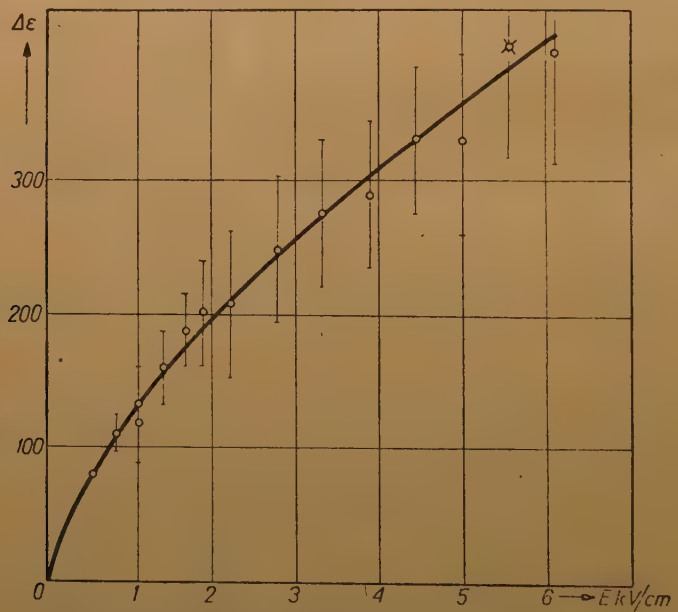


Fig. 13. The change of the dielectric constant after application of the AC-bias, below the Curie point at 20°C

5. Dependence of the dielectric constant on the AC-biasing field. The dielectric constant as a function of the applied AC-biasing field was next examined. The change $\Delta\varepsilon$ of the dielectric constant measured below the Curie

point when the AC-biasing field was applied is shown in Fig. 13. The frequency of the field was 50 c/s, the strength up to 6 kV/cm. Under these conditions a permanent increase of the dielectric constant was observed. The change of the dielectric constant measured above the Curie point is shown in Fig. 14. The frequency of the field was also 50 c/s, the strength used, up to 5 kV cm. In this case we can see the change reversing its sign from positive to negative at about 2 kV cm under the measuring conditions.

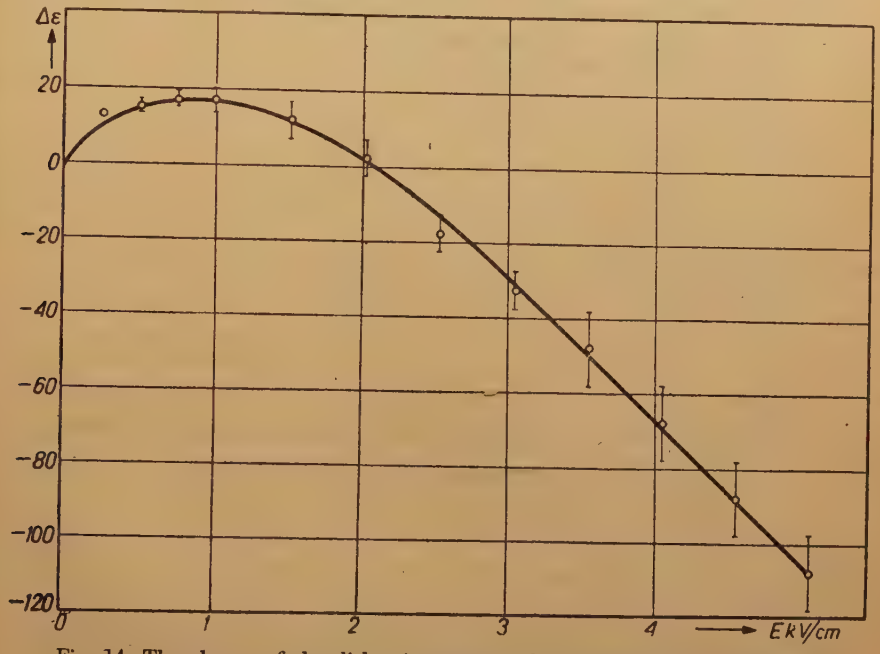


Fig. 14. The change of the dielectric constant after application of the AC-bias, above the Curie point at 66°C

More detailed studies of the influence of the DC- and AC-biasing fields on the dielectric constant of the ferroelectric titanates are being carried out.

The authors wish to express their gratitude to the Committee for Advancing Scientific and Artistic Activities Attached to the Council of Ministers for the award of a research grant that has enabled them to carry out this investigation.

## КРАТКОЕ СОДЕРЖАНИЕ

А. Пекара и З. Пайонк, *Зависимость диэлектрической проницаемости сегнетоэлектрических титанатов от напряженности электрического поля.*

Измерялась диэлектрическая проницаемость поликристаллических титанатов бария и бария-стронтия в зависимости от температуры, времени, напряженности переменного измеряющего и приложенного электрического поля. В особенности была исследована зависимость между диэлектрической проницаемостю и постоянным приложенным полем. Получено кривые зависимости диэлектрической проницаемости от постоянного поля для квазистатических состояний ниже и выше точки Кюри. Замечено влияние предва-

рительной поляризации образца на временной ход диэлектрической проницаемости ниже точки Кюри. Это явление проявилось в разных величинах диэлектрической проницаемости, соответствующих разным направлениям приложенного электрического поля.

## REFERENCES

Partington J. R., Planer G. V. and Boswell I. I., *Phil. Mag.*, **40**, 157 (1949).
Piekara A. and Pająk Z., *Acta Phys. Pol.*, **11**, 256 (1952).
Roy N., *Dokl. Akad. Nauk SSSR*, **81**, 545 (1951).

# VACUUM POLARIZATION IN A NON-LOCAL ELECTRODYNAMICS

By W. HANUS and J. RAYSKI

Department of Physics, Nicholas Copernicus University, Toruń

*(received January 17, 1953)*

The vacuum polarization current produced by an external electromagnetic field is computed in the framework of a non-local electrodynamics formulated by one of the authors. The vacuum polarization current is free of the usual divergencies, but does not agree with experiment owing to a pole in the power series expansion in momentum space. This pole may be removed and the agreement with experiment reestablished by means of a realistic compensation (simultaneous coupling of the electromagnetic field with charged fermions and bosons).

It is well known that the problem of the vacuum polarization current produced by a given external electromagnetic field $A_\mu$ leads to serious difficulties within the local quantum electrodynamics. First of all, one encounters (already in the lowest order of approximation) ambiguous expressions of the type of an infinite photon self-mass, contradicting the gauge invariance of the formalism (see, e.g., Pauli and Villars 1949). Moreover, one finds a divergent term of a charge renormalization type (Schwinger 1949).

The first of these difficulties could be surmounted with the aid of a realistic compensation (Rayski 1948, Umezawa 1948, Jost and Rayski 1949, Källén 1949). It has been shown that by taking a suitable mixture of charged fermions and bosons, the non-gauge invariant terms may be compensated. On the other hand, no admixture of fields could compensate the divergent terms of the self-charge type.

It seems to be worth while to investigate the problem of the vacuum polarization within the framework of the non-local electrodynamics and to compare the results with those of the traditional electrodynamics.

The non-local quantum electrodynamics, formulated by one of us, (Rayski 1951, 1952) belongs to the class of the so called "form-factor theories". The form-factor appearing in this formalism is derived from the postulate of reciprocity (Born 1949, Yukawa 1950). Owing to this form-factor, the theory is free of the well-known divergencies inherent in local quantum electrodynamics. This new electrodynamics differs in several aspects from the traditional one, in particular, the gauge invariance is restricted to changes of potentials by constant values $A_\mu \to A_\mu + C_\mu$ only.

Let us consider a vacuum state of the quantized charged field (or several charged fields) whose charge and current density is $ej_\mu(x)$. The rule for constructing

the density $j_\mu(x)$ within the framework of the non-local theory has been given in the cited paper of one of us. Let us introduce also a given non-quantized charge and current distribution $eJ_\mu(x)$. This current produces an external electromagnetic field, which induces, at the same time, a vacuum polarization current $\langle ej_\mu(x)\rangle_0$. The connection between the two current densities and the electromagnetic field $A_\mu$ is

$$(\Box - \varkappa^2)A_\mu(x) = -e(J_\mu(x) + \langle j_\mu(x)\rangle_0), \tag{1}$$

where the "photon rest mass" $\varkappa$ has been introduced for the sake of a subsequent renormalization of the mass constant to the experimental value zero. In the momentum space the same equation reads

$$(k^2 + \varkappa^2)A_\mu(k) = e(J_\mu(k) + \langle j_\mu(k)\rangle_0). \tag{1'}$$

It will be shown in Appendix I that the vacuum polarization current induced by the field $A_\mu$ may be written in the well-known form

$$\langle j_\mu(x)\rangle_0 = -e\int dx' K_{\mu\nu}(x - x')A_\nu(x') \tag{2}$$

or, in momentum space,

$$\langle j_\mu(k)\rangle_0 = -eK_{\mu\nu}(k)A_\nu(k), \tag{2'}$$

where $K_{\mu\nu}(x)$ or $K_{\mu\nu}(k)$ are straightforward generalizations of the analogous well-known expressions of the local electrodynamics (see e.g. Jost and Rayski 1949). A general form of a tensor $K_{\mu\nu}(k)$ is

$$K_{\mu\nu}(k) = a(-k^2)k_\mu k_\nu + b(-k^2)\delta_{\mu\nu}. \tag{3}$$

Taking account of the supplementary Lorentz condition $k_\nu A_\nu(k) = 0$, valid also in the non-local electrodynamics in the lowest order of approximation, we may write simply

$$\langle j_\mu(k)\rangle_0 = -eb(-k^2)A_\mu(k), \tag{4}$$

whence (1') becomes

$$(k^2 + \varkappa^2)A_\mu(k) = e(J_\mu(k) - eb(-k^2)A_\mu(k)). \tag{5}$$

It is interesting to notice that the vacuum polarization current satisfies the continuity equation (at least in the lowest order of approximation) although the non-local formalism does not guarantee the existence of the continuity equation. Indeed we have from (4)

$$k_\mu\langle j_\mu(k)\rangle_0 = -eb(-k^2)k_\mu A_\mu(k) = 0, \tag{6}$$

where use has been made of the Lorentz condition.

We have also from (2')

$$k_\mu\langle j_\mu(k)\rangle_0 = -ek_\mu K_{\mu\nu}(k)A_\nu(k), \tag{7}$$

so that

$$k_\mu K_{\mu\nu}(k) = 0 \tag{8}$$

on account of the complete arbitrariness of $A_\nu$. As the polarization tensor $K_{\nu\mu}$ is symmetrical (at least in the lowest order of approximation) it must be also

$$k_\mu K_{\nu\mu}(k) = 0, \tag{8}$$

which shows that $K_{\mu\nu}$ satisfies the condition of gauge invariance exactly as in the local electrodynamics.

Let us assume, for a while, that $b(-k^2)$ admits a power series expansion:

$$b(-k^2) = b_0 + b_1 k^2 + b_2 k^4 + \ldots \tag{9}$$

By introducing (9) into (5) and rearranging the terms, we get

$$[(1 + e^2 b_1) k^2 + (\varkappa^2 + e^2 b_0)] A_\mu(k) = e J_\mu(k) - e^2 b_2 k^4 A_\mu(k) + \ldots \tag{10}$$

from where it is seen that the renormalization of the photon rest-mass constant requires

$$\varkappa^2 = -e^2 b_0, \tag{11}$$

while the experimental charge $\varepsilon$ is

$$\varepsilon = \frac{e}{1 + e^2 b_1}. \tag{12}$$

We express the charge $e$ by means of the experimental charge $\varepsilon$:

$$e = \varepsilon(1 + b_1 \varepsilon^2 + \ldots). \tag{13}$$

If we restrict ourselves to terms of the order $\varepsilon^2$, then we may simply put $e = \varepsilon$, so that there is no charge renormalization in the lowest order of approximation provided $b_1$ is finite (in fact, $b_1$ is finite within the framework of the non-local electrodynamics). Thus, the renormalized equation (10) is (up to the order $\varepsilon^2$)

$$k^2 A_\mu(k) = \varepsilon J_\mu(k) - \varepsilon^2 (b_2 k^4 + b_3 k^6 + \ldots) A_\mu(k), \tag{14}$$

where

$$-\varepsilon (b_2 k^4 + b_3 k^6 \ldots) A_\mu(k) = \langle j_\mu(k) \rangle_0^R \tag{15}$$

is the renormalized vacuum polarization current. Thus, in order to infer the observable vacuum polarization effects, we have to compute the coefficients $b_2, b_3, \ldots$ of the power series expansion (9). Of course, it must be proved first whether $b(-k^2)$ exists and whether it admits a series expansion of the form (9). We shall show that $b(-k^2)$ exists, but possesses a pole:

$$b(-k^2) = \frac{b_{-1}}{k^2} + b_0 + b_1 k^2 + b_2 k^4 + \ldots \tag{16}$$

unless a suitable mixture of charged fields of Fermi and Bose types is assumed. If the number of boson fields of spin 0 is twice the number of fermion fields, then the term $\frac{b_{-1}}{k^2}$ disappears.

The computation of the tensor $K_{\mu\nu}(k)$, given in Appendix I, yields

$$K_{\mu\nu}^{1/2}(k^2) = \frac{4}{(2\pi)^3} P \int d^4p \, J^4(p, k) \frac{\delta(p^2 + m^2)}{(p - k)^2 + m^2}$$

$$\times \{p_\mu (p_\nu - k_\nu) + p_\nu (p_\mu - k_\mu) - \delta_{\mu\nu} [p_\lambda (p_\lambda - k_\lambda) + m^2]\} \tag{17'}$$

$$K^0_{\mu\nu}(k^2) = -\frac{1}{(2\pi)^3} P\int d^4p\, J^4(p,k)\,\frac{\delta(p^2+M^2)}{(p-k)^2+M^2}$$
$$\times\{p_\mu(p_\nu-k_\nu)+p_\nu(p_\mu-k_\mu)+p_\mu p_\nu$$
$$+(p_\mu-k_\mu)(p_\nu-k_\nu)-\delta_{\mu\nu}[p_\lambda(p_\lambda-k_\lambda)+2M^2]\}, \tag{17''}$$

where $K^{1/2}_{\mu\nu}$, $K^0_{\mu\nu}$ apply to the fields with spin $^1/_2$ and 0 respectively. The above formulae differ from the traditional ones merely by the form factor

$$J(p,k) = \int d^4r\, e^{\frac{i}{2}k_\nu r_\nu}\,\varrho(p,r) = \begin{cases} \dfrac{1}{\sqrt{a}}\sin\sqrt{a} & \text{for} \quad a \geqslant 0 \\ 0 & \text{for} \quad a < 0 \end{cases} \tag{18}$$

where:

$$a = \frac{\lambda^4}{4}[(p_\mu k_\mu)^2 - p_\mu^2 k_\nu^2], \tag{18'}$$

while $\lambda$ plays the role of a fundamental length.

In order to compute $b(-k^2)$, we may assume a special frame of reference and generalize subsequently the obtained result for arbitrary Lorentz frames. This procedure is unambiguous in the framework of a convergent formalism. For a time-like four-vector $k_\mu (k_\mu^2 = -\varrho^2,\ \varrho^2 > 0)$, we assume the frame of reference where $\vec{k} = 0, k_0 = \varrho$, and from (3) we have

$$K_{\mu\mu} = -a(\varrho^2)\varrho^2 + 4b(\varrho^2), \qquad K_{44} = -a(\varrho^2)\varrho^2 + b(\varrho^2), \tag{19}$$

whence

$$b(\varrho^2) = \frac{1}{3}(K_{\mu\mu} - K_{44}) = \frac{1}{3}K_{ii}\,. \tag{20}$$

The detailed computation in Appendix II yields $K_{44} = 0$, whence we have

$$b(\varrho^2) = \frac{1}{3}K_{\mu\mu} \tag{21}$$

independently of the particular frame of reference. The same expression holds also for a space-like $k_\mu$. By evaluating the trace, we get from (17) and (20) in the cases of fermions and bosons respectively (see Appendix II)

$$b^{1/2}(\varrho^2) = -\frac{1}{3\pi^2} P\int_0^\infty dp\,\frac{2p^2+3m^2}{\sqrt{p^2+m^2}}\,\frac{p^2}{p^2+m^2-\frac{\varrho^2}{4}}\left(\frac{\sin\frac{1}{2}\lambda^2\varrho p}{\frac{1}{2}\lambda^2\varrho p}\right)^4, \tag{22'}$$

$$b^0(\varrho^2) = \frac{1}{6\pi^2} P\int_0^\infty dp\,\frac{2p^2+3\left(M^2-\frac{\varrho^2}{4}\right)}{\sqrt{p^2+M^2}}\,\frac{p^2}{p^2+M^2-\frac{\varrho^2}{4}}\left(\frac{\sin\frac{1}{2}\lambda^2\varrho p}{\frac{1}{2}\lambda^2\varrho p}\right)^4, \tag{22''}$$

where $p$ is the length of the vector $\vec{p}$. The integrals (22) have been computed approximately in Appendix III. Taking account of the orders of magnitude of the parameters

$$m \approx 5 \cdot 10^{10}\ \mathrm{cm}^{-1}, \quad M \approx 10^{13}\ \mathrm{cm}^{-1}, \quad \lambda \leqslant 10^{-13}\ \mathrm{cm}, \tag{23}$$

we get

$$b^{1/2}(\varrho^2) = -\frac{1}{3\pi^2}\left\{\frac{8\ln 2}{\lambda^4}\frac{1}{\varrho^2} + \left[-\frac{1}{2}m^2 + \frac{3}{8}10^{-4}m^4\lambda^2 - \frac{3}{16}10^{-8}m^6\lambda^4\right]\right.$$
$$+\left[\frac{1}{12}10^8 - \frac{5}{12} + \frac{1}{4}10^{-4}m^2\lambda^2 - \frac{1}{2}\ln\left(\frac{1}{2}10^{-2}m\lambda\right)\right]\varrho^2$$
$$\left.+\left[-\frac{1}{240}10^{12}\lambda^2 + \frac{1}{20}m^2\right]\varrho^4 + \ldots\right\}, \tag{24'}$$

$$b^0(\varrho^2) = \frac{1}{6\pi^2}\left\{\frac{8\ln 2}{\lambda^4}\frac{1}{\varrho^2} + \left[-\frac{1}{2}M^2 + \frac{3}{8}10^{-4}M^4\lambda^4 - \frac{3}{16}10^{-8}M^6\lambda^4\right]\right.$$
$$+\left[\frac{1}{12}10^8 + \frac{1}{3} - \frac{5}{16}10^{-4}M^2\lambda^2 + \frac{1}{4}\ln\left(\frac{1}{2}10^{-2}M\lambda\right)\right]\varrho^2$$
$$\left.+\left[-\frac{1}{240}10^{12}\lambda^2 - \frac{1}{80}M^2\right]\varrho^4 \ldots\right\} \tag{24''}$$

From (24) it is seen that assumption (9) does not hold for the separate fields (possessing poles at the point $k^2 = 0$). The coefficients $b_{-1}$ are very large, which obviously contradicts the experimental data.

The agreement with experiment may be established easily if we introduce a suitable mixture of charged fields obeying Fermi-Dirac and Bose-Einstein statistics. The resulting $b(\varrho^2)$ is the sum of the contributions of the separate fields:

$$b(\varrho^2) = \sum_1^n b^{1/2}(\varrho^2) + \sum_1^N b^0(\varrho^2), \tag{25}$$

where $n$ is the number of spinor fields (with masses $m_1, \ldots m_n$) and $N$ is the number of boson fields (with masses $M_1, \ldots M_N$). The condition for the removal of the pole is

$$N = 2n \tag{26}$$

and hence the resulting $b(\varrho^2)$ is of the desired form (9):

$$b(\varrho^2) = \frac{1}{6\pi^2}\left\{\frac{1}{2}\left(2\sum_1^n m_i^2 - \sum_1^N M_i^2\right) - \frac{3}{8}10^{-4}\lambda^2\left(2\sum_1^n m_i^4 - \sum_1^N M_i^4\right)\right.$$
$$\left.+\frac{3}{16}10^{-8}\lambda^4\left(2\sum_1^n m_i^6 - \sum_1^N M_i^6\right) + \left[\left(n + \frac{N}{4}\right)\ln\left(\frac{1}{2}10^{-2}\lambda\right)\right.\right.$$

$$+\left(\sum_1^n \ln m_i + \frac{1}{4}\sum_1^N \ln M_i\right) + \frac{1}{6}(5n+2N) - \frac{1}{16}10^{-4}\lambda^2\left(8\sum_1^n m_i^2 + 5\sum_1^N M_i^2\right)\Big]\varrho^2 - \frac{1}{80}\left[8\sum_1^n m_i^2 + \sum_1^N M_i^2\right]\varrho^4 \ldots\Big\}. \tag{27}$$

Condition (26) is the same as the first of the two conditions given in the paper of Jost and Rayski (which were found necessary to secure the gauge invariance of the vacuum polarization current and to remove an infinite photon self-mass in the local electrodynamics). In this formalism the same condition reappears in a somewhat different context. The second condition of the cited paper

$$2\sum_1^n m_i^2 - \sum_1^N M_i^2 = 0 \tag{28}$$

is not necessary in the non-local formalism, since the photon rest-mass may be renormalized to the experimental value (the renormalization procedure is correct, from the mathematical point of view, within the framework of a convergent formalism). Nevertheless we notice that, if condition (28) is satisfied, the coefficient $b_0$ (responsible for the mass renormalization) is very small and tends to zero for $\lambda \to 0$.

The coefficient $b_1$ (responsible for the self-charge) contains terms of the type $\ln \lambda$ tending to infinity for $\lambda \to 0$. The sign and the relation 4 : 1 of the coefficients of fermions and bosons is in complete agreement with the sign and relation of the coefficients attached to the logarithmically divergent integrals in the local electrodynamics. We notice a further term in $b_1$ which is independent of the fundamental length $\lambda$ and is of the order of unity. This term has no counterpart within the local electrodynamics.

On the other hand, the coefficient $b_2$ describing the observable vacuum polarization current is identical with that provided by the traditional quantum electrodynamics.

In conclusion it may be repeated that the non-local quantum electrodynamics, with a form-factor suggested by the postulate of reciprocity, avoids the usual inconsistencies, connected with divergent self-mass and self-charge, well-known from the local electrodynamics. However, in consequence of the appearance of a pole, an agreement with experiment may be achieved only by simultaneous introduction of several charged fields presumably existing in Nature. If we limit our considerations to charged particles with spin 1/2 and 0, then the number of different kinds of particles with spin 0 must be twice as large as the number for particles with spin 1/2.

As the procedure of realistic compensation enables us to avoid the difficulties of the self-mass type even within the framework of the local electrodynamics, the main progress provided by the non-local electrodynamics consists in surmounting the difficulties connected with an infinite self-charge.

The question whether other types of form-factors will enable us to avoid the pole at $k^2 = 0$ and to provide a satisfactory electrodynamics (without need of a realistic compensation) is still open. The existence of a form-factor securing (*i*) convergence, (*ii*) relativistic invariance, (*iii*) correspondence with the local theory, and preserving, at the same time, gauge invariance (at least in the restricted sense of invariance against changes of electromagnetic potentials by additive constants) seems improbable.

APPENDIX I. Computation of the vacuum expectation value of the induced current.

The non-local spinor field quantities satisfy the following integral field equations

$$\psi(y,r) = \psi_0(y,r) - ie\int d^4x'd^4r'd^4s'\,\bar{S}(y-y',r,s')\gamma^\mu\psi(y',r')A_\mu(x'),$$

$$\bar{\psi}(y,r) = \bar{\psi}_0(y,r) - ie\int d^4x'd^4r'd^4s'\,\bar{\psi}(y',r')\gamma^\mu\bar{S}(y'-y,r,s')A_\mu(x'), \qquad (1)$$

where $y = x - \frac{1}{2}(r+s)$. They may be computed from (1) by means of iteration as a power series

$$\psi = \psi_0(y,r) + e\psi_1(y,r) + \ldots$$
$$\bar{\psi} = \bar{\psi}_0(y,r) + e\bar{\psi}_1(y,r) + \ldots. \qquad (2)$$

The charge and current density is given by the formula

$$j_\mu(x) = \frac{ie}{2}\int d^4r\,d^4s\,[\bar{\psi}(y,s),\gamma_\mu\psi(y,r)]. \qquad (3)$$

By introducing the power series expansion (2) into (3), we have in the first approximation

$$i_\mu(x) = j_\mu^{(0)}(x) + j_\mu^{(1)}(x) = \frac{ie}{2}\int d^4r\,d^4s\,[\bar{\psi}_0(y,s),\gamma^\mu\psi_0(y,r)]$$

$$+\frac{ie}{2}\int d^4r\,d^4s\,([\bar{\psi}_0(y,s),\gamma^\mu\psi_1(y,r)]+[\psi_1(y,s),\gamma^\mu\psi_0(y,r)]). \qquad (4)$$

Substituting for $\psi_1, \bar{\psi}_1$ the expressions obtained from (1) by means of iteration and taking the vacuum expectation value $\langle j_\mu\rangle_0$, we find

$$\langle j_\mu(x)\rangle_0 = \langle j_\mu^{(1)}(x)\rangle_0 = -e^2\int d^4x'\,K_{\mu\nu}^{1/2}(x-x')A_\nu(x'), \qquad (5')$$

where

$$K_{\mu\nu}^{1/2}(x-x') = -\int d^4r\,d^4s\,d^4r'\,d^4s'\langle B\rangle_0, \qquad (5'')$$

with

$$B = \frac{1}{2}([\bar{\psi}_0(y,s),\gamma^\mu\bar{S}(y-y',r,s')\gamma^\nu\psi_0(y',r')]$$
$$+[\bar{\psi}_0(y',s')\gamma^\nu\bar{S}(y'-y,s,r')\gamma^\mu\psi_0(y,r)]), \qquad (5''')$$

where $y' = x' - \frac{1}{2}(r' + s')$. The tensor $K_{\mu\nu}$ is the non-local counterpart of the usual polarization tensor known from the local electrodynamics:

$$K^{loc}_{\mu\nu}(x-x') = -\frac{1}{2}\gamma_\mu [S^{(1)}(x-x')\gamma^\nu \bar{S}(x'-x) + \bar{S}(x-x')\gamma^\nu S^{(1)}(x'-x)]$$

$$= 4\left\{\frac{\partial \Delta^1(x-x')}{\partial x_\mu}\frac{\partial \bar{\Delta}(x-x')}{\partial x_\nu} + \frac{\partial \Delta^{(1)}(x-x')}{\partial x_\nu}\frac{\partial \bar{\Delta}(x-x')}{\partial x_\mu} - \delta_{\mu\nu}\left[\frac{\partial \Delta^{(1)}(x-x')}{\partial x_\lambda}\frac{\partial \bar{\Delta}(x-x')}{\partial x_\lambda} + m^2 \Delta^{(1)}(x-x')\bar{\Delta}(x-x')\right]\right\} \tag{6}$$

and may be also obtained directly from (6) by means of the general rules of transcription of local into non-local quantities:

$$S^{(1)}(x-x') \to S^{(1)}(y-y', r, s') = \left(\gamma_\mu \frac{\partial}{\partial x_\mu} - m\right)\Delta^{(1)}(y-y', r, s'),$$

$$\bar{S}(x-x') \to \bar{S}(y-y', r, s') = \left(\gamma_\mu \frac{\partial}{\partial x_\mu} - m\right)\bar{\Delta}(y-y', r, s'), \tag{7'}$$

or

$$\Delta^{(1)}(x-x') \to \Delta^{(1)}(y-y', r, s'),$$

$$\bar{\Delta}(x-x') \to \bar{\Delta}(y-y', r, s'), \tag{7''}$$

where

$$\Delta^{(1)}(y-y', r, s) = \frac{1}{(2\pi)^4}\int d^4k \Delta^{(1)}(k, r, s) e^{ik(y-y')}$$

$$\Delta^{(1)}(k, r, s) = \Delta^{(1)}(k)\varrho(k, r)\varrho(k, s) = 2\pi\delta(k_\mu^2 + m^2)\varrho(k, r)\varrho(k, s),$$

$$\bar{\Delta}(y-y', r, s) = \frac{1}{(2\pi)^4} P\int d^4k \bar{\Delta}(k, r, s) e^{ik(y-y')}$$

$$\bar{\Delta}(k, r, s) = \bar{\Delta}(k)\varrho(k, r)\varrho(k, s) = \frac{1}{k^2 + m^2}\varrho(k, r)\varrho(k, s), \tag{8}$$

$$\varrho(k, r) = N(k)\delta(k_\mu r_\mu)\delta(r_\mu^2 + \lambda^4 k_\mu^2) \tag{9}$$

($m$ is the mass constant, $N(k)$ denotes a normalizing factor and $\lambda$ is a constant playing the role of an elementary length). After carrying out the integrations over the variables $r, s, r', s'$ we are left with the expression[1]

[1] Taking account of the properties:

$$J(p, q) = J(-p, q) = J(p, -q) = J(-p, -q) = J(p, p\alpha + q)$$

with $\alpha$ denoting an arbitrary constant.

$$K^{1/2}_{\mu\nu}(x-x') = -\frac{4}{(2\pi)^7} P\int d^4p\, d^4q\, e^{i(p+q)(x-x')} \frac{\delta(p^2+m^2)}{q^2+m^2}$$
$$\{p_\mu q_\nu + p_\nu q_\mu - \delta_{\mu\nu}(p_\lambda q_\lambda - m^2)\} J^4(p,q), \tag{10}$$

where

$$J(p,q) = \int d^4r\, e^{\frac{i}{2} q_\nu r_\nu}\, \varrho(p,r) = \frac{1}{\sqrt{a}} \sin\sqrt{a}\,, \tag{11}$$

$$a = \frac{\lambda^4}{4}\{(p_\mu q_\mu)^2 - p_\mu^2 q_\nu^2\}. \tag{11'}$$

The Fourier transform $K_{\mu\nu}(k)$ is (for $k = p+q$)

$$K^{1/2}_{\mu\nu}(k) = \frac{4}{(2\pi)^3} P\int d^4p \frac{\delta(p^2+m^2)}{(p-k)^2+m^2}$$
$$\times\{p_\mu(p_\nu - k_\nu) + p_\nu(p_\mu - k_\mu) - \delta_{\mu\nu}[p_\lambda(p_\lambda - k_\lambda) + m^2]\} J^4(p,k), \tag{12}$$

which differs from the analogous expression in the local theory merely by the appearance of the form-factor $J^4(p,k)$.

We do not need repeat the calculations for the charged fields with spin 0, but may immediately transcribe the well-known expression of the local theory (cf. Jost and Rayski 1949) by supplementing the tensor $K^0_{\mu\nu}$ by the form-factor $J$:

$$K^0_{\mu\nu}(x-x') = \frac{1}{(2\pi)^7} P\int d^4p\, d^4q\, e^{i(p+q)(x-x')} \frac{\delta(p^2+M^2)}{q^2+M^2}$$
$$\times\{p_\mu q_\nu + p_\nu q_\mu - p_\mu p_\nu - q_\mu q_\nu + \delta_{\mu\nu}(p_\lambda^2 + q_\lambda^2 + 2M)\} J^4(p,q) \tag{10'}$$

or

$$K^0_{\mu\nu}(k) = -\frac{1}{(2\pi)^3} P\int d^4p \frac{\delta(p^2+M^2)}{(p-k)^2+M^2}$$
$$\times\{p_\mu(p_\nu - k_\nu) + p_\nu(p_\mu - k_\mu) + p_\mu p_\nu + (p_\mu - k_\mu)(p_\nu - k_\nu)$$
$$- \delta_{\mu\nu}[p_\lambda^2 + (p_\lambda - k_\lambda)^2 + 2M^2]\} J^4(p,k). \tag{12'}$$

APPENDIX II. The evaluation of the components of $K_{\mu\nu}(k)$ in a special frame of reference.

Assuming a time-like $k_\mu$ ($k_\mu^2 = -\varrho^2 < 0$) we introduce the frame of reference where $\vec{k} = 0$, $k_0 = \varrho$. In this frame of reference the form-factor assumes a comparatively simple form:

$$J^4(p,k) = \left(\frac{\sin\frac{1}{2}\lambda^2 p\varrho}{\frac{1}{2}\lambda^2 p\varrho}\right)^4, \tag{1)}$$

where $|\vec{p}| = p$. We may put also

$$\frac{\delta(p_\mu + m^2)}{(p_\mu - k_\mu)^2 + m^2} = \frac{1}{\varrho}\frac{\delta(p^2 - p_0^2 + m^2)}{\varrho - 2p_0} \tag{2)}$$

Now

$$K_{ij}^{1/2} = \frac{4}{(2\pi)^3}\left\{\frac{2}{\varrho}P\int \vec{dp}\, p_i p_j J^4(p,k)\int dp_0 \frac{\delta(p^2-p_0^2+m^2)}{2p_0-\varrho}\right.$$
$$\left. -\delta_{ij}P\int \vec{dp}\, J^4(p,k)\int dp_0 \frac{\delta(p^2-p_0^2+m^2)}{2p_0-\varrho}\right\},$$

$$K_{i4}^{1/2} = \frac{4}{(2\pi)^3}\frac{i}{\varrho}P\int \vec{dp}\, p_i J^4(p,k)\int dp_0\, \delta(p^2-p_0^2+m^2),$$

$$K_{44}^{1/2} = -\frac{4}{(2\pi)^3}P\int \vec{dp}\, J^4(p,k)\int dp_0 p_0\, \delta(p^2-p_0^2+m^2). \tag{3}$$

For reasons of symmetry, we find

$$K_{i4}^{1/2} = K_{44}^{1/2} = K_{ij}^{1/2} = 0 \qquad \text{for } i \neq j, \tag{4'}$$

$$K_{ij}^{1/2} = \frac{2}{(2\pi)^3}P\int \vec{dp}\, \frac{1}{\sqrt{p^2+m^2}}\, \frac{p_i p_j}{p^2+m^2-\frac{\varrho^2}{4}} J^4(p,k). \qquad \text{for } i=j \tag{5'}$$

After evaluating the trace $K_{ii}^{1/2}$ the integration over the angles may be immediately carried out and we are left with

$$K_{ii}^{1/2} = -\frac{1}{\pi^2}P\int_0^\infty \frac{dp}{\sqrt{p^2+m^2}}\, p^2\, \frac{2p^2+3m^2}{p^2+m^2-\frac{\varrho^2}{4}}\left(\frac{\sin\frac{1}{2}\lambda^2\varrho p}{\frac{1}{2}\lambda^2\varrho p}\right)^4. \tag{6'}$$

In the same way

$$K_{i4}^0 = K_{44}^0 = K_{ij}^0 = 0 \qquad \text{for } i \neq j, \tag{4''}$$

$$K_{ij}^0 = -\frac{1}{(2\pi)^3}P\int \vec{dp}\, \frac{1}{\sqrt{p^2+M^2}}\left(\frac{p_i p_j}{p^2+M^2-\frac{\varrho^2}{4}} - \delta_{ij}\right) J^4(p,k), \text{ for } i=j \tag{5''}$$

$$K_{ii}^0 = \frac{1}{2\pi^2}P\int_0^\infty \frac{dp}{\sqrt{p^2+M^2}}\, p^2\, \frac{2p^2+3\left(M^2-\frac{\varrho^2}{4}\right)}{p^2+M^2-\frac{\varrho^2}{4}}\left(\frac{\sin\frac{1}{2}\lambda^2\varrho p}{\frac{1}{2}\lambda^2\varrho p}\right)^4. \tag{6''}$$

## APPENDIX III. Numerical evaluation of the integrals $b(\varrho^2)$.

$$b^{1/2}(\varrho^2) = -\frac{1}{3\pi^2}P\int_0^\infty \frac{dp}{\sqrt{p^2+m^2}}\, \frac{p^2(2p^2+3m^2)}{p^2+m^2-\frac{\varrho^2}{4}}\left(\frac{\sin\frac{1}{2}\lambda^2\varrho p}{\frac{1}{2}\lambda^2\varrho p}\right)^4, \tag{1'}$$

$$b^0(\varrho^2) = \frac{1}{6\pi^2} P \int_0^\infty \frac{dp}{\sqrt{p^2+M^2}} \frac{p^2\left[2p^2+3\left(M^2-\frac{\varrho^2}{4}\right)\right]}{p^2+M^2-\frac{\varrho^2}{4}} \left(\frac{\sin\frac{1}{2}\lambda^2\varrho p}{\frac{1}{2}\lambda^2\varrho p}\right)^4. \quad (1'')$$

Since we exclude the creation of pairs of charged particles, we assume $\varrho$ to be not too large: $\varrho < 2m$, so that the symbol $P$ denoting the principal value may be omitted (it may be easily verified that the integrals are convergent in the sense of Cauchy also for $\varrho > 2m$). The integrations may be carried out approximately on account of the inequalities (21). By dividing the domain of integration into two parts

$$\int_0^\infty dp = \int_0^A dp + \int_A^{+\infty} dp, \quad (2)$$

where $A$ is assumed equal to $A = \frac{10^2}{\lambda} \geqslant 10^{15}$, we may assume in the first integral

$$\left(\frac{\sin\frac{1}{2}\lambda^2\varrho p}{\frac{1}{2}\lambda^2\varrho p}\right)^4 = 1, \qquad 0 \leqslant p \leqslant A \quad (3)$$

with a very good accuracy. In the second integral we may omit $m^2$ (or $M^2$) and $\frac{\varrho^2}{4}$ in comparison with $p^2$. The error introduced by these approximations does not exceed $10^{-4}$ in either case.

Thus

$$b^{1/2,0}(\varrho^2) = -\frac{1}{3\pi^2}(I_I^{1/2,0} + 2J_{II}), \quad (4)$$

where

$$I_I^{1/2}(\varrho^2) = \int_0^A \frac{dp}{\sqrt{p^2+m^2}} \frac{2p^4+3m^2p^2}{p^2+m^2-\frac{\varrho^2}{4}},$$

$$I_I^0(\varrho^2) = \int_0^A \frac{dp}{\sqrt{p^2+M^2}} \frac{2p^4+3\left(M^2-\frac{\varrho^2}{4}\right)p^2}{p^2+M^2-\frac{\varrho^2}{4}},$$

$$I_{II}^{1/2}(\varrho^2) = I_{II}^0(\varrho^2) = I_{II}(\varrho^2) = \int_A^\infty dp\, p \left(\frac{\sin\frac{1}{2}\lambda^2\varrho p}{\frac{1}{2}\lambda^2\varrho p}\right)^4. \quad (5)$$

The integrations denoted by I are elementary:

$$I_{\mathrm{I}}^{1/2}(\varrho^2) = 2N_m^{(2)} + 3m^2 N_m^{(1)}, \tag{6'}$$

$$I_{\mathrm{I}}^{0}(\varrho^2) = 2N_M^{(2)} + 3\left(M^2 - \frac{\varrho^2}{4}\right) N_M^{(1)} \tag{6''}$$

with

$$N_\mu^{(1)} = \frac{1}{2}\left\{ -\ln\frac{\sqrt{1+\alpha^2}-1}{\sqrt{1+\alpha^2}+1} + \frac{2}{\beta}\sqrt{1-\beta^2}\left[\operatorname{arc\,tg}\left(\frac{1}{\beta}\sqrt{1-\beta^2}\,\sqrt{1+\alpha^2}\right) - \frac{\pi}{2}\right]\right\}, \tag{7'}$$

$$N_\mu^{(2)} = \frac{\mu^2}{4}\left\{ 2\,\frac{\sqrt{1+\alpha^2}}{\alpha^2} + (3-2\beta^2)\ln\frac{\sqrt{1+\alpha^2}-1}{\sqrt{1+\alpha^2}+1} - 4(1-\beta^2)\frac{1}{\beta}\sqrt{1-\beta^2}\left[\operatorname{arc\,tg}\left(\frac{1}{\beta}\sqrt{1-\beta^2}\,\sqrt{1+\alpha^2}\right) - \frac{\pi}{2}\right]\right\}, \tag{7''}$$

$$\alpha = \frac{\mu}{A}, \quad \beta = \frac{\varrho}{2\mu}, \quad \mu = \begin{cases} m \\ M. \end{cases} \tag{7'''}$$

Since $\alpha \ll 1$, $\beta < 1$, we may use a power series expansion of[2] $N_\mu$.

Thus, we get up to $\alpha^4$, $\beta^4$

$$I_{\mathrm{I}}^{1/2} = \frac{10^4}{\lambda^2} - \frac{1}{2}m^2 + \frac{3}{8}10^{-4}m^4\lambda^2 - \frac{3}{16}10^{-8}m^6\lambda^4 + \left[-\frac{5}{12} + \frac{10^{-4}}{4}m^2\lambda^2 - \frac{1}{2}\ln\left(\frac{10^{-2}}{2}m\lambda\right)\right]\varrho^2 + \frac{1}{20m^2}\varrho^4 + \ldots$$

$$I_{\mathrm{I}}^{0} = \frac{10^4}{\lambda^2} - \frac{1}{2}M^2 + \frac{3}{8}10^{-4}M^4\lambda^2 - \frac{3}{16}10^{-8}M^6\lambda^4 + \left[\frac{1}{3} - \frac{5}{4}10^{-4}M^2\lambda^2 + \frac{1}{4}\ln\left(\frac{10^{-2}}{2}M\lambda\right)\right]\varrho^2 - \frac{1}{80M^2}\varrho^4 + \ldots$$

$$I_{\mathrm{II}} = \left(\int_0^\infty - \int_0^A\right) dp\,p\left(\frac{\sin\frac{1}{2}\lambda^2\varrho p}{\frac{1}{2}\lambda^2\varrho p}\right)^4 = \frac{4\ln 2}{\lambda^4\varrho^2} - \frac{1}{2}\frac{10^4}{\lambda^2} + \frac{1}{24}10^8\varrho^2 - \frac{1}{480}10^{12}\lambda^2\varrho^4 \ldots \tag{8}$$

[2] The power series expansion for arctg converges slowly for $\beta \to 1$, but taking $\varrho \leqslant 10^{-1}2m$ (i. e. $\beta \leqslant 10^{-1}$) we assure a sufficiently rapid convergence.

Now, collecting the terms in $I_{\mathrm{I}}$ and $I_{\mathrm{II}}$, we find

$$b^{1/2}(\varrho^2) = -\frac{1}{3\pi^2}\left\{\frac{8\ln 2}{\lambda^4\varrho^2} - \frac{1}{2}m^2 + \frac{3}{8}10^{-4}m^4\lambda^2 - \frac{3}{16}10^{-8}m^6\lambda^4 + \left[\frac{1}{12}10^8 - \frac{5}{12} + \frac{1}{4}10^{-4}m^2\lambda^2 - \frac{1}{2}\ln\left(\frac{10^{-2}}{2}m\lambda\right)\right]\varrho^2 + \left[-\frac{1}{240}10^{12}\lambda^2 + \frac{1}{20m^2}\right]\varrho^4 + \ldots\right\}$$

$$b^0(\varrho^2) = \frac{1}{6\pi^2}\left\{\frac{8\ln 2}{\lambda^4\varrho^2} - \frac{1}{2}M^2 + \frac{3}{8}10^{-4}M^4\lambda^2 - \frac{3}{16}10^{-8}M^6\lambda^4 + \left[\frac{1}{12}10^8 + \frac{1}{3} - \frac{5}{16}10^{-4}M^2\lambda^2 + \frac{1}{4}\ln\left(\frac{10^{-2}}{2}M\lambda\right)\right]\varrho^2 + \left[-\frac{1}{240}10^{12}\lambda^2 - \frac{1}{80M^2}\right]\varrho^4 + \ldots\right\}. \quad (9)$$


## КРАТКОЕ СОДЕРЖАНИЕ

В. Ганус и Й. Райский, *Поляризация вакуума.*

Вакуумный поляризационный ток произведённый внешним электромагнитным полем был вычислен с применением неместной электродинамики формулированной одним из автогов. Вакуумный поляризационный ток свободен от обычных расхождений, но не соглашается с экспериментом благодаря полюсу (особой точке) в разложении на степенной ряд по моментам. Этот полюс может быть устранен и согласие с экспериментом вновь установлено при помощи реалистичной компенсации (одновременное сопряжение электромагнитного поля с заряжёнными фермионами и бозонами).


## REFERENCES


Born M. and Green H. S., *Proc. Roy. Soc. Edinb.* A, **92,** 470 (1949).
Jost R. and Rayski J., *Helv. Phys. Acta,* **22,** 457 (1949).
Källen G., *Helv. Phys. Acta,* **22,** 637 (1949).
Pauli W. and Villars F., *Rev. Mod. Phys.,* **21,** 433 (1949).
Rayski J., *Acta Phys. Pol.,* **9,** 129 (1948).
Rayski J., *Proc. Phys. Soc.,* **64,** 957 (1951).
Rayski J., *Acta Phys. Pol.,* **11,** 109 (1952).
Schwinger J., *Phys. Rev.* **75,** 651 (1949).
Umezawa H., Yukawa J. and Yamada E., *Progr. Theor. Phys.,* **3,** 317 (1948).
Umezawa H. and Kawabe R., *Progr. Theor. Phys.,* **4,** 1949 (1949).
Yukawa H., *Phys. Rev.,* **77,** 219 (1950).

# PHOTOCONDUCTIVE AND PHOTOVOLTAIC LEAD SELENIDE LAYERS

By Halina Chęcińska

Institute of Experimental Physics, Warsaw University, Warszawa

*(received January 27, 1953)*

A method was worked out for activating thin (about $1\mu$) microcrystalline layers of lead selenide. These layers displayed photoconductivity and the internal photovoltaic effect. They were prepared by evaporating in vacuo lead selenide which possessed an excess of lead (above the stechiometric ratio). The layers were treated with oxygen under low pressure and then reduced by heating in vacuo with the purpose of securing photosensitivity. The photoconducting layers, when subjected in vacuo to an electric current at about 250° and then rapidly cooled to room temperature, obtained photovoltaic sensitivity. This method of producing photosensitive layers gives sufficiently reproductible results, but further improvements seem possible.

The conductivity, photosensitivity, and thermoelectric efficiency were measured during various stages of activation of the layers. Changes of type $n$ to type $p$ conductivity were observed during oxidation and the reverse during reduction. The general properties of lead selenide layers are similar to the well known properties of analogous PbS layers; the main difference consists in their greater sensitivity to the action of oxygen. The behaviour of the layers during activation operations, data obtained from examining the Hall effect, and the strict connection existing between the photoconductivity and the photovoltaic effect agree with the barrier theory of L. Sosnowski (1949). The layers produced by the above method possess a sensitivity to radiation in the range $0{,}5-3{,}6\mu$. The threshold of sensitivity i.e. the smallest value of radiation energy causing noticeable effects amounts to $10^{-8}$ W/cm$^2$ at room temperature and increases at low temperatures.

## INTRODUCTION

There exists a group of semiconductors which in a pure state do not possess photoelectric properties, but which with certain admixtures are photosensitive. To this type of substances belong besides such elements as germanium and silicon, simple chemical compounds of a mixed (ion-valency) bond type such as PbS, PbO, CuO, PbSe, PbTe, $Tl_2S$, etc. They are usually semiconductive substances which may very easily appear as excess as well as defect semiconductors.

The interpretation of electronic phenomena in semiconductors is based mainly on the band theory evolved by Wilson and Mott and independently by the Frenkel school in the U.S.S.R.

According to the fundamental principles of this theory, the electric properties of semiconductors are conditioned by the presence in the crystalline net of impurity centres, which form for the electron local levels, placed in the forbidden

zone between the ground band and the conductivity band. If the impurity centres possess a metallic character, they may supply the conductivity band with electrons. In such a case there exists excess conductivity, called "type $n$" conductivity. If the impurity centres possess an electronegative character, they may capture electrons from the ground band forming "holes" which act as positive current carriers. This conductivity is usually called the $p$ type, and the semiconductor is described as defective.

The Wilson-Mott-Frenkel theory concerned itself with monocrystals and in calculations it treated their dimensions as infinite. In spite of this simplification it satisfactorily explained a number of electric phenomena in semiconductors, among others it succesfully explained the existence of two types of conductivity: the electronic and the hole type, in agreement with experiment, since investigations of the Hall effect and of changes in the direction of the thermoelectric force indicated the presence of positive and negative carriers in the semiconductors.

The development, however, of research on semiconductors and, in particular, the investigation of their photoelectric properties, brought to light great deficiencies of the theory and the necessity of further improvements. The investigyations of Sosnowski (1946, 1949) and, independently, of other scientists in the U.S.S.R., U.S.A. and in Germany on the properties of microcrystalline layers of PbS, have been one of the main stages of progress in this field.

It appeared that the phenomena occurring on the boundary surfaces of the microcrystals play the main part in semiconductors. These investigations became the foundation for enlarging the theory and for a new interpretation of photoelectric phenomena in semiconductors.

## Photoconductivity of a monolithic layer

Photosensitivity may be defined as the relative change of conductivity under the influence of a unitary flux of energy $I$:

$$S = \frac{\sigma^1 - \sigma}{\sigma I},$$

where $\sigma^1$ is the conductivity of the illuminated film, and $\sigma$ of the nonilluminated one. At the base of the interpretation of photoelectric phenomena is the hypothesis that a radiation quantum transfers an electron from the ground band or an impurity centre to the conductivity band. As a result of this action a hole appears in the ground band. Electrons and holes can recombine and may also be captured by centres. A change of their concentration under the influence of illumination causes the change of conductivity. This depends on the number and type of impurity centres existing in the crystalline structure. Under the influence of constant illumination an equilibrum — a stationary state — is achieved between the increase in the number of electrons transferred to the conductivity band, and its decrease due to recombination. Let us call the relative concentration of holes and electrons under the influence of unitary illumination $I$ (in the stationary

state) as $\frac{n_h' - n_h}{n_h I} = S_h$ for holes and correspondingly as $S_e = \frac{n_e' - n_e}{n_e I}$ for electrons, where $n_e$ and $n_h$ are respectively the numbers of electrons and of holes in the nonilluminated conductor, and $n_e'$ and $n_h'$ the number of electrons and holes per 1 ccm in the illuminated conductor.

These quantities were approximately estimated for PbS on the base of calculation as well as of experiment (Sosnowski, 1949). The calculations were based on the condition of thermodynamic equilibrium in darkness and in light between electrons and holes, and on quantum-statistical considerations leading to the determination of Fermi's level in each type of the semiconductor.

In the case of a defect semiconductor $S_e \approx 10$, $S_h \approx 10^{-5}$. Conversely, for excess PbS $S_e \approx 10^{-5}$, $S_h \approx 10$ (with $I = 1$ W/cm$^2$). The concentration of electrons $n_e$ in an excess semiconductor and of holes $n_h$ in a defect semiconductor is very large in darkness. As $S_e$ and $S_h$ denote relative changes of their concentration under the influence of light, in the case of large $n_e$ and $n_h$ in darkness, the relative changes under the influence of light will be small. The photosensitivity of a semiconductor $S$ depends on changes in the concentration of holes as well as of electrons. For a defect conductor, in which the number of electronegative centres $N_1$ is much larger than the number of electropositive centres $N_2$, the participation of electrons in the conductivity may be neglected and we may assume $S \approx S_h$. In an excess conductor, where $N_2 \gg N_1$, the participation of minority carriers may be omitted and we assume $S \approx S_e$. As it appeared from calculated estimates in the case of PbS the values of $S_h$ for a defect conductor and of $S_e$ for an excess conductor are very small. This would indicate that the photosensitivity of PbS of $n$ or $p$ type conductivity should be much smaller than that which we observe in reality. The photosensitivity of microcrystalline layers of PbS, suitably activated by the introduction of oxygen centres into the crystalline structure, surpasses a hundred and even a thousand times the sensitivity of monocrystals and cannot be explained by the presence of evenly distributed impurity centres.

## Photoconductivity of a policrystalline layer

The theory of photoconductivity based on Wilson and Mott's hypothesis does not supply a satisfactory explanation when applied to monocrystals, and in the case of policrystals it completely fails. Only when the photovoltaic effect in PbS was discovered (Sosnowski 1946, 1949) it was possible to form a new "contact" interpretation of photoelectric phenomena in semiconductors. A more precise analysis proved that the sensitivated microcrystalline photovoltaic and photoconductive layer is composed of a mosaic of excess and defect crystals, and that the contacts between them are responsible for the photoelectric phenomena.

The theory of the contact "n" — "p" based on investigations of photoelectric phenomena in PbS layers was stated by Sosnowski (1949). Such a contact is schematically presented in Fig. 1.

On each side of the contact the semiconductor possesses $N_1$ electronegative and $N_2$ electropositive centres per 1 ccm of the substance. On the left side $N_1 \gg N_2$ and on the right side $N_1 \ll N_2$. In a state of equilibrium the electron density on each energy level must be equal on both sides of the contact. This is possible only if the levels of the area possessing more electrons (excess area) are displaced by a certain distance in respect to the area which is poorer in electrons (Fig. 1). This displacement and the consequent potential difference on the contact is obviously connected with the transition of a part of the electrons from the electropositive centres on the right hand side to the electronegative ones on the left hand side. The areas may possess a sharp boundary as on Fig. 1, or else the transition from type $n$ to type $p$ conductivity may be gradual.

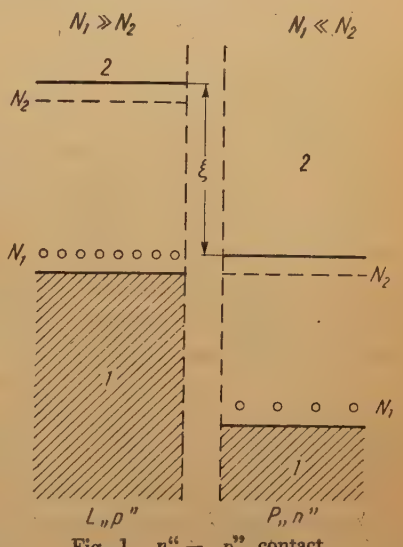

Fig. 1. „$n$" — „$p$" contact

As a result of illumination the concentration of current carriers will increase on both sides of the contact. On considering the photoconductivity of a monolithic layer it appears that the relative changes of concentration of holes $S_h^L$ on the left hand side and of electrons $S_e^R$ on the right hand side will be very small and may be neglected without great error. On the other hand, the relative change of concentration of electrons $S_e^L$ on the left hand side and of holes $S_h^R$ on the right hand side will be considerable. These electrons will occupy the lowest part of the conductivity band on the left hand side and may instantly diffuse to the conductivity band on the other side of the barrier. This passage is particularly facilitated in this direction as it will take the direction from the higher to the lower concentration of electrons on the given level. On the other hand, the probability of recombination of electrons with centres diminishes as a result of the occupation of a part of the electronegative centres on the left hand side, hence their larger share in the conductivity band. A similar reasoning for holes explains their transition from the right to the left side of the contact.

Illumination of the contact results therefore in a transition of electrons from the defect to the excess side and of holes in the opposite direction. This considerably lowers the contact potential barrier. The large change of concentration of minority current carriers under the influence of light and the consequent lowering of the contact barrier are the main factors of a large sensitivity of the contact in regard to the photoconductivity effect.

Exact calculations (Sosnowski, 1949) lead to the following formula for a current passing through an illuminated contact

$$I' = C_1 e^{-\zeta/kT}[1 + S_1 \cdot I - e^{-eV/kT}] + C_2 e^{-\zeta/kT}[1 + S_2 \cdot I - e^{-eV/kT}], \qquad (1)$$

where $C_1$, $C_2$ are constants, $V$ is the applied *E.M.F.*, $\zeta$ is the displacement of energy levels on the contact, $S_e$, $S_h$ are concentration changes of electrons on the left hand side and of holes on the right hand side of the contact under the influence of illumination of unit intensity $I$.

Such an interpretation of photoelectric phenomena in microcrystalline PbS layers, which form a mosaic of miniature contact barriers between areas of type $n$ and type $p$ conductivity, satisfactorily explains their high photosensitivity. Examination of the structure of these layers by means of illumination with a point source about 30 $\mu$ in size, actually proved the existence of microbarriers distributed at random in the photosensitive layers.

Although the theory of photoelectric phenomena in PbS proposed by Sosnowski has a semiempirical character and is based on approximate calculations, further development of investigations on semiconductors proved it to be successful. Contact phenomena between $p$ and $n$ type semiconductors became the foundation for constructing diodes and semiconducting transistors, and supplied physics of the solid state with a new field of research, which possesses wide practical applications.

On the other hand the new interpretation may possibly be applied to other semiconducting substances, which may eventually facilitate obtaining larger photosensitivities or widen the sensitivity spectrum in the direction of longer waves.

Lead selenide is one of the nearest analogues of PbS. As far back as Simpson (1947) pointed out the analogy of PbS and PbSe in regard of the action of oxygen on microcrystalline layers evaporated in vacuo. The next step was achieved when it was discovered (Blackwell and Simpson 1947) that such layers exhibit at low temperatures a photosensitivity reaching further into the infrared area than for PbS layers. Starkiewicz (1948) constructed the first PbSe cells which were also sensitive at room temperature. Up to date no major work on the subject of lead selenide has appeared in the available literature. Short announcements (Millner and Watts 1948; Moss and Chasmar 1948; Gibson, Lawson and Moss 1951) of papers on the subject of photocells made of lead selenide did not contain any information on the methods of producing such cells, and the descriptions of their properties were not always in agreement between each other.

The present paper constitutes an attempt to find independent methods of activating PbSe photoconductive layers. The possible analogy between PbSe and PbS and the possibility of employing for PbSe methods used for PbS were the guiding idea of the investigations.

## I. PRODUCTION APPARATUS

Photosensitive layers were formed in high vacuum in conditions of great purity. The cell containing the layer was connected with a vacuum system (Fig. 2) which was constructed of several "duran" tubes of about 1 cm² diameter, connected with a mercury diffusion pump *PD*, which ensured a vacuum of the order

of $10^{-6}$ mm Hg. The initial vaccum was provided by an oil rotation pump connected with the system. Together with a U-type manometer $M_1$ for measuring the initial vacuum, a container $Z_1$, and a drying contraption $S$ containing $P_2O_5$ for absorption of water vapour. A freezer $L_1$ was mounted directly behind the diffusion pump to prevent the spreading of mercury vapours over the whole system. During work the freezer was immersed in a Dewar flask with liquid air. At the temperature of liquid air mercury vapours condensed in the freezer. A second freezer $L_2$ was mounted directly below the small flask in which the layer was formed. This freezer

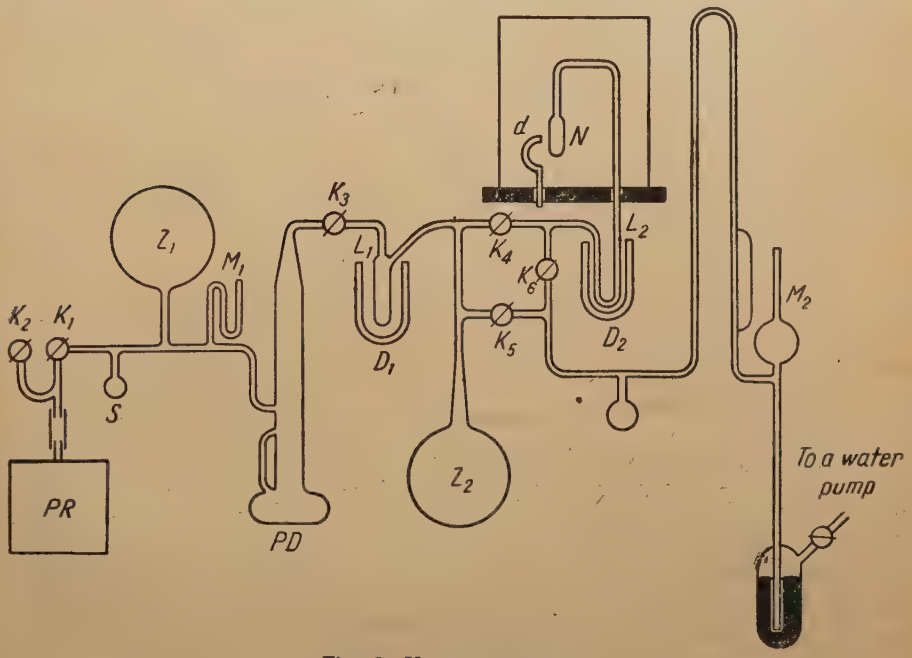


Fig. 2. Vacuum apparatus

served to condense volatile decomposition and oxidation products formed during the production. This is the quickest way of removing them from that part of the system in which the photosensitive layer should be produced in a state of the greatest possible purity. This condensation facilitated an analysis of the composition of obtained by-products and their influence on the properties of the layer as it was possible by removing the Dewar flask $D_2$ to bring the condensed substances back into a volatile state, in which they diffused into the photocell, separated in this case from the pump. According to need oxygen was freed from the container $T$ filled with potassium chlorate by heating with a Bunsen burner.

A McLeod manometer $M_2$ was used to investigate the state of the vaccum and the pressure of oxygen evolved from the potassium chlorate. Taps $K_1 \ldots K_6$ facilitated the separation of various parts of the system.

The whole apparatus was placed on an iron grating. An electric furnace of 5,5 $kW$ maximum power served to subject the film to thermal processes. The furnace had the shape of a cylinder. It was suspended by means of pulleys and

a rope at the top of the grating. This facilitated its quick and easy raising when the cell was cooled to room temperature.

The photosensitive layer was formed in a "duran" flask connected with the vacuum system by a capillary tube. Fig. 3 is a schematic diagram of such a flask. The flasks had the shape of low cylinders of about 30 mm diameter and about 7 mm height. Two tungsten electrodes $W_1$ and $W_2$ were fused into the walls of the cylinder and are connected with graphite electrodes painted in the interior of the cell with a colloidal "Aquadag" graphite solution.

During the production it was necessary to note changes of conductivity and of the photoelectric properties of the layer. For this purpose the cell inserted in

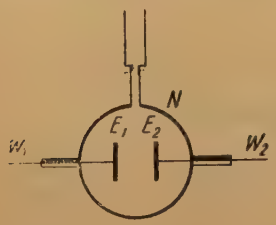


Fig. 3. Flask for the formation of the photoconductive layer

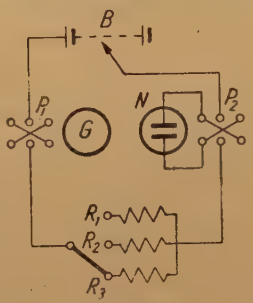


Fig. 4. Electrical circuit

the furnace was connected with an electric circuit. Fig. 4 is a diagram of this cir cuit. It contained a "Multiplex" type sensitive galvanometer $G$ (sensitivity up to $10^{-8}$ A/mm), an anode battery $B$, resistors $R_1$, $R_2$ and $R_3$, and keys $P_1$ and $P_2$. As the resistance of the cell changed gretly in various stages of its preparation, the galvanometer had to possess several ranges of sensitivity. This was obtained by appropriate shunts.

A 40 $W$ power bulb attached to the grating was used for illuminating the cell in order to test its photoconductive properties.

## II. PRODUCTION METHODS

### Materials

Lead selenide, obtained by the reaction of suitable amounts of lead and selenium in vacuo, served as the object of investigation. The elements used in the reaction were labeled by the producing factory as chemically pure; moreover, selenium was distilled in vacuo many times before using. The flask in which the reaction took place was heated for about one hour in vacuo to 600° before filling with the reacting elements.

Six various samples of PbSe were prepared with the reacting substances added partly in stechiometric amounts and partly in amounts which differed from the stechiometric proportion. The best results were obtained with lead selenide containing an 5% excess of lead. This material was, therefore, subjected to further tests.

### The forming of the layer

After several miligrams of lead selenide are inserted in the flask, this is fused to the vacuum system and evacuated. Next, the flask is heated in the furnace at a temperature of about 600°, till all the lead selenide sublimates and gathers in the coolest part of the flask. This usually takes an hour or so. Products of partial oxidation of PbSe in the form of $SeO_2$ and $CO_2$ from the graphite electrode are condensed in the freezer. PbSe is made to collect on the front wall of the cell through cooling this wall with a stream of cooler air from a blower, while the whole flask is kept at the furnace temperature (of about 580°). After the lead selenide is collected in the shape of a dark spot of about 1 cm in diameter, the cell is cooled to room temperature. Now we direct the stream of air from the blower on to the back wall on which the electrodes are painted, and with the help of a gas-air flame we transfer the lead selenide to this wall. This process is executed in vacuo and it takes about one minute. From this moment on, the layer is connected with the electrodes and its electric and photoelectric properties may be observed.

### Properties of the unactivated layer

The microcrystalline PbSe layer formed by this method takes the form of a dark incrustation with a metallic surface tinged a dark blue. It has uneven thickness. The thickest and non-transparent layer appears between the graphite electrodes. Approximate estimations of its thickness led to the value of about $1\,\mu$. The incrustation occupies the whole surface of the far wall of the cell, and often extends to the sides. Layers formed in this way in macroscopically identical conditions showed, after cooling to room temperature, an electric resistance of 500 $\Omega$ to 30 000 $\Omega$. They did not display any photoelectric effect. Of 16 layers prepared in this fashion only one showed traces of photoconductivity.

### Methods of activation

To activate the semiconductive microcrystalline layers they are submitted to the action of oxygen, or else the results of this action are partially removed by heating the layers in vacuo. Oxygen may be introduced at various pressures and at various temperatures. In our experiments it was impossible to verify what changes in the structure of the layer are caused by oxygen. Of the many changeable parameters influencing the properties of layers only the following could be kept under control: temperature, oxygen pressure, amount of oxygen absorbed and changes of conductivity of the layer. In view of this a statistical method was employed, that is, numerous activating operations were completed in various conditions and those which led to a higher sensitivity were noted. About two hundred activating operations were performed. Each layer was revaporized several times and submitted to numerous operations (see Fig. 5 and 6). As a result 36 photosensitive cells were obtained.

Oxygen was introduced by one of the following methods:

a) by revaporizing the material in oxygen,

b) by the action of oxygen on the layer at room temperature,

c) by heating the layer in the presence of oxygen.

The amount of oxygen introduced could be reduced by

d) heating the layer in vacuo.

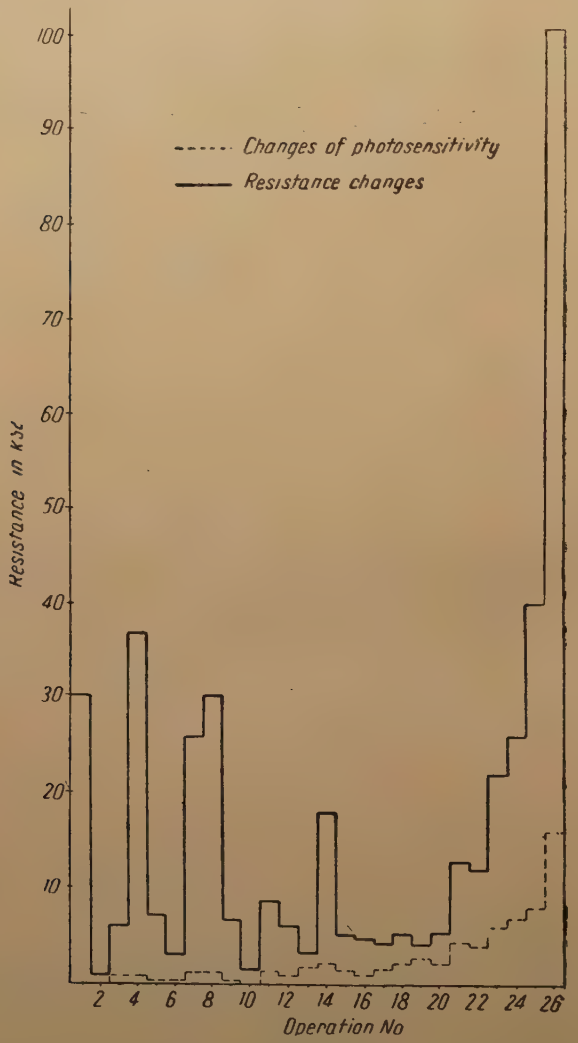


Fig. 5. Production diagram of cell No 21. The diagram gives the values of resistance and of relative sensitivity after the operations and cooling the cell to room temperature

Operation 1 — revaporizing in vacuo by means of a burner
Operation 2 — heating in oxygen up to 300°C under 0,02 mm Hg pressure
Operation 3 — Heating at 460°C in vacuo
Operation 4 — heating in vacuo up to 200°C
Operation 5 — heating in vacuo up to 400°C
Operation 6 — heating in oxygen up to 300°C under 0,03 mm Hg pressure
Operation 7 — heating in vacuo up to 470°C

Operation 8 — heating in oxygen up to 300C° under 0,001 mm Hg pressure
Operation 9 — heating in vacuo up to 450C°
Operation 10 — heating in oxygen up to 450°C under 0,03 mm Hg pressure
Operation 11 — 5 consecutive repetitions of heating in vacuo to 460°C and rapid cooling to room temperature
Operation 12 — heating in vacuo up to 450°C
Operation 13 — heating in oxygen up to 250°C under 0,05 mm Hg pressure
Operation 14 — three consecutive repetitions of heating in vacuo up to 470°C
Operation 15 — heating in oxygen up to 250°C under 0,03 mm Hg pressure
Operation 16 — heating in vacuo up to 450°C
„ 17 — heating in oxygen up to 300°C under 0,03 mm Hg pressure
Operation 18 — heating in vacuo up to 480°C
„ 19 — heating in oxygen up to 460°C under 0,02 mm Hg pressure
Operation 20 — heating in vacuo up to 480°C
Operation 21 — heating in vacuo up to 330°C
„ 22 — heating in vacuo up to 450°C
„ 23 — action of oxygen at room temperature under 0,1 mm Hg pressure
Operation 24 — heating in vacuo up to 350°C
„ 25 — separation of the photocell
„ 26 — changes after 3 — 4 weeks.

a. Revaporizing in oxygen

The substance which has collected on the front wall of the flask in the first phase, after cooling down to room temperature was resublimated onto the far wall in an atmosphere of oxygen, the pressure of which was kept within the limits of 0,001 to 0,1 mm Hg. This operation may be accomplished either by heating the flask in an electric furnace to the temperature of about 550° and by simoultaneous cooling of the far wall with a current of compressed cool air (in this case the operation takes several minutes) or by heating the substance on the front wall with a gas-air burner with simoultaneous cooling of the far wall with compressed cool air. In this case the operation takes about 1 minute. The second method was more frequently employed. After revaporizing in oxygen the layers displayed larger resistance and higher photosensitivity than those heated in a furnace.

b. Action of oxygen at room temperature

A layer formed by the above method (resublimated in vacuo) and cooled to room temperature is submitted to the action of oxygen introduced into the cell at a definite pressure of 0,001 to 0,1 mm Hg). The action of oxygen even under low pressure (0.001 mm Hg) led to the rise of resistance of the layer. Evacuation of the oxygen did not influence the properties of the activated layers. After this process the layers achieved a certain photosensitivity.

c. Heating in the presence of oxygen

The cell was filled with oxygen at room temperature and then heated in the furnace. At the same time conductivity changes were measured. About a hundred such operations were performed under various conditions of oxygen pressure (0,001—0,1 mm Hg) and of maximum temperature (200—450°C). We did not succeed in establishing conditions which would markedly influence the growth of the photosensitivity, PbSe acting in this respect differently than PbS which is strongly influenced by this operation. After heating to 200°C and cooling, the

layers possessed a resistance somewhat higher than before the operation, and a certain small sensitivity. Heating to 450°C caused a decrease of conductivity and a disappearance of sensitivity.

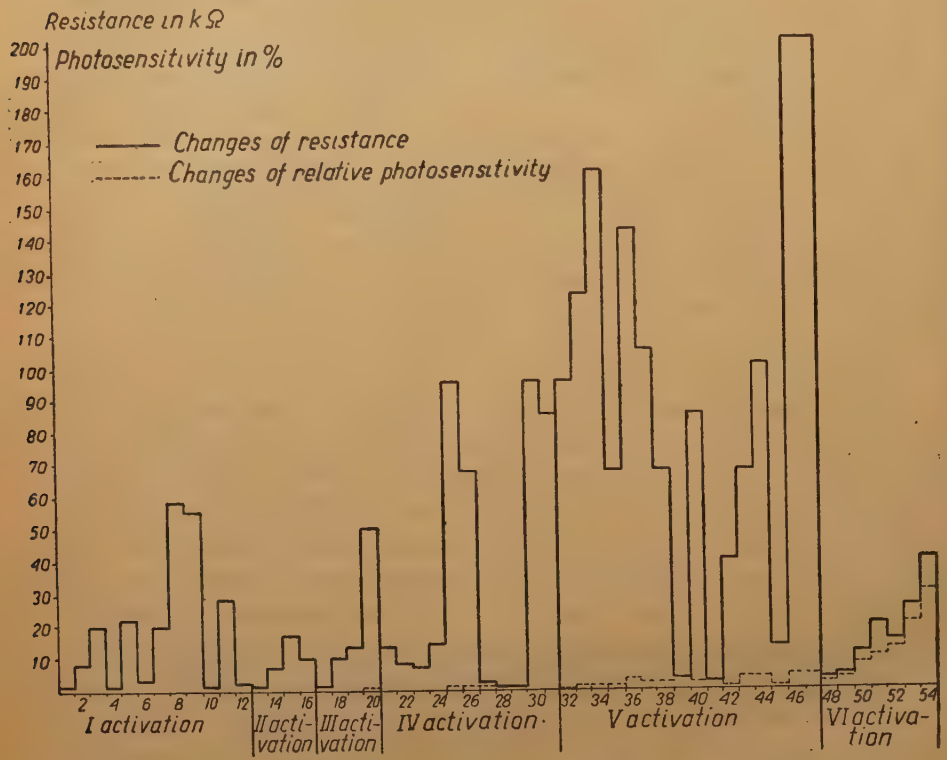


Fig. 6. Production diagram of cell No. 29 — 6 activations, 54 operations

*Operations 1—12 — I activation*

Operation 1 — revaporizing in vacuo
„ 2 — heating in oxygen up to 300° C under 0,03 mm Hg pressure
Operation 3 — heating in vacuo up to 400° C
„ 4 — heating in vacuo up to 430° C
„ 5 — heating in oxygen up to 350° C under 0,02 mm Hg pressure. Traces of photosensitivity.
Operation 6 — heating in vacuo up to 400° C
„ 7 — heating in oxygen up to 300° C under 0,02 mm Hg pressure.
Operation 8 — an interruption for 2 hours. The layer remains in vacuo.
Operation 9 — heating in oxygen up to 350° C under 0,8 mm Hg pressure
Operation 10 — heating in vacuo up to 400° C
„ 11 — heating in oxygen up to 350° C under 0,02 mm Hg pressure. Traces of photosensitivity
Operation 12 — heating in vacuo up to 400° C. The photosensitivity disappears.

*Operations 13—16 — II activation*

Operation 13 — revaporizing in vacuo
„ 14 — heating in oxygen up to 350° C under 0,03 mm Hg pressure
Operation 15 — heating in vacuo up to 400° C
„ 16 — action of oxygen at room temperature.

*Operations 17—20 — III activation*

Operation 17 — revaporizing in vacuo
„ 18 — heating in oxygen up to 400° C under 0,03 mm Hg pressure
Operation 19 — heating in vacuo up to 380° C
„ 20 — a 3-day interruption. The freezers were not immersed in liquid air.

*Operations 21—31 — IV activation*

Operation 21 — revaporizing in oxygen under 0,004 mm Hg pressure

Operation 22 — heating in vacuo up to 400° C
„ 23 — heating in oxygen up to 300° C under 0,004 mm Hg pressure
Operation 24 — heating in vacuo up to 380° C
„ 25 — heating in vacuo up to 250° C
„ 26 — heating in oxygen up to 300° C under 0,006 mm Hg pressure
Operation 27 — heating in vacuo up to 450° C
„ 28 — a 2-day interruption
„ 29 — action of oxygen at room temperature
Operation 30 — heating in oxygen up to 300° C under 0,006 mm Hg pressure
Operation 31 — heating in vacuo up to 300° C, traces of photosensitivity.

*Operations 32—47 — V activation*

Operation 32 — revaporizing in oxygen under 0,008 mm Hg pressure
Operation 33 — heating in vacuo up to 250° C
„ 34 — heating in vacuo up to 250° C higher voltage applied
Operation 35 — heating in vacuo up to 400° C
„ 36 — interruption for 3 hours (vacuum)
Operation 37 — interruption for 24 hours
„ 38 — heating in oxygen up to 300° C under 0,02 mm Hg pressure
Operation 39 — heating in vacuo up to 450° C
„ 40 — heating in oxygen up to 250° C under 0,03 mm Hg pressure
Operation 41 — heating in vacuo up to 470° C
„ 42 — heating in oxygen up to 470° C under 0,01 mm Hg pressure
Operation 43 — heating in oxygen up to 450° C under 0,01 mm Hg pressure
Operation 44 — heating in oxygen up to 450° C under 0,01 mm Hg pressure
Operation 45 — an interruption
„ 46 — heating in vacuo up to 300° C
„ 47 — action of oxygen at room temperature.

*Operations 48—54 — VI activation*

Operation 48 — revaporizing in oxygen under 0,01 mm Hg pressure in a furnace (the layer is thicker than those revaporized with a burner)
Operation 49 — heating in vacuo up to 400° C
„ 50 — heating in vacuo up to 450° C
„ 51 — vacuum for 15 minutes at room temperature
Operation 52 — heating in vacuo up to 400° C
„ 53 — the cell is removed in vacuo
„ 54 — after three weeks. Vacuum in the interior

d. Heating in vacuo

After each of the processes mentioned above (a, b, c) the layers displayed only small photosensitivity and comparatively low resistance. The layers were next subjected to thorough evacuation and additional heating in vacuo, for the purpose of increasing their resistance, and, which usually follows, of their photosensitivity. Heating to 450° during 1—2 minutes led to an increase of conductivity, then to a rapid decrease, and again to an increase. If the process was interrupted by rapid cooling to room temperature when the conductivity was at a minimum, then the photosensitivity and resistance increased to a greater degree. The same effect was obtained by heating for a longer period (about 15 minutes) to a temperature of at most 300°C. During heating the cell first underwent an increase of conductivity and then a slow decrease. After rapid cooling to room temperature the resistance and photosensitivity were much larger.

Other operations. If the Dewar flask with liquid air is removed from the freezer, then $SeO_2$ vaporizes and enters the cell. The diffusion was slow. Visible changes in the layer appeared after the Dewar flask had been removed for 15—20 minutes. This depends to a high degree upon the diameter of the capillary connection between the photocell and the vacuum system. The resistance in some cells increased under the influence of $SeO_2$, but, as only a small number of these

operations was performed, it is difficult to evolve general inferences as to the effect of $SeO_2$ on photoesnsitivity.

Combined operations. None of the operations described, if employed singly, gave a layer of sufficient photosensitivity. At least one oxidizing process was necessary, and it had to be followed by heating in vacuo. The revaporization of the substance in the presence of oxygen by means of an air-gas burner seems to be the most effective one in regard to photoconductive properties. Generally speaking layers possessing a larger resistance displayed a higher photosensitivity. The main principle, therefore, of producing photosensitive layers is to use such a combination of sensitivating operations as will lead to the highest resistance. The best results were obtained by the following combinations of operations:

*either I.* 1) revaporizing the substance in an atmosphere of oxygen at 0,01 mm Hg pressure with the use of a gas-air burner,

2) heating the layer in vacuo at a temperature up to 300°C,

*or II.* 1) revaporizing the substance in vacuo,

2) heating the layer in an atmosphere of oxygen under the pressure of 0,01 mm Hg at a temperature up to 250°C,

3) heating the layer in vacuo up to 450°C during 2 minutes and rapidly cooling to room temperature,

*or III.* 1) revaporizing in vacuo,

2) action of oxygen under the pressure of mm Hg at room temperature,

3) heating in vacuo up to 300°C rapidly cooling to room temperature.

In all cases heating in vacuo was the last process. After cooling to room temperature and separating the cell from the vacuum system, the resistance of the layer increased and the photosensitivity grew in the course of some three weeks. After this time, the properties of the layers remained practically constant if the cell remained evacuated. This method of producing cells is sufficiently developed to let each activation result in obtaining a fairly sensitive cell. The results are reproducible in a sufficient degree. It seems, however, that the methods employed are not the best ones and that further improvements are possible.

## III. PROPERTIES OF THE PHOTOSENSITIVE LAYERS

The following electric properties of PbSe layers were tested:

1) Electric resistance at room temperature and at low temperatures.

2) Value and direction of the thermoelectric E.M.F. in various stages of the production.

3) Hall's constant.

Also the following quantities characterizing photoelectric properties were measured:

4) Relative sensitivity at room temperature and at low temperatures.

5) Total absolute reactivity.

6) Threshold sensitivity.
7) Spectral distribution of reactivity and its dependence on temperature.
8) The photoeffect relaxation period.

## 1. Resistance

The resistance of photosensitive microcrystalline PbSe layers at room temperature was from 10 to 300 k$\Omega$. Assuming with a large approximation that the mean thickness of the layer between the graphite electrodes is 1$\mu$ and that the surface area is 0,5 cm$^2$, we may estimate the specific resistance of a non-illuminated layer to be 2—60 $\Omega$ cm. The resistance at low temperatures was measured for 16 cells. The following table gives the resistances of cells at room temperature and at —130°C.

| No. of cell | Resistance at room temperature in k$\Omega$ | Resistance at — 130° in k$\Omega$ |
|---|---|---|
| 20 | 118 | 8300 |
| 21 | 100 | 1800 |
| 18 | 53 | 200 |
| 16 | 33 | 60 |
| 22 | 42 | 1000 |
| 23 | 15 | 600 |
| 24 | 12,5 | 14 |

On the whole, resistance of PbSe cells in darkness grows with lower temperatures. The experimental material was too sparse to establish on which factors these changes depend.

Resistance changes due to the lowering of the temperature of cell No. 30 are shown below. In a voltage range of 0—100 V the intensity of a current flowing

| Temperature in °C | Resistance in $k$ |
|---|---|
| 20 | 118 |
| —46 | 500 |
| —80 | 833 |
| —100 | 1430 |
| —120 | 4170 |
| —130 | 8300 |

through a layer is in accordance with Ohm's law. Higher voltage was not employed because of the risk of damaging the photosensitive layer.

## 2. Investigation of the thermoeffect in PbSe layers

The size and direction of the thermoelectric E.M.F. which appeared in the layer as a result of temperature differences was measured in order to elucidate the nature of the conductivity. The PbSe layer was in contact with the graphite

electrodes in the cell. If these contacts were kept at different temperatures a thermoelectric E.M.F. appeared in the circuit graphite — lead selenide — graphite. By attaching a sensitive millivoltmeter to tungsten electrodes which were in contact with the graphite ones, it was possible to measure the thermoelectric E.M.F. which appears in PbSe with respect to graphite. The thermoelectric E.M.F. of a semiconductor with respect to a metal (graphite in this connection may bet treated as a metal) depends mainly on the type and character of the semiconductor. If the cooler contact acquires a lower potential, we consider the sign of the thermoelectric E.M.F. as negative. Converesely, a higher potential of the cooler contact proves the direction of the thermoelectric E.M.F. to be positive.

Semiconductors of the hole type, i.e. those possessing an excess of positive electricity carriers, display a positive thermoelectric E.M.F. A negative thermoelectric E.M.F. is characteristic of a semiconductor of the excess, or electron, type of conductivity.

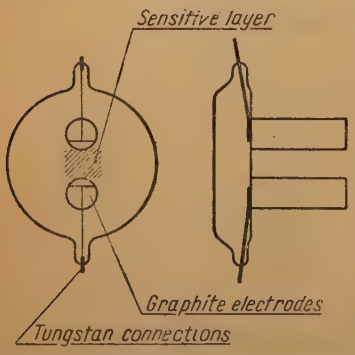


Fig. 7. Photocell for the examination of the thermoeffect

Cells of the type employed by Sosnowski (1949) (see Fig. 7) were used to measure changes of the thermoelectric E.M.F. On the flat far wall of such a cell two tubes are fused. In these tubes there were placed the outlets of blow-pipes. Compressed air introduced through one of these blowpipes was cooled or heated by a suitable bath of liquid air or of boiling water, in which the inlet tube was immersed. The current of air directed at the other electrode was kept at room temperature. The temperature difference of the two electrodes was measured by means of a thermoelement and a sensitive millivoltmeter.

The thermoeffect was investigated for several layers, which were subjected to various operations. The value and direction of the thermoelectric E.M.F. varied in a rather wide range from — 1 mV/°C through zero to 10 mV/°C. Layers which were not submitted to oxygen displayed a negative sign of the thermoelectric power. This indicates conductivity of the electron type, which proves the excess character of lead selenide used as basic material. After any oxidation process the layers displayed a positive sign of thermoelectric ability, which proves the presence of an excess of oxygen centres in the crystalline structure of PbSe and, consequently, of hole type conductivity. By heating the layer to 450°C in vacuo the direction of the thermoeffect is changed back to negative. A repetition of revaporizing, oxidation, and alternate heating in vacuo proved the repetitive character of the phenomenon.

Under the influence of gases diffusing from the freezer ($SeO_2$) the direction of the thermoelectric power changed from negative to positive. Layers with a negative thermoelectric ability were not photo sensitive, nor was photosensitivity observed in layers with zero thermoelectric ability.

### 3. Investigation of Hall's effect

If a conductor through which a current is flowing is placed in a strong magnetic field, the current carriers will be displaced, and an additional current appears which is perpendicularto the main current and to the magnetic field. This phenomenon is called the Hall effect. The E.M.F. value of Hall's current may be calculated from the formula

$$V = R\frac{iH}{d},$$

where $i$ is the current intensity, $H$ is the magnetic field intensity, $d$ is the thickness of the layer and $R$ is Hall's constant. This constant is characteristic of the given semiconductor and depends on the number, sign, and mobility of the current carriers. We may therefore estimate the value of these factors by calculations of Hall's constant. Type $p$ semiconductors show a positive value of the Hall effect, while type $n$ ones display a negative value. The value of Hall's constant is directly proportional to the thickness of the layer, while the conductivity is conversely proportional to the cross-section of the conductor, and therefore to the thickness of the layer. The product $R\sigma$ of Hall's constant multiplied by the conductivity is virtually independent of the thickness of the layer it is proportional to the mobility of the current carriers and plays a prominent role in practical applications of the experimental material.

Measurements of Hall's constant were effected by Sosnowski's method (1949). This constant could not be measured for finished, closed cells. The layers were prepared for measurements in the same way as photocells, but after their separation from the vacuum system the front wall had to be filed off, and this exposed the layer to the action of atmospheric oxygen. Hall's constant was measured for several layers prepared from stechiometric and excess material in various conditions. The following table gives the results for three layers, the first of which was prepared from stechiometric material and activated with oxygen, the second prepared from excess material and submitted only to the action of atmospheric oxygen after the cell has been opened, and the third, prepared from excess material revaporized in oxygen and subsequently heated in vacuo at a temperature of about 500°C.

| Layer No. | $R$ emu | $R\sigma$. $10^9$ | $\sigma\Omega^{-1}\text{cm}^{-1}$ | $n$ cm $^3$ | mobility $a$ cm $\text{sec}^{-1}/\text{Vcm}^{-1}$ |
|---|---|---|---|---|---|
| 1 | 2,5 | 3.75 | 1,5 | $2{,}9 \cdot 10^{19}$ | 0,32 |
| 2 | 1,5 | 16,85 | 11,3 | $4{,}9 \cdot 10^{19}$ | 1,4 |
| 3 | −1,02 | 12,24 | 12 | $7{,}2 \cdot 10^{19}$ | 1,04 |

The PbSe layers can have a positive as well as a negative value of Hall's constant. Those which were oxidized had a positive value. Those oxidized and subsequently heated in vacuo to 500°C had a negative value even after they had been exposed to the action of atmospheric oxygen when the cell was opened.

Estimations based on measurement of Hall's effect proved that the PbSe microcrystalline layers possess a large concentration of current carriers. The concentration is of an order of $10^{19}/cm^3$. The mobility of the current carriers calculated on the basis of these measurements is of an order of 1 cm $sec^{-1}/V\ cm^{-1}$. Hogarth's calculations (1951) of Hall's constant for PbSe monocrystals (of a current carrier concentration of the same order) led to higher mobility values by several orders of magnitude.

## 4. Relative photosensitivity

The relative change of conductivity under the influence of light of a definite intensity is called the *relative photosensitivity of a photocell.* For the purpose of comparing photosensitivity it is convenient to define it as the percentage change of intensity of the current, which flows through a layer, under the influence of a definite illumination:

$$S = \frac{i_2 - i_1}{i_1} 100,$$

where $i_1$ is the current intensity in a non-illuminated cell and $i_2$ is the current intensity in an illuminated cell in identical conditions. If the current intensity under the influence of light doubles, we say the cell has a sensitivity of 100%. The following table presents the sensitivities of several PbSe cells calculated in this way, compared with PbS cells of average sensitivity, under the influence of radiation of *0'05 W*/cm² intensity (an ordinary bulb).

| cell No. | Resistance of the non-illuminated cell in $k\ \Omega$ | Relative sensitivity % |
|---|---|---|
| PbSe 16 | 33 | 18 |
| PbSe 18 | 53 | 15 |
| PbSe 20 | 118 | 50 |
| PbSe 21 | 100 | 40 |
| PbSe 22 | 37 | 17 |
| PbSe 29 | 80 | 25 |
| PbSe 23 | 15 | 8 |
| PbS 5 | 50 | 100 |
| PbS 6 | 900 | 280 |

The sensitivity of PbSe cells increases with a decrease of temperature. Not all the layers showed this change in the same degree. The sensitivity at low temperatures was measured for 16 layers. This number was too small to permit a conclusion as to what factors determine, to a smaller or larger degree, the increase of photosensitivity at low temperatures.

The following table shows the sensitivity of several cells at room temperature and at — 130°C. The photoeffects were produced by the light of an ordinary bulb of about *0'05 W*/cm² intensity.

| Cell No. | Relative sensitivity at room temperature | (%) at − 130°C |
|---|---|---|
| PbSe 16 | 18 | 25 |
| PbSe 18 | 15 | 70 |
| PbSe 20 | 50 | 200 |
| PbSe 21 | 40 | 220 |
| PbSe 22 | 17 | 35 |
| PbSe 23 | 12 | 36 |
| PbSe 24 | 10 | 16 |
| PbSe 26 | 8 | 8 |

## 5. Measurements of global reactivity

Sensitive photocells should react even to very weak radiation. A valve amplifier was used to investigate the photoeffects caused by such radiation. The selective amplifier employed had a frequency of 735 cycles per second, band width of 20 cycles per second, and total amplification coefficient of 180000. Measurements were executed with the use of modulated illumination. A perforated rotating shield placed between the source of light and the cell served as modulator. For these measurements the cell was connected in series with a battery and a resistor $R$. The terminals of the resistor were connected with the clamps of the amplifier. Under the influence of light impulses, voltage impulses were generated, which could be expressed by the formula

$$\Delta V = \Delta i (R - R_c),$$

where $R$ is the resistance connected in series with the cell, $R_c$ is the resistance of the non-illuminated cell, and $i$ is the current intensity in the circuit. The change of current intensity $\Delta i$ depends on the change in the resistance of the cell under the influence of light and is proportional to the sensitivity of the photocell.

Impulses $\Delta i\, R$ of an order of $1 \mu V$ were directed to the clamps of the amplifier. These impulses, when amplified, were observed on the final voltmeter as signals of an order of several volts.

The ratio of the electric signal generated in the cell by radiation measured in $\mu V$, to the intensity of that radiation is called the *global reactivity*. Its unit is $\mu V / \mu W \mathrm{cm}^{-2}$.

As a standard radiation source a black body was used. From the chamber of this body there is emitted through the aperture a radiation, the energy of which may be calculated from the formula

$$d\Phi = A \cos \Theta \frac{d\Omega}{\pi} \sigma T^4 = A \cos \Theta \frac{S}{\pi R^2} \sigma T^4 \frac{\mathrm{cal}}{\mathrm{sec}},$$

where $T$ is the absolute temperature, $A$ is the aperture area, $d\Omega = \frac{S}{R^2}$ is the spheric angle in which the radiation band is propagated, $\sigma = 1{,}38 \cdot 10^{-12} \mathrm{cal\ sec}^{-1} \mathrm{cm}^{-2}$, $\Theta$ is the angle between the direction of the radiation band and the normal to the aperture plane. The intensity of the radiation band is proportional to $T^4$

and if the other conditions remain unchanged it is uniquely determined by this temperature. The energy of a radiation band from a standard source in the wave-length range from $\lambda_1$ to $\lambda_2$ was calculated according to Planck's formula

$$E = A \cos \Theta \frac{\Omega}{\pi} \int_{\lambda_1}^{\lambda_2} \frac{c_1 \lambda^5}{e^{c_2/\lambda T} - 1} d\lambda ,$$

where $T$ is the absolute temperature, $\Omega$ is the solid angle, and $c_1$, $c_2$ are the constants of Planck's equation.

The wave lengths $\lambda_1 = 0{,}5\,\mu$ and $\lambda_2 = 3{,}5\,\mu$ were taken as integration limits to calculate the global reactivity of the photocells. The measurements were effected with a black body at 200°C, of 3 mm aperture, placed at a distance of 10 cm from the photocell. The value of the amplified signal in volts was read on the voltmeter of the amplifier. The results are shown in the following table.

| Cell No. | Global reactivity in $\mu V/\mu W\,cm^{-2}$ | Global reactivity in $\mu V/\mu W\,cm^{-2}$ at 500 $\mu$A | Threshold sensitivity W $cm^{-2}$ |
|---|---|---|---|
| PbSe 20 | 84,4 | 76,5 | $14 \cdot 10^{-8}$ |
| PbSe 32 from the side of the thicker wall | 53,6 | 42,1 | $26{,}8 \cdot 10^{-8}$ |
| PbSe 32 from the side of the thinner wall | 61,6 | 47,5 | $22 \cdot 10^{-8}$ |
| PbSe 31 thin wall | 33,7 | 2,32 | $7{,}54 \cdot 10^{-8}$ |
| PbSe 33 thin wall | 56 | 128 | $5{,}5 \cdot 10^{-8}$ |

The reactivity depends on the intensity of the current flowing through the photosensitive layer. Values of the reactivity given in the first column are taken for equal voltages in the photocell circuits; in the second column the reactivity is given in respect to the same current intensity — 500 $\mu A$.

## 6. Measurements of the threshold of sensitivity

Measurements of the threshold of sensitivity are connected with measurements of the global reactivity. They were executed on the same apparatus for modulated radiation, emitted by a black body of a 3 mm aperture at 200°C with the help of a valve amplifier.

The lowest intensity of radiation energy expressed in $W/cm^2$, which is necessary to induce a noticeable electric signal in the photocell circuit, is called the *threshold of sensitivity of the cell.* The measurements of weak electric signals are limited by electric fluctuations existing in every circuit and caused by natural thermal oscillations — the so-called *shot effect.* The photoelectric cell, after a voltage has been applied, shows, even in the absence of radiation, fluctuations of this voltage which appear as a saw-line of light on an oscillograph or as constant small oscillations of the pointer of the exit voltmeter of the amplifier. The amplifier itself also causes shot noises. The mean value of these disturbances is called

the noise level. A radiation intensity for which the signal is equal to the noise level is called the *threshold sensitivity of the cell.*

The cell placed at a distance of 10 cm from the black body, just as in measuring the global reactivity, was gradually removed from the source of radiation and the diminishing signal was observed on the voltmeter. At a certain distance he magnitude of the signal is equal to the noise level. The number of microwatts

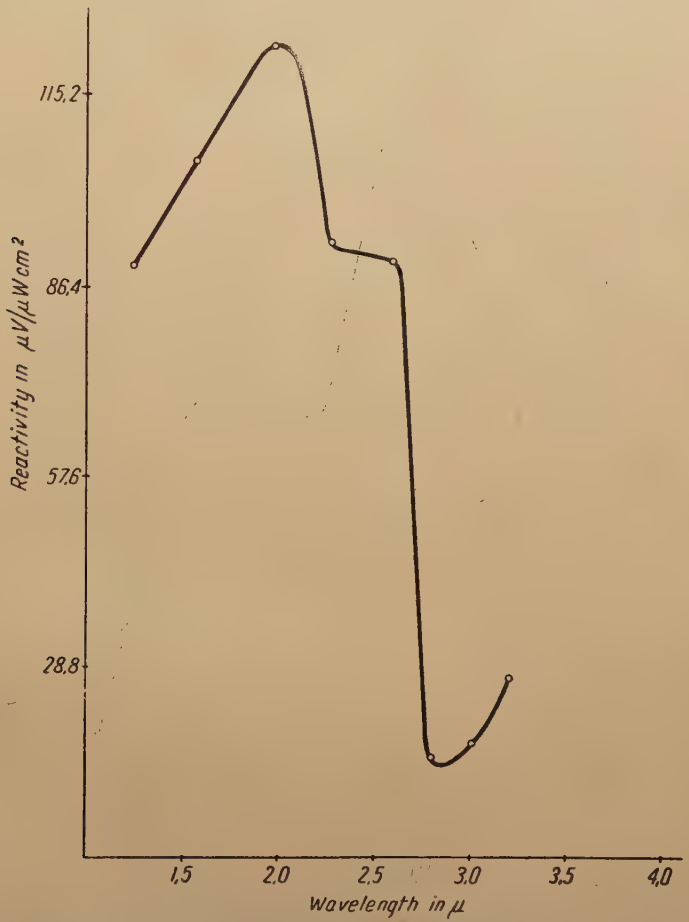


Fig. 8. Spectrum reactivity distribution of PbSe cell No. 20. "Globar" source of light, quartz optics

falling from this distance on 1 square cm of the photosensitive layer and calculated according to Planck's formula gives the value of the threshold of sensitivity for the cell. Thresholds for several cells are given in the table on page 212

## 7. Spectral distribution of reactivity

Neither the relative and the limiting sensitivity nor the global reactivity form a full picture of the photoelectric properties of cells, as their values depend upon the wave-length of the radiation which causes these effects. Only an exami-

nation of the spectral distribution of reactivity leads to a complete conception of the photoelectric properties. This distribution was investigated by means of a Kipp& Zonnen spectrophotometer. A quartz prism coupled with a so-called Wadsworth mirror were the main parts of this apparatus. The system prism — mirror permitted only those rays, which passed through the prism at an angle of lowest deflection, to enter the slit of a detector. The spectrophotometer was provided with reflection optics.

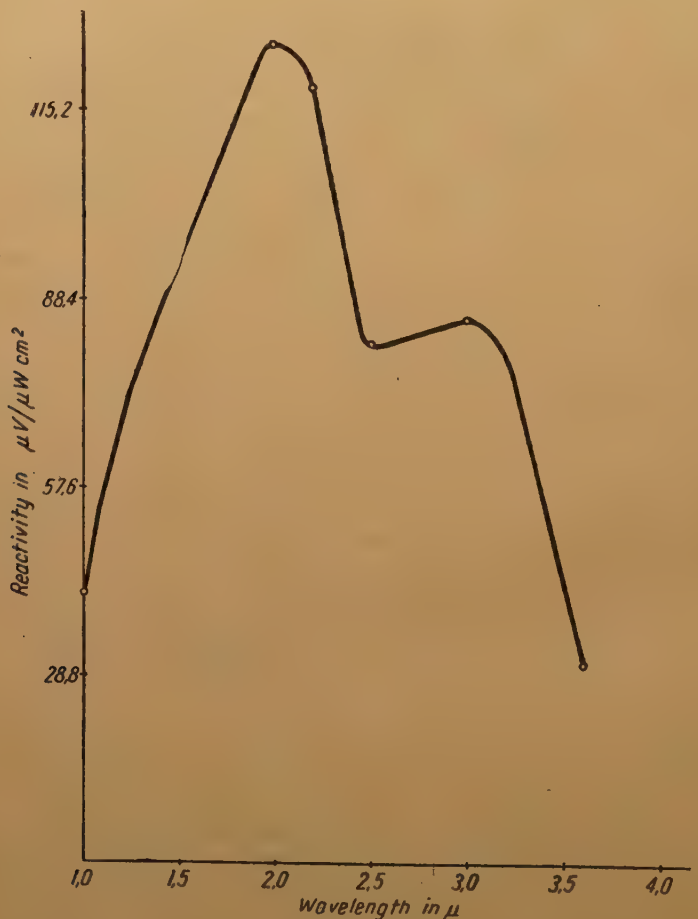


Fig. 9. Spectrum reactivity distribution of PbSe cell No. 20. "Globar" source of light, NaCl optics

Two detectors were used. The original Kipp&Zonnen one was composed of a thermocouple, a Moll-Burger type thermorelais and two galvanometers. Deflections of the galvanometer, which was coupled with the thermorelais, were observed by means of an appropriate scale. The deflections were proportional to the radiation passing through the entrance slit and falling on the thermocouple. The distribution of radiation intensity with respect to the wave-lengths $T(\lambda)$

was measured with the help of this detector. The photocell mounted in the place of the thermocouple, served as the second detector.

The radiation which entered the photocell was modulated, and the electric signal caused by impulses of light was amplified. The magnitude of the appearing signal $\Delta V$ depended both on the spectral distribution of the sensitivity of the photocells and on the radiation intensity distribution with respect to the wave-

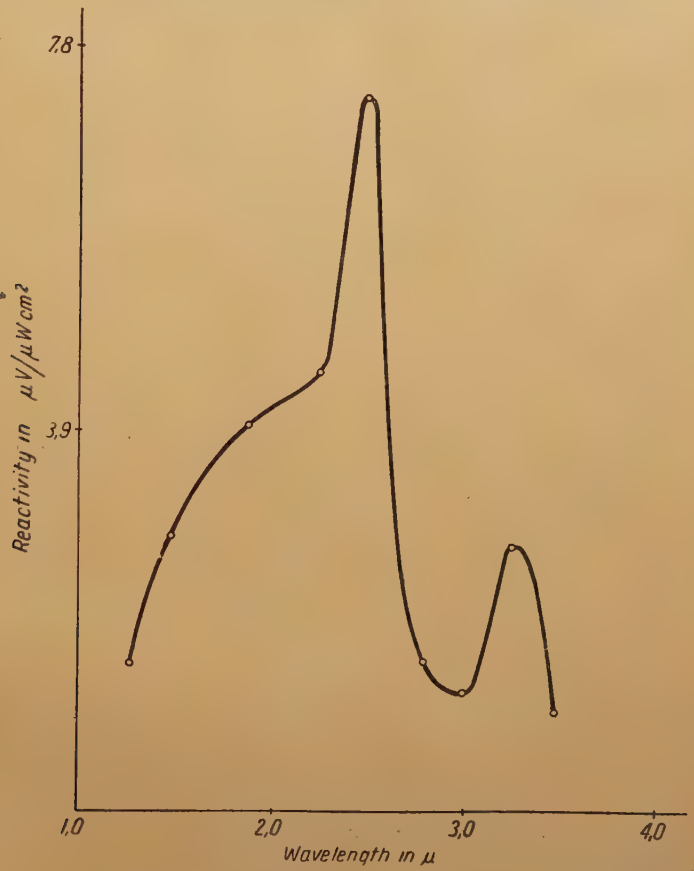


Fig. 10. Spectrum reactivity distribution of PbSe cell No. 32. "Globar" source of light, quartz optics

lengths $T(\lambda)$. The latter distribution was measured with the help of the Moll-Burger thermocouple. The dependence of the size of the signal on the wavelength $S(\lambda)$ was measured by using the photocell as a detector. The spectral distribution of the relative reactivity takes the form of the quotient

$$R_w(\lambda) = \frac{S(\lambda)}{T(\lambda)}.$$

The spectral distribution of relative reactivity $R_w(\lambda)$ differs, by a certain constant which must be calculated, from the distribution of absolute reactivity:

$$R_b(\lambda) = R_w(\lambda) \cdot C$$

To calculate this constant, measurements of global reactivity were executed with the help of a black body. If the signal at a certain temperature of the black body amounted to $K$, then

$$K = \int_{\lambda_1}^{\lambda_2} R_b(\lambda)\, I(\lambda)\, d\lambda = C \int_{\lambda_1}^{\lambda_2} R_w(\lambda)\, I(\lambda)\, d\lambda,$$

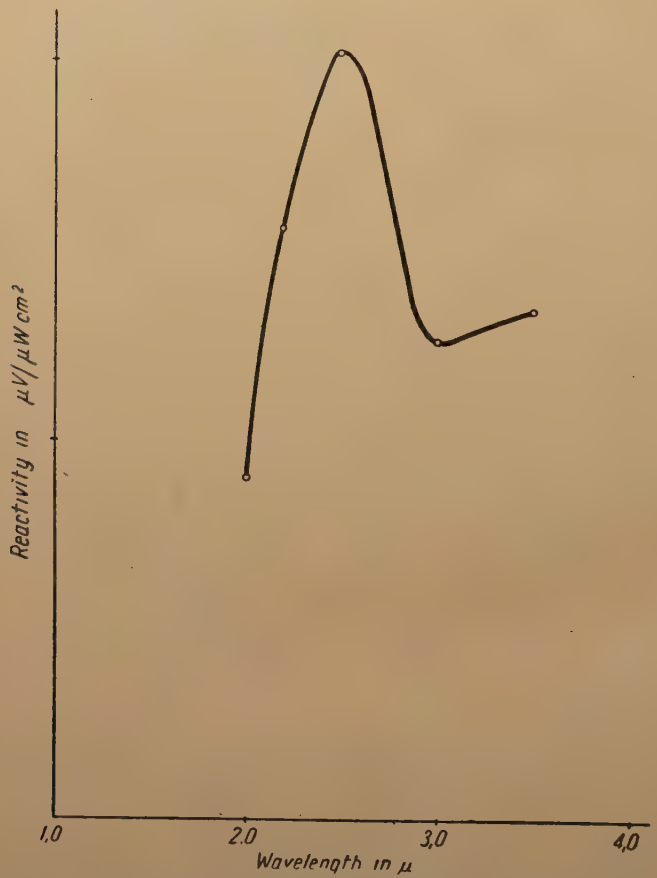


Fig. 11. Spectrum reactivity distribution of PbSe cell No. 32. "Globar" source of light, NaCl optics

Here $I(\lambda)$ is the spectral intensity distribution, and $\lambda_1$, $\lambda_2$ are the limits of the spectrum range. Hence

$$C = \frac{K}{\int_{\lambda_1}^{\lambda_2} R_w(\lambda)\, I(\lambda)\, d\lambda}.$$

The results obtained are represented on diagrams in Fig. 8, 9, 10 and 11. The wave-lengths in $\mu$ are plotted as abscissae and the absolute or relative reactivities as ordinates.

The spectral distribution was examined within the wave-length limits of $\lambda_1 = 0{,}5\,\mu$ and $\lambda_2 = 3{,}6\,\mu$. The resolving power of the method is characterized by the minimum width of the spectrum range which could be isolated. This range amounted to $0{,}05\,\mu$. The lowest reactivity at which measurements were still possible amounted to about $0{,}2\,\mu V/\mu W\,\mathrm{cm}^{-2}$.

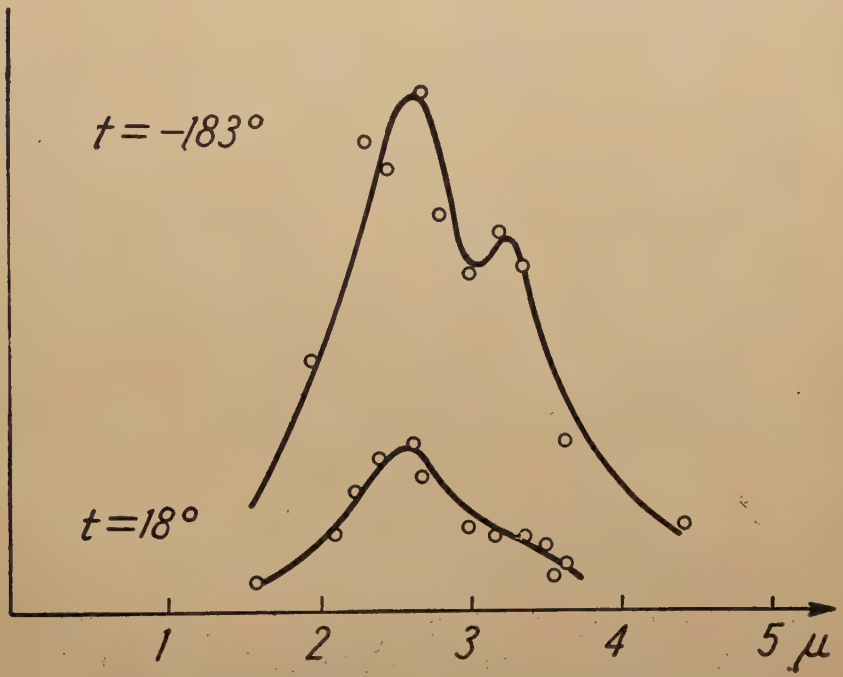


**Fig. 12. Spectral distribution of reactivities for photocell No. 32**

The influence of temperature on the spectrum distribution of reactivity. The cells were cooled to — 183° C and the spectrum distribution of reactivity was measured at various temperatures. As cooling proceeded the absolute values of reactivity increased for all the wavelengths within the limits of sensitivity. The character of the curve of spectral distribution of reactivity remains essentially the same. It seems that in the vicinity of $3\mu$ the reactivity at low temperatures increases relatively more than at other wave-lengths. This was noticed in several cells. The reactivity distribution curve at room temperature and at — 183° C for photocell No. 32 is shown in Fig. 12.

## 8. The photoeffect relaxation period

With the help of Sosnowski's method (1949) the photoeffect relaxation periods were investigated for several PbSe layers. PbSe photocells possess the short-

est relaxation periods as yet observed in semiconductors. The following table gives the results for three layers.

| cell No. | relaxation period in $\mu$ sec | resistance of the layer in $k\Omega$ | relative sensitivity |
|---|---|---|---|
| PbSe 21 | 1,1 | 100 | 40% |
| PbSe 18 | 0,3 | 15 | 18% |
| PbSe 23 | 0,2 | 25 | 12% |

## IV. PHOTOVOLTAIC CELLS

The appearance of an electromotive force in a semiconductor under the influence of radiation only is called the *internal photovoltaic effect*. The discovery of this effect (Sosnowski 1946, 1949) became one of the most important experimental foundations on which is based the new interpretation of photoelectric phenomena in semiconductors. A thorough discussion of this effect is given by Sosnowski (1949); it is based on the fact that a contact between two regions of the $n$ and $p$ type respectively becomes under the influence of light a source of an electromotive force. If in the formula for a current flowing through a contact (page 210), we put $V=0$ ,i.e. no external potential difference is applied, the formula takes the form

$$I_s = C_1 S_h + C_2 S_e \, e^{-\zeta/kT} \cdot I,$$

which means that under the influence of light an electron stream flows through the contact, and therefore an E.M.F. is generated. The magnitude of this force may be calculated by assuming $I_s = 0$:

$$V_0 = \frac{kT}{e} \log (1 + S_0 \cdot I),$$

where

$$S_0 = \frac{C_1 S_h + C_2 S_e}{C_1 + C_2}.$$

The photosensitive layer is a mosaic of $n$ and $p$ type microcrystals. Under the influence of light, their contacts become sources of electromotive forces. In a normal photosensitive layer these forces compensate each other since potential barriers on the contacts are distributed at random. If under the influence of an external factor (a photovoltaic activation process) the contacts are redistributed in an organized manner, the photovoltaic potential differences of several contacts add up and a macroscopic contact n-p appears; the layer becomes a photocell.

The photovoltaic process for photoconductive cells is effected by directing an electric current to flow through the layer at 250° C in vacuo. At this temperature oxygen centres which rule the $p$ type conductivity are mobile to such a degree

that under the influence of the electric field they may migrate and gather in the vicinity of one of the electrodes. If at a certain moment the process is interrupted and the cell is rapidly cooled to room temperature, this state will be "freezed" and a macroscopic barrier will appear between the region which is rich in oxygen centres and the *n* type region which does not contain them or contains very few.

Examination of the layers by means of a spotlight of 30$\mu$ diameter (Sosnowski 1949) proved that they are composed of a mosaic of *n* and *p* microcrystals. It was also proved that the flow of an activating current has an electrolitic character, and that the migration of oxygen centres does appear in reality. A region possessing an excess of oxygen centres, when subjected to illumination, acquires a positive potential.

## PbSe photovoltaic cells

The production of PbSe photovoltaic cells is similar to that of the photoconducting cells. A PbSe layer, prepared in the usual way, which possessed a certain photosensitivity was subjected to a certain additional photovoltaic activation. For this purpose an electric current of about 1 mA intensity was permitted to flow through the layer in vacuo at a temperature of about 250° C. During this process the conductivity of the layer initially increased, then decreased, reached a minimum and again increased. At this moment the cell was rapidly cooled down to room temperature. After cooling, the layer possessed photovoltaic properties. Heating the layer in vacuo with simultaneous observations of conductivity changes (a certain electromotive force is therefore applied) is, as a rule, the last operation during the production of photosensitive PbSe layers. This, therefore, served at the same time as a photovoltaic operation. Nearly all the photosensitive layers possessed at the same time photovoltaic properties.

The photovoltaic E.M.F. generated in PbSe cells under the influence of illumination with a bulb of radiation intensity 0,05 $W/cm^2$ are presented in the following table. For purposes of comparison data concerning two PbS cells produced in this Institute are included in the table. The photovoltaic E.M.F. of some layers increases at low temperatures. In the last column the E.M.F. of two cells at — 130° C are given.

| cell No. | Intensity of the photovoltaic current in $A \cdot 10^{-8}$ | Photovoltaic E.M.F. at room temp. in $mV$ | Photovoltaic E.M.F. at — 130°C in $mV$ |
|---|---|---|---|
| PbSe 18 | 15 | 7,5 | 33 |
| PbSe 21 | 15 | 4,6 | 22 |
| PbSe 23 | 12 | 1,8 | |
| PbSe 24 | 9 | 2,6 | |
| PbS Piw 5 | 30 | 60 | |
| PbS Piw 1 | 6 | 20 | |

## V. DISCUSSION OF RESULTS

### A. Interpretation of sensitization processess

The material used possessed initially a type *n* conductivity due to an excess of lead. This is proved by the negative sign of the thermoelectric power for unactivated layers. Activation took place through introducing oxygen into the crystalline structure. The presence of oxygen centres could be detected by means of measurements of the thermoelectric ability and of Hall's constant. It was sufficient for the formation of oxygen centres to submit the layer to the action ofoxygen under low pressure, even at room temperature. This seems to prove that a microcrystalline PbSe structure is an unusually fit medium for oxygen absorption. If oxygen was evacuated from the cell the sign of the thermoelectric E.M.F. did not change. This then was not a surface process, but oxygen diffused into the layer and was held fast. This is confirmed by Simpson (1947) who investigated the entering of oxygen into the cracks between crystals. Only a prolonged heating at 450° C (or at a higher temperature) in vacuo removes the oxygen centres and changes the sign of the thermoelectric ability and of Hall's constant back to negative.

The influence of oxygen on PbSe layers is the first considerable difference when their behaviour is compared with that of PbS layers. In the case of PbS the most important factor is an oxidizing operation at a temperature of 450° C. At this temperature there takes place in PbS a series of chemical reactions, which were examined and determined. By analogy similar operations were performed on PbSe. In the execution of the present research the chemical composition of the layers during the operations was not examined and it was impossible to determine what chemical reactions took place. By analogy to PbS it may be assumed hat the following reactions occured

$$2PbSe + 3O_2 = 2PbO + 2SeO_2$$

or

$$PbSe + 2O_2 = PbSeO_4.$$

As $SeO_2$ is the only selene oxide known in chemistry these reactions seem probable. $SeO_2$ was condensed in the freezer, lead selenate and lead oxide would remain in the structure forming a microcrystalline mosaic. After such operations, the layers possessed a positive sign of the thermoelectric E.M.F. and of Hall's constant, and this proves an excess of oxygen centres in the structure. Such operations did not lead to a considerable photosensitivity. This emphasizes the difference between the bevaviour of PbS and of PbSe. The decisive process for PbS of heating at high temperatures in the presence of oxygen is scarcely effective in the case of PbSe. The layers obtained were hardly sensitive to the action of oxygen, they possessed a relatively small resistance and a small photosensitivity.

The evacuation of oxygen and prolonged heating at 450° C (or at a higher temperature) in vacuo lead to a change of the direction of the thermoelectric ability and of Hall's constant from positive to negative, as a result of the removal of oxygen centres in the structure. Since the analogy with PbS ends with the

action of oxygen at higher temperatures, it is difficult to forsee what further chemical reactions take place when the layer is heated in vacuo. In the case of PbS the reduction in vacuo led to the formation of lead centres, which probably does not take place in PbSe. This might be the reason for the necessity of using a material containing an excess of lead, and therefore of lead centres, to obtain sensitive photocells.

After a prolonged heating at 450° C in vacuo the layers exhibited similar, but not identical, properties as the initial material. The sign of the thermoelectric E.M.F. and of Hall's constant changed to negative, the sensitivity to the action of oxygen at room temperatures was smaller; some of these layers did not change the sign of Hall's constant and of the thermoelectric E.M.F. back to positive under the influence of oxygen at room temperature, as is always the case with unactivated layers.

A greater sensitivity was obtained only after a short heating in vacuo at 450° C. This would agree with the $n-p$ contact interpretation. At 450° C the oxygen centres disappear. If the operation is performed rapidly, not all the microcrystals undergo changes; some of them obtain a $n$ type conductivity and some retain the $p$ type. A rapid cooling to room temperature "freezes" this state. As a result there form in the layer a number of contact barriers between $n$ and $p$ type regions.

The appearance of the internal photovoltaic effect also confirms the contact interpretation of photoconductivity phenomena in PbSe. Nearly all the photosensitive PbSe layers showed the photovoltaic effect to a larger or smaller degree.

The mobility of current carriers estimated on the basis of calculations of Hall's effect is lower by several orders of magnitude than in the case of monocrystals. This would also be in favour of the barrier interpretation.

## B. A comparison of PbSe and PbS layers

Relative sensitivities to the light of a usual bulb of the PbSe layers are at room temperatures about 10 times smaller than of PbS cells. The relative sensitivity to infrared radiation is somewhat smaller; it was measured during the illumination of the layer through a system consisting of 2 crossed polaroids eliminating the visible spectrum beginning with $0{,}8\mu$. In the case of PbSe cells this change is proportionaly smaller than in the case of PbS. Even this simple comparative measurement indicates that the sensitivity of PbSe lies mostly in the infrared part of the spectrum. The following table gives relative sensitivities of several PbSe and PbS cells to visible and infrared radiation.

| Cell No. | Sensitivity (%) to infrared and visible radiation of a usual bulb | Sensitivity (%) to infrared radiation only of the same bulb | Loss of sensitivity (%) |
|---|---|---|---|
| PbSe 20 | 50 | 42,7 | 14,6 |
| PbSe 21 | 40 | 77 | 18 |
| PbSe 26 | 8 | 7 | 12,5 |
| PbS 6 | 280 | 180 | 36 |

Since the layers are formed in duran glass containers the comparison of relative sensitivities of PbSe and PbS cells is conducted in conditions unfavourable for the former, as duran glass strongly absorbs radiation of about $3\mu$ wave-length.

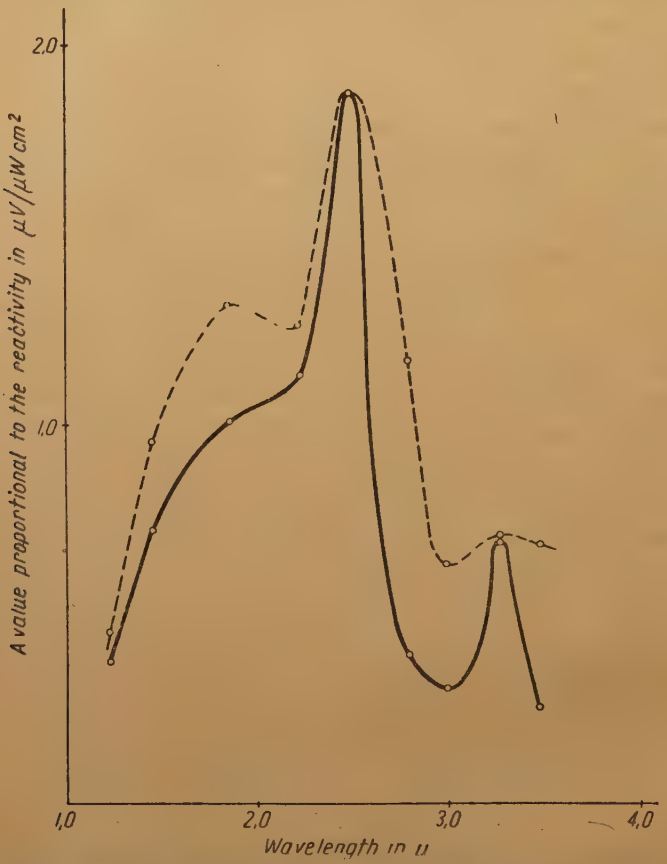


Fig. 13. Spectrum reactivity distribution of PbSe cell No. 32. "Globar" source of light, quartz optics. Full line — on the side of the thicker wall. Broken line — on the side of the thinner wall

The examination of the reactivity spectrum distribution of PbSe layer confirms this hypothesis. The PbSe layers exhibit a measurable reactivity even at a wave-length of $3{,}6\mu$. This is visible from the diagrams in Fig. 8, 9, 10 and 11. In the vicinity of $3\mu$ the curves possess a minimum due to the absorption in glass. A number of special cells were prepared to prove this. Their front walls were provided with thin-walled windows. The average thickness of the walls of normal cells ammounted to 1,4 mm. The windows were about 0,3 mm thick. The thin-walled cells were prepared by a method similar to the method of production of usuall cells.

The reactivity spectrum distribution for thin-walled and normal PbSe cells is represented on the diagrams in Fig. 13 and 14. The diagrams indicate the low-

ering of reactivity of the cells in the vicinity of $3\mu$ due to the absorption in glass.

Photosensitive PbSe layers are sensitive mainly to infrared radiation. If they are to be used as detectors in this range of the spectrum the methods of production should be modified in such a way as to eliminate the absorption in glass. This seems possible.

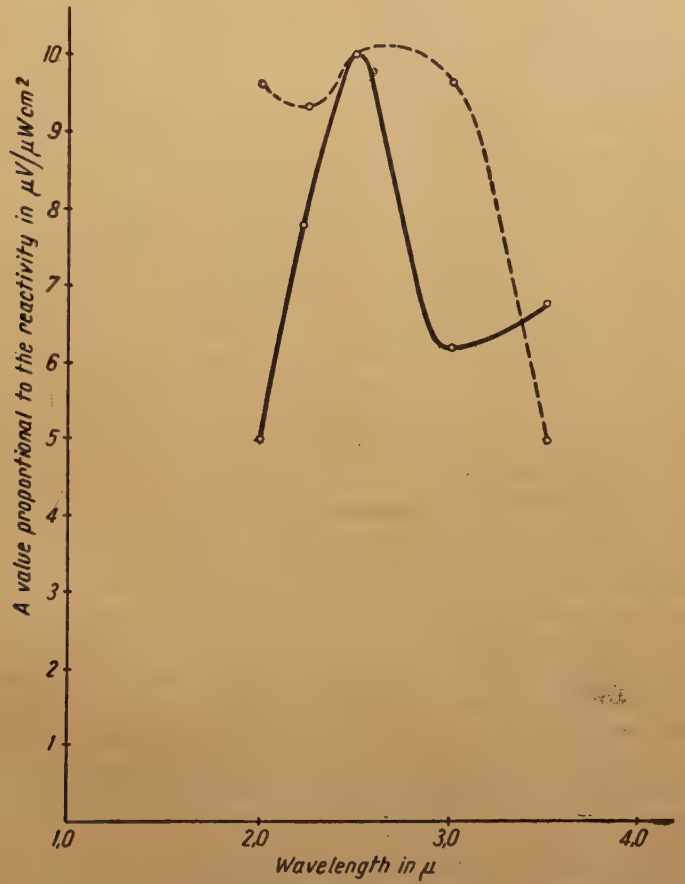


Fig. 14. Spectrum reacivity distribution of PbSe cell No. 32." Globar" source of light, NaCl optics. Full line — on the side of the thicker wall. Broken line — on the side of the thinner wall. A value proportionate to the reactivity in $\mu V/\mu W cm^{-2}$

I wish to thank Professor S. Pieńkowski for his permission to carry out this work in the Institute and for the kind interest he took during its preparation. It is a pleasure to express my sincere gratitude to Professor L. Sosnowski who suggested this investigation and guided the work through all its stages. Thanks are also due to my colleagues in the Institute of Physics of the Warsaw University, who have collaborated in various stages ot this work: Professor L. Sosnowski with Mr. M. Chmielewski, MPh., executed measurements of the photoeffect re-

laxation period; Dr T. Piwkowski helped the author with measurements of global reactivities, of threshold sensitivities, and of the reactivity spectrum distribution; Mr. J. Bogdanowicz MPh examined the effect of temperature on the reactivity spectrum distribution; Mr M. Kozłowski, MPh, measured Hall's constant.

## КРАТКОЕ СОДЕРЖАНИЕ

Г. Хенциньская, *Фотовольтаические и фотопроводимые слои из селенового свинца.*

Разработано метод активации тонких (около 1 μ) микрокристаллических слоев селенового свинца, проявляющих фотопроводимость и внутренний фотовольтаический эффект. Такие слои формировано выпариванием в вакууме селенового свинца, содержащего излишек свинца сверх стехиометрического отношения. С целью получения фоточувствительности подвергнуто препараты действию под низким давлением кислорода и восстановлению, вследствии грения в вакууме. Фотопроводимые слои подвергнутые действию электрического тока при температуре около 250° С в вакууме и быстро охлажденные до комнатной температуры, приобретали фотовольтаическую чувствительность. Метод выработки приводит к результатам повторяемым в достаточной степени, хотя дальнейшие улучшения представляются возможными.

Измерялась проводимость, фоточувствительность и термоэлектрическая способность разных фаз процесса получения чувствительности слоя. Проведено наблюдения над переменой проводимости типа „*n*" на „*p*" под влиянием кислорода и наоборот при восстановлении.

Общие черты слоев из селенового свинца напоминают хорошо известные свойства схожих слоев сернистового свинца; главной разницей являетя большая их чувствительность на влияние кислорода. Поведение слоев во время процессов, данные полученные после исследования явлений Галла и плотная связь между фотопроводимостью и фотовольтаическим явлением, соответствует барьерной теории, представленной Л. Сосновским.

Таким способом выработанные слои обладают чувствительностью на излучение в пределах от 05, μ до 3,6 μ. Порог чувствительности в комнатной температуре, т. е. малейшее значение энергии излучения, проявляющее видимые эффекты, равняется $10^{-8}$W/см$^2$ и возрастает при низких температурах.

## REFERENCES

**Blackwell D. and Simpson O.**, *Nature*, London, **160,** 793 (1947).
Chasmar R. *Nature* Lond., **161,** 281 (1948).
Gibson A., Lawson W., and Moss T., *Proc. Phys. Soc.*, London, **64,** 383 (1951).
Hogarth, *Proc. Phys. Soc.* London, **64,** 822 (1951).
Millner and Watts, *Nature*, London, **161,** 281 (1948).
Moss T. and Chasmar R., *Nature*, London, **161,** 244 (1948).
Simpson O. *Nature*, London, **160**, 791 (1947).
Sosnowski L., *Proc. Soc. Sci.*, Warsaw, (1949).
Starkiewicz J., *J. Opt. Soc. Amer.*, 481 (1948).
Starkiewicz J., Sosnowski L. and Simpson O., *Nature*, London, **158,** 28 (1946).
Starkiewicz J., Sosnowski L. and Simpson O., *Nature*, London, **159,** 818 (1947).

# EINE EINFACHE ABLEITUNG DES AUSDRUCKES FÜR DIE KIRCHHOFFSCHE BEUGUNGSWELLE

Von A. Rubinowicz

Staatliches Mathematisches Institut, Warszawa

*(Erhalten am 16. Februar 1953)*

Es wird eine sehr einfache Ableitung des Ausdruckes für die Kirchhoffsche Beugungswelle gegeben, die sich auf den Stokesschen Satz stützt, jedoch kein spezielles Koordinatensystem benutzt und die die Beugungswelle unmittelbar in der vom Verfasser (1917) angegebenen Gestalt liefert.

Die Wellenbewegung, die an der Schattenseite eines beugenden Schirmes den Beugungsvorgang beschreibt, wird nach Kirchhoff durch das Integral

$$u_K = \int_F V_n \, df \tag{1}$$

gegeben, wo $\vec{V}$ das Vektorfeld

$$\vec{V} = \frac{1}{4\pi}\left\{\frac{e^{ikr}}{r}\,\mathrm{grad}\,\frac{e^{ik\varrho}}{\varrho} - \frac{e^{ik\varrho}}{\varrho}\,\mathrm{grad}\,\frac{e^{ikr}}{r}\right\} \tag{2}$$

bedeutet. Hier bezeichnet $F$ eine die beugende Öffnung überspannende Fläche und $\vec{n}$ die Normale an $F$, die nach dem durch $F$ und den beugenden Schirm begrenzten, die Lichtquelle $L$ enthaltenden Halbraum hin gerichtet ist. $\varrho$ bzw. $r$ sind die Entfernungen eines Raumpunktes $Q$ von der Lichtquelle $L$ bzw. vom Beobachtungspunkte $P$.

G. A. Maggi (1888) hat zuerst gezeigt, dass man die durch (1) gegebene Wellenbewegung in zwei Teile aufspalten kann:

1) in eine direkt einfallende Welle $u_E$. Sie wird in allen Raumpunkten $P$, in denen nach der geometrischen Optik Licht vorhanden ist, durch die Funktion $e^{ikR}/R$ $(R = LP)$ gegeben, welche die unbehinderte Ausbreitung des Lichtes beschreibt.

2) in eine von den einzelnen Punkten des Schirmrandes $B$ ausgehende Beugungswelle

$$u_B = \frac{1}{4\pi a}\int_B e^{ik2\zeta}\,\frac{a^2 - \vartheta^2}{\zeta^2 - \vartheta^2}\,d\omega. \tag{3}$$

Dabei bedeuten:

$$\zeta = \frac{r+\varrho}{2}, \quad \vartheta = \frac{r-\varrho}{2},$$

$2a = R$ die Entfernung des Beobachtungspunktes $P$ von der Lichtquelle $L$ und $\omega$ den Winkel, den eine durch die beiden Punkte $L$ und $P$ hindurchgehende Halb-

ebene $E$ mit einer festen durch eben diese Punkte gehenden Halbebene bildet. Die Integration ist hier über einen Bereich der Veränderlichen $\omega$ zu erstrecken, der einem ganzen Umlauf längs des beugenden Randes entspricht.

Maggi hat seine Formel (3) mit Hilfe des Stokesschen Satzes unter Verwendung der rotationssymmetrischen elliptischen Koordinaten $\zeta, \vartheta, \omega$ abgeleitet.

Der Verfasser (1917) der vorliegenden Note hat durch eine direkte Umformung des Kirchhoffschen Ausdruckes (1), aber ohne Benutzung spezieller Koordinaten, die Beugungswelle in einer Gestalt angegeben, die vektoriell in der Form

$$u_B = -\frac{1}{4\pi}\int_B \frac{e^{ik(r+\varrho)}}{r\varrho}\,\frac{(\vec{r}\times\vec{\varrho})\,\vec{ds}}{r\varrho + \vec{r}\,\vec{\varrho}} \tag{4}$$

geschrieben werden kann. Hier ist $\vec{ds}$ ein Linienelement des beugenden Randes $B$. Die Vektoren $\vec{r}$ und $\vec{\varrho}$ werden durch $\vec{r} = \vec{P}ds$ und $\vec{\varrho} = \vec{L}ds$ gegeben.

Der Ausdruck (4) lässt sich auch aus der Formel von Maggi (3) durch eine geometrische Umformung gewinnen.

Vom physikalischen Standpunkt ist der Ausdruck (4) für die Beugungswelle $u_B$ insofern vorzuziehen als er die Rolle des beugenden Randes $B$ in unmittelbare Evidenz setzt und daher ohne weiteres vom Standpunkt der Youngschen Anschauungen über das Zustandekommen der Beugungserscheinungen gedeutet werden kann. Der in der Formel von Maggi (3) auftretende Winkel $\omega$ ist dagegen physikalisch vollkommen uninteressant. Bei allen bisher bekannt gewordenen Anwendungen[1] wurde die Beugungswelle in der Gestalt (4) verwendet.

Ähnlich wie Maggi hat Kottler (1923) mit Hilfe des Stokesschen Satzes, nur unter Benutzung anderer rotationssymmetrischer elliptischer Koordinaten, den Kirchhoffschen Ausdruck (1) in die direkt einfallende und die Beugungswelle aufgespaltet. Er erhielt dabei für die Beugungswelle einen der Formel von Maggi (3) äquivalenten Ausdruck, den er dann durch Umrechnung auf die Gestallt (4) transformierte.

Keine der bisher angegebenen Ableitungen kann als einfach bezeichnet werden. Der Weg über den Stokesschen Satz erfordert bei Benutzung rotationssymmetrischer elliptischer Koordinaten längere Rechnungen, wie z.B. die ausführliche Darstellung bei Baker und Copson (1939 oder 1950) zeigt. Der vom Verfasser (1917) angegebene Weg (vgl. auch die Darstellungen bei Försterling, 1928, und bei Sommerfeld, 1950) ist zwar kürzer, führt aber über geometriche Betrachtungen.

Die vorliegende Note hat daher den Zweck zu zeigen, dass man auf einem sehr kurzen Weg und zwar unter Verwendung des Stokesschen Satzes aber ohne Benutzung irgend eines speziellen Koordinatensystems den Ausdruck (4) für die Beugungswelle ganz einfach ableiten kann.

Wir gehen von der Bemerkung aus, dass das Vektorfeld $V$, (2), mit Rücksicht darauf, dass $e^{ikr}/r$ sowie $e^{ik\varrho}/\varrho$ der Wellengleichung $\Delta u + k^2 u = 0$ genügen, als

[1] Vgl. z.B. Baker-Copson (1939 und 1950), Bouwkamp (1940), Franz (1949), Höller (1952), Kottler (1923), Martin (1943 und 1949), Mc Donald-Harris (1952), Rubinowicz (1917, 1924 und 1938).

Funktion des Punktes $Q$ quellenfrei ist. Es muss daher durch ein Vektorpotential $\vec{W}$:

$$\vec{V} = \text{rot}\, \vec{W} \tag{5}$$

darstellbar sein. Um für dieses Vektorpotential $\vec{W}$ einen plausiblen Ansatz zu finden, bemerken wir, dass das Vektorfeld $\vec{V}$ mit Rücksicht auf grad $r = \vec{r}/r$ und grad $\varrho = \vec{\varrho}/\varrho$ in der Gestalt

$$\vec{V} = \frac{e^{ik(r+\varrho)}}{4\pi r\varrho}\left\{\left(\frac{ik}{\varrho} - \frac{1}{\varrho^2}\right)\vec{\varrho} - \left(\frac{ik}{r} - \frac{1}{r^2}\right)\vec{r}\right\} \tag{6}$$

geschrieben werden kann und daher die Vektoren $\vec{V}$ des Feldes (6) stets in einer durch den Lichtpunkt $L$ und den Beobachtungspunkt $P$ hindurchgehenden Halbebene $E$ liegen. Um nun sicherzustellen, dass $\vec{V}$ keine Komponente senkrecht zu der Halbebene $E$ besitzt, nehmen wir an, dass die Komponenten von $\vec{W}$ in dieser Halbebene verschwinden und daher der Vektor $\vec{W}$ stets senkrecht auf der durch den betreffenden Raumpunkt $Q$ hindurchgehenden Halbebene $E$ steht. Das Vektorpotential $\vec{W}$ setzen wir somit in der Gestalt

$$\vec{W} = \vec{r} \times \vec{\varrho}\, g \tag{7}$$

voraus, wo $g$ eine skalare Funktion ist.

Mit Rücksicht auf rot $(\vec{r} \times \vec{\varrho}) = 2(\vec{r} - \vec{\varrho})$ folgt dann aus (5) und (7) für das Vektorfeld $\vec{V}$ der Ausdruck

$$\vec{V} = g\,\text{rot}\,(\vec{r} \times \vec{\varrho}) + \text{grad}\, g \times (\vec{r} \times \vec{\varrho})$$
$$= 2(\vec{r} - \vec{\varrho})g + \vec{r}(\vec{\varrho}\,\text{grad}\, g) - \vec{\varrho}(\vec{r}\,\text{grad}\, g).$$

Beachten wir dass

$$2g + \vec{r}\,\text{grad}\, g = \frac{1}{r^2}\vec{r}\,\text{grad}\,(r^2 g)$$

und dass eine analoge Gleichung mit $\vec{\varrho}$ und $\varrho$ statt $\vec{r}$ und $r$ besteht, so wird

$$\vec{V} = \vec{r}\,\frac{1}{\varrho^2}[\vec{\varrho}\,\text{grad}\,(\varrho^2 g)] + \vec{\varrho}\,\frac{1}{r^2}[\vec{r}\,\text{grad}\,(r^2 g)]. \tag{8}$$

Werden die beiden Ausdrücke für $\vec{V}$, (6) und (8), einander gleichgesetzt und die erhaltene Beziehung vektoriell mit $\vec{r}$ bzw. $\vec{\varrho}$ multipliziert, so ergeben sich schliesslich für die Funktion $g$ die beiden Differentialgleichungen:

$$-\frac{e^{ik(r+\varrho)}}{4\pi}\frac{r}{\varrho}\left(\frac{ik}{\varrho} - \frac{1}{\varrho^2}\right) = \vec{r}\,\text{grad}\,(r^2 g), \tag{9a}$$

$$-\frac{e^{ik(r+\varrho)}}{4\pi}\frac{\varrho}{r}\left(\frac{ik}{r} - \frac{1}{r^2}\right) = \vec{\varrho}\,\text{grad}\,(\varrho^2 g). \tag{9b}$$

Um zunächst eine Lösung der Differentialgleichung (9a) zu finden, spalten wir von der Funktion $g$ den Exponentialfaktor $\exp ik(r+\varrho)$ ab, setzen also

$$r^2 g = e^{ik(r+\varrho)} f. \tag{10}$$

Ein solcher Ansatz für die Funktion $g$ wird durch die Tatsache nahegelegt, dass der Faktor $\exp ik(r+\varrho)$ bei allen Differentiationen von (10) erhalten bleibt und daher auch in dem Ausdruck $\vec{r}\,\mathrm{grad}\,(r^2 g)$ auftreten wird, wie dies die linke Seite der Differentialgleichung (9a) verlangt.

Mit Rücksicht auf

$$\vec{r}\,\mathrm{grad}\,(r+\varrho) = \frac{1}{\varrho}\,[r\varrho + \vec{r}\vec{\varrho}]$$

sowie die Gl. (10) erhalten wir dann die Beziehung

$$\vec{r}\,\mathrm{grad}\,(r^2 g) = \vec{r}\,\mathrm{grad}\,(e^{ik(r+\varrho)} f) = ik\,\frac{1}{\varrho}\,[r\varrho + \vec{r}\vec{\varrho}]\,e^{ik(r+\varrho)} f + e^{ik(r+\varrho)}\,\vec{r}\,\mathrm{grad}\,f.$$

Die Tatsache, dass in der Differentialgleichung (9a) die Konstante $k$ ausser in $\exp ik(r+\varrho)$ sonst nur einmal und zwar als ein Faktor in der ersten Potenz auftritt, legt die Annahme nahe, dass die Funktion $f$ die Konstante $k$ nicht mehr enthält. Der Vergleich des letzten Ausdruckes für $\vec{r}\,\mathrm{grad}\,(r^2 g)$ mit der Differentialgleichung (9a) ergibt dann zwangsläufig

$$f = -\frac{1}{4\pi}\,\frac{r}{\varrho}\,\frac{1}{[r\varrho + \vec{r}\vec{\varrho}]}, \tag{11a}$$

$$\vec{r}\,\mathrm{grad}\,f = \frac{1}{4\pi}\,\frac{r}{\varrho^3}. \tag{11b}$$

Dass die durch (11a) definierte Funktion $f$ der Differentialgleichung (11b) genügt ergibt sich daraus, dass mit Rücksicht auf $\mathrm{grad}\,\vec{r}\vec{\varrho} = \vec{r} + \vec{\varrho}$ die Beziehung

$$\vec{r}\,\mathrm{grad}\,\frac{\varrho}{r}\,[r\varrho + \vec{r}\vec{\varrho}] = \frac{1}{r\varrho}\,[r\varrho + \vec{r}\vec{\varrho}]^2$$

besteht.

Aus (10) und (11a) folgt aber, dass die Differentialgleichung (9a) mit

$$g = -\frac{1}{4\pi}\,\frac{e^{ik(r+\varrho)}}{r\varrho\,[r\varrho + \vec{r}\vec{\varrho}]} \tag{12}$$

vereinbar ist.

Da die Differentialgleichungen (9a) und (9b) bei Vertauschung von $\vec{r}$ und $\vec{\varrho}$ sowie $r$ und $\varrho$ in einander übergehen und der Ausdruck (12) für $g$ in diesen Grössen symmetrisch ist, so erfüllt er auch die Differentialgleichung (9b). Die Funktion $g$, (12), ist somit eine Lösung der beiden Differentialgleichungen (9a) und (9b).

Aus (1), (5), (7) und (12) folgt mit Hilfe des Stokesschen Satzes für die Beugungswelle $u_B$ schliesslich der Ausdruck (4).

Bezüglich des Auftretens der direkt einfallenden Welle $u_E$ ist folgendes zu bemerken: Bezeichnen wir mit $\alpha$ den Winkel zwischen $\vec{r}$ und $\vec{\varrho}$, so wird

$$\frac{|\vec{r} \times \vec{\varrho}|}{r\varrho + \vec{r}\vec{\varrho}} = \frac{\sin \alpha}{1 + \cos \alpha} = \operatorname{tg} \frac{\alpha}{2} .$$

Dieser Ausdruck wird auf der Verbindungslinie $LP$ unendlich, da ja hier $\alpha = \pi$ wird. Hat daher diese Verbindungslinie mit der Fläche $F$ einen Durchstosspunkt $Q_0$ gemeinsam, so muss man diesen Punkt $Q_0$ bei der Anwendung des Stokesschen Satzes durch eine ihn umschliessende Kurve $K$ aus der Fläche $F$ ausschneiden. Man kann aber das Ausrechnen des über $K$ erstreckten Integrales vermeiden, wenn man die Fläche $F$ bei Vorhandensein eines Durchstosspunktes $Q_0$ über den Beobachtungspunkt $P$ hinwegzieht (vgl. Baker-Copson, 1939, S. 75). Dadurch entfällt der Durchstosspunkt, so dass der Stokessche Satz nun auf die ganze deformierte Fläche $F$ angewandt werden kann. Bei diesem Hinüberziehen der Fläche $F$ über den Beobachtungspunkt $P$ hinweg, erscheint aber gleichzeitig die einfallende Welle $u_E$.

## КРАТКОЕ СОДЕРЖАНИЕ

А. Рубинович. *Простой вывод формулы на диффракционную волну в теории Кирхгоффа.*

В настоящей работе очень простым способом выведено выражение на диффракционную волну, выступающую в теории диффракции Кирхгоффа, при чём эта волна получается непосредственно в форме данной впервые автором (1917). Это доказательство основано на теореме Стокса, хотя в нём не употребляются никакие специального рода координаты.

## LITERATURHINWEISE

Baker B. B. and Copson E. T., *The Mathematical Theory of Huygens' Principle,* Oxford 1939 und 1950 (erste bzw. zweite Auflage).

Bouwkamp C. J., *Physica* **7**, 485 (1940).

Försterling K., *Lehrbuch der Optik,* Leipzig 1928.

Franz W., *ZS. Phys.* **125**, 563 (1949).

Höller P., *ZS. f. angew. Phys.* **3**, 424 (1952).

Kottler F., *Ann. d. Phys.* **70**, 405 (1923).

Maggi G. A., *Ann. di Matem.* (2), **16**, 21 (1888).

Martin L. C., *Proc. Phys. Soc.* **55**, 104 (1943); ebenda *Sec.* B, **62**, 713 (1949).

McDonald K. L. and Harris F. S. Jr., *Journ. of Opt. Soc. of America,* **42**, 321 (1952).

Rubinowicz A., *Ann. d. Phys.* **53**, 257 (1917); ebenda **73**, 339 (1924); *Phys. Rev.* **54**, 931 (1938).

Sommerfeld A., *Vorlesungen über theoretische Physik,* Bd. IV, *Optik,* Wiesbaden 1950.

# EINDEUTIGKEITSBEWEISE FÜR EINIGE HYPERBOLISCHE DIFFERENTIALGLEICHUNGEN DER THEORETISCHEN PHYSIK

VON J. PLEBAŃSKI

Institut für Theoretische Physik an der Universität Warschau

*(Erhalten am 19. Februar 1953)*

Ausgehend vom Grundgedanken des Rubinowiczschen Eindeutigkeitsbeweises für Maxwellsche Gleichungen, wird ein Hilfsatz bewiesen, der sehr einfach Eindeutigkeitsbeweise für viele lineare hyperbolische Differentialgleichungen der theoretischen Physki durchzuführen gestattet.

Der Hilfsatz lautet: $I^\nu$ sei ein Vektorfeld für welches $I^0 \geqslant 0$, $I^\nu I^\nu \geqslant 0$, $I^\nu_{,\nu} \leqslant 0$ angenommen wird. Wenn $I^\nu$ in einem endlichen dreidimensionalen raumartigen Gebiete $R$ verschwindet, so verschwindet es auch in dem dreidimensionalen raumartigen Gebiete $R'$, wobei $R'$ in der nachstehenden Weise definiert ist. $R'$ ist der Schnitt einer beliebigen raumartigen Fläche $\sigma'$ (die oberhalb $R$ verläuft) mit dem vierdimensionalen Gebiete, das durch die Lichtkegeln begrenzt wird, deren Spitzen sich auf der Begrenzung von $R$ befinden.

Besonders einfach können wir unseren Hilfsatz bei den Eindeutigkeitsbeweisen für die Maxwellschen, Procaschen und Diracschen Gleichungen zur Anwendung bringen.

1. Einführung. Der von Rubinowicz (1926) angegebene Beweis für die Eindeutigkeit der Lösung der Maxwellschen Gleichungen ist vom physikalischen Standpunkt besonders befriedigend, da er die endliche Ausbreitungsgeschwindigkeit des Lichtes zum Ausdruck bringt. Durch eine Integration der Differentialgleichung des Energieerhaltungssatzes über ein entsprechendes vierdimensionales Gebiet war es möglich den Eindeutigkeitsbeweis einfach durchzuführen.

Friedrichs und Lewy (1927) haben das Eindeutigkeitsproblem für einige allgemeinere hyperbolische Differentialgleichungen untersucht, wobei sie aber die Anfangsbedingungen auf beliebigen raumartigen Hyperflächen vorgegeben haben. Ihre allgemeinen Resultate kann man aber nicht einfach und einheitlich auf die verschiedenen in der Physik vorkommenden Differentialgleichungen anwenden.

In dieser kurzen Mitteilung wollen wir anschliessend an die Grundgedanken des Beweises von Rubinowicz einen Hilfsatz aufstellen, aus dem sehr einfach die Eindeutigkeitsbeweise für die verschiedenen Differentialgleichungen der Physik folgen. Dabei werden differentielle Erhaltungssätze angewandt, welche bei verschiedenen physikalischen Feldern aus den Feldgleichungen sich ergeben. Besonders einfach ist, wie es weiter gezeigt wird, die Benutzung unseres Hilfsatzes im

Falle der Maxwellschen, Procaschen und Diracschen Gleichungen. Die Anfangsbedingungen werden wir dabei auf beliebigen raumartigen Flächen vorgeben.

2. Hilfsatz. Wir bezeichnen mit $x^\nu$ die Koordinaten der Punkte des 4-dimensionales Raumes[1], mit $ds^2 = g_{\alpha\beta}dx^\alpha dx^\beta$, wo $g_{00} > 0$, $g_{0k} = 0$, $g_{kl} = -a_{kl}$. Die quadratische Form $a_{kl}y^k y^l$ wird als positiv definit vorausgezetzt. Im allgemeinen können die $g_{\alpha\beta}$ Funktionen der Koordinaten $x^\nu$ sein.

Wir wollen nun an die geometrische Konstruktion des in unseren Beweisen benutzten Abhängigkeitsgebietes herantreten. Auf einer 3-dimensionalen raumartigen Fläche $\sigma$ (d.h. mit einer zeitartigen Normale $n^\nu$: $n^\nu n_\nu > 0$) ziehen wir ein endliches Gebiet $R$ in Betracht, das von der 2-dimensionalen Fläche $F$ begrenzt wird. Wir nehmen an, dass durch jeden Punkt $x^\nu \in F$ die Spitze eines Lichtkegels hindurchgeht, der aus allen durch $x^\nu$ hindurchgehenden geodätischen Nullinien besteht (vgl. Fig. 1.).

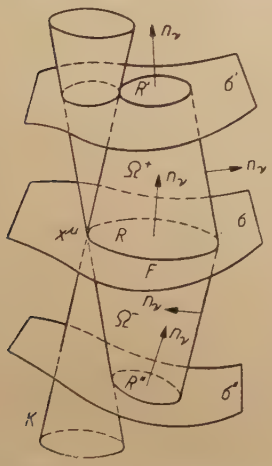


Fig. 1. Schema der Hyperflächen in der 4-dimensionalen Raumzeitwelt ($K$ = Kegel mit Spitze im Punkte $x^\mu$ von $F$)

Mit $\Omega_0^+$ bezeichnen wir das Gebiet, das aus allen jenen oberhalb $\sigma$ gelegenen Punkten besteht, welche mit einem inneren Punkte von $R$ durch eine solche stetige Kurve verbunden werden können, die keinen Punkt mit den oben angegebenen Lichtkegeln gemeinsam hat.

Die aus den geodätischen Nullinien gebildete Fläche, welche gemeinsam mit $R$ das vierdimensionale Gebiet $\Omega_0^+$ begrenzt, bezeichnen wir mit $T_0^+$. Die Normale $n_\nu$ der Fläche $T_0^+$ ist ein Nullvektor: $n_\nu n^\nu = 0$.

Wir schneiden jetzt $\Omega_0^+$ durch eine neue oberhalb $\sigma$ gelegene raumartige Fläche $\sigma'$ und bezeichnen ihren mit $\Omega_0^+$ gemeinsamen Teil mit $R'$; $\sigma'$ soll so nahe an $\sigma$ geführt werden, dass das Gebiet $R'$ dreidimensional wird. Den durch $R$, $R'$ und den entsprechenden Teil von $T_0^+$ (er heisse $T^+$) begrentzten Teil von $\Omega_0^+$ bezeichnen wir mit $\Omega^+$.

Die Normalen auf $R$ und $R'$ sollen mit der positiven $x^0$ Richtung spitze Winkel bilden; wir haben hier also $n_0 > 0$. Auf der Fläche $T^+$ wählen wir die Normale als äussere Normale, so dass $n_0$ positiv ist.

Ganz ähnlich werden wir jetzt das Gebiet $\Omega_0^-$ definieren. Es wird durch die Flächen $T_0^-$ und $R$ begrenzt und besteht aus allen unterhalb $\sigma$ liegenden Punkten, welche durch stetige Linien, die keine gemeinsamen Punkte mit den Lichtkegeln haben, mit inneren Punkten von $R$ verbunden werden können (vgl. Fig. 1).

Den gemeinsamen Teil von $\Omega_0^-$ mit der unterhalb der Fläche $\sigma$ liegenden Fläche $\sigma''$ bezeichnen wir mit $R''$. Mit $\Omega^-$ bezeichnen wir das Teilgebiet von $\Omega_0^-$

[1] Wir werden die Bezeichnungen der Relativitätstheorie benutzen: lateinische Buchstaben für 1, 2, 3, griechische für 0, 1, 2, 3; über zwei gleiche Indizes wird summiert. $\alpha_{,\nu}$ bedeutet die Ableitung $\partial\alpha/\partial x^\nu$.

das durch $R, R''$ und den entsprechenden Teil $T^-$ von $T_0^-$ begrenzt wird. Die Normale auf $R'$ bildet mit $x^0$ wieder einen spitzen Winkel, so dass $n_0 > 0$. Auch auf der Fläche $T^-$ wählen wir die Normale so dass $n_0 > 0$ ist, d. h. als innere Normale. Auf $T^-$ wird die Normale selbstverständlich durch einen Nullvektor gegeben: $n^\nu n_\nu = 0$.

Wir behaupten nun: wenn $I^\nu$ ein Vektorfeld ist, für das die beiden folgenden Annahmen gelten

$$I^0 \geqslant 0 \qquad (1), \qquad I^\nu I_\nu \geqslant 0, \qquad (2)$$

so ist $\lambda = I^\nu n_\nu$ auf den Flächen $R, R', R''$ und $T^+$ sowie $T^-$ sind positiv.

Auf den Flächen $R, R', R''$ ist

$$n_0 > 0 \qquad (3), \qquad n^\nu n_\nu > 0 \qquad (4)$$

und wegen $I_0 = g_{00} I^0$ kann man $\lambda$ auch in der Gestalt $\lambda = \dfrac{(n_0 I_0 - g_{00} a_{kl} I^k n^l)}{g_{00}}$ schreiben. Aus (1), (2) und (3), (4) folgt dann

$$I_0 \geqslant \sqrt{g_{00} a_{kl} I^k I^l} \qquad (5), \qquad n_0 > \sqrt{g_{00} a_{kl} n^k n^l}, \qquad (6)$$

während aus $a_{kl} y^k y^l \geqslant 0$ sich für beliebige $y^k$

$$\sqrt{g_{00} a_{kl} I^k I^l} \cdot \sqrt{g_{00} a_{nm} n^n n^m} \geqslant |g_{00} a_{kl} I^k n^l| \qquad (7)$$

ergibt[2]. Es wird dann

$$\lambda \geqslant \frac{1}{g_{00}} (n_0 I_0 - |g_{00} a_{kl} I^k n^l|) \geqslant \frac{1}{g_{00}} [n_0 I_0 - \sqrt{g_{00} a_{kl} I^k I^l} \cdot \sqrt{g_{00} a_{nm} n^n n^m}] \qquad (8)$$

Aus (8) erhalten wir aber schliesslich, wegen (5) und (6), $\lambda \geqslant 0$. Damit ist unsere Behauptung für die Flächen $R, R'$ und $R''$ bewiesen. Der Beweis für $T^+$ und $T^-$ ist ganz ähnlich zu führen; in (6) wird zwar an Stelle des Ungleichheitszeichens ein Gleichheitszeichen auftreten, was aber ohne Einfluss auf unseren Beweis ist.

Es soll nun weiters gezeigt werden, dass falls $\lambda$ auf $R, R'$ oder $R''$ verschwindet, dort auch $I^\nu = 0$ sein muss. In der Tat folgt aus $\lambda = 0$ im Falle $I^0 \neq 0$, dass $n_0 = g_{00} a_{kl} I^k n^l / I_0$ ist, mit Hilfe von (6) erhalten wir also $g_{00} a_{kl} I^k n^l > I_0 \sqrt{g_{00} a_{kl} n^k n^l}$. Diese Ungleichheit wird verstärkt, wenn wir an Stelle von $I_0$ mit Rücksicht auf (5) den Ausdruck $\sqrt{g_{00} a_{kl} I^k I^l}$ einsetzen. Wir bekommen also

$$\sqrt{g_{00} a_{kl} I^k I^l} \cdot \sqrt{g_{00} a_{nm} n^n n^m} < g_{00} a_{kl} I^k n^l,$$

was offenbar mit Rücksicht auf (7) falsch ist. Es ist also $I_0 = 0$, was aber nach (5) wegen des positiv definiten Charakters von $a_{kl} I^k I^l$ schliesslich auch $I^k = 0$ ergibt.

Um nun den sogleich zu formulierenden Hilfsatz I zu beweisen, nehmen wir noch an, dass $Q = -I^\nu_{,\nu}$ positiv ist. Durch eine Integration des Ausdruckes $Q + I^\nu_{,\nu}$ über das vierdimensionale Gebiet $\Omega^+$ erhalten wir

[2] Es ist $g_{00} a_{kl} (I^k \mu + n^k)(I^l \mu + n^l) \geqslant 0$ für beliebiges $\mu$; das negative Vorzeichen der Diskriminante dieser Ungleichheit für $\mu$ wird durch (7) garantiert.

$$\int\limits_{\Omega^+} Q\, d\tau_{(4)} - \int\limits_{R} I^\nu n_\nu d\tau_{(3)} + \int\limits_{R'} I^\nu n_\nu d\tau_{(3)} + \int\limits_{T^+} I^\nu\, n_\nu\, d\tau_{(3)} = 0$$

Wenn also $I_0$ (und deswegen $I_\nu$) auf $R$ verschwindet, so wird auf $R$ auch $\lambda = 0$ werden. Es werschwindet also eine Summe von Integralen mit positiven Integranden und daher auch die Integranden selbst. Unter anderem verschwindet auf $R'$ der Ausdruck $\lambda = I^\nu n_\nu$, woraus $I^\nu = 0$ auf $R'$ folgt.

Hilfsatz I. Falls ein Vektorfeld $I^\nu$, für das $I^0 \geqslant 0$, $I^\nu I_\nu \geqslant 0, I^\nu{}_{,\nu} \leqslant 0$ gilt, auf der Fläche $R$ verschwindet, so muss es auch auf der Fläche $R'$ verschwinden. Dabei wird angenommen, dass der metrische Tensor $g_{\alpha\beta}$ die nachstehenden Eigenschaften aufweist: $g_{00} > 0$, $g_{0k} = 0$ und $- g_{kl}\, y^k y^l$ ist positiv definit. Die Bedeutung der Flächen $R$ und $R'$ wurde oben angegeben.

Einen ähnlichen Hilfsatz können wir beweisen, wenn wir $Q + I^\nu_{,\nu}$ über das vierdimensionales Gebiet $\Omega^-$ integrieren. Mit Berücksichtigung der Normalenrichtungen bekommen wir dann

$$0 = \int\limits_{\Omega^-} Q\, d\tau_{(4)} - \int\limits_{R''} n_\nu I^\nu d\tau_{(3)} - \int\limits_{T^-} n_\nu I^\nu d\tau_{(3)} + \int\limits_{R} n_\nu I^\nu d\tau_{(3)}.$$

Wir betrachten hier nur den Fall $Q = 0$. Wenn $I^0$ (also auch $I^\nu$) auf $R$ verschwindet, so verschwindet auch die Summe der positiven Grössen $\int\limits_{R''} n_\nu I^\nu d\tau_{(3)} + \int\limits_{T^-} n_\nu I^\nu\, d\tau_{(3)}$ und daher auch $I_\nu$ auf $R$.

Hilfsatz II. Falls ein Vektorfeld $I^\nu$, für das $I^0 \geqslant 0, I^\nu I_\nu \geqslant 0, I^\nu{}_{,\nu} = 0$ gilt, auf der Fläche $R$ verschwindet, so musss es auch auf der Fläche $R''$ verschwinden.

Für $Q \neq 0$ ist dieser Hilfsatz ungültig.

3. Eindeutigkeitsbeweise. Wir nehmen an dass die Funktionen $\varphi^A$ $(A = 1, \ldots, N)$ irgendwelche lineare Differentialgleichungen erfüllen. Ferner soll vorausgesetzt werden, dass aus den Feldgleichungen ein Erhaltungssatz $I^\nu_{,\nu} = -Q$ folgt, in dem $Q$ und $I^0$ positive Grössen sind und $I^\nu$ bei entsprechender Wahl des metrischen Tensors $g_{\alpha\beta}$ zeitartig ist. Das Verschwinden von $I^\nu$ soll auch ein Verschwinden von $\varphi^A$ nach sich ziehen und umgekehrt.

Mit Rücksicht auf unsere Hilfsätze genügen diese Voraussetzungen um den Eindeutigkeitsbeweis für die Feldgleichungen zu erbringen. Wir behaupten: ist das Feld $\varphi^A$ auf $R$ vorgegeben, so ist es dadurch auf $R'$ eindeutig bestimmt. In der Tat, wenn zwei Lösungen $\varphi^A_1, \varphi^A_2$ der Feldgleichungen existieren, die auf $R$ identisch sind, so können wir wegen der Linearität der Feldgleichungen die neue Lösung $\varphi^A_* = \varphi^A_2 - \varphi^A_1$ bilden. $\varphi^A_*$ verschwindet aber auf $R$, woraus mit Rücksicht auf unsere Annahmen folgt, dass das dem Felde $\varphi^A_*$ zugeordnete Vektorfeld $I^\nu$ auf $R$ verschwindet. Aus unserem Hilfsatz I folgt dann, dass $I^\nu$ auf $R'$ verschwinden muss. Daraus ergibt sich aber weiter, dass $\varphi^A_*$ auf $R'$ verschwindet, also $\varphi^A_1 = \varphi^A_2$ auf $R'$ sein muss.

Im Falle $Q = 0$ bestimmt das auf $R$ gegebene Feld auch das in der Vergangenheit liegende Feld auf $R''$. Um das zu beweisen bilden wir ganz ähnlich wie oben die Differenz zweier Lösungen und benutzen Hilfsatz II.

Da $R'$ einen Schnitt von $\Omega_0^+$ durch eine beliebige raumartige Fläche darstellt, so ist es klar, dass durch die Vorgabe von $\varphi^A$ auf $R$ das Feld $\varphi^A$ im ganzen Bereiche $\Omega_0^+$ eindeutig bestimmt wird. In dem Spezialfalle $Q = 0$ wird aus dem gleichen Grunde durch $\varphi^A$ auf $R$ auch $\varphi^A$ im ganzen Bereiche $\Omega_0^-$ gegeben.

Wir wollen jetzt einige Beispiele untersuchen.

4. Maxwellsche Gleichungen. Aus den Gleichungen:

$$\text{rot}\,\vec{H} - \frac{\varepsilon}{c}\frac{\partial \vec{E}}{\partial t} = \frac{4\pi\sigma}{c}\vec{E} \qquad (9) \qquad div\varepsilon\vec{E} = 4\pi\varrho \qquad (11)$$

$$\text{rot}\,\vec{E} + \frac{\mu}{c}\frac{\partial \vec{H}}{\partial t} = 0 \qquad (10) \qquad div\mu\vec{H} = 0, \qquad (12)$$

wo $\varepsilon, \mu, \sigma$ positive Funktionen von $(x, y, z)$ sind, folgt der differentielle Energieerhaltungssatz

$$div\,\vec{S} + \frac{\partial W}{\partial t} = -Q, \qquad (13)$$

$$\text{wo} \quad \vec{S} = \frac{c}{4\pi}\vec{E}\times\vec{H}, \qquad W = \frac{1}{8\pi}(\varepsilon E^2 + \mu H^2), \qquad Q = \sigma E^2 \geqslant 0.$$

Es sei $(x^0, x^1, x^2, x^3) = (ct, x, y, z)$ und $I^0 = cW$, $I^1 = S_x \ldots$; der metrische Tensor sei durch $dS^2 = (dx^0)^2/\varepsilon\mu - (dx^1)^2 - (dx^2)^2 - (dx^3)^2$ gegeben. Die Gleichung (13) kann jetzt auch in der Gestalt $I^\nu{}_{,\nu} = -Q$ geschrieben werden.

$I^\nu$ erfüllt, wie sofort ersichtlich ist, die beiden Annahmen unserer Hilfsätze:

$$I^0 = \frac{c}{8\pi}(\varepsilon E^2 + \mu H^2) \geqslant 0, \quad I^\nu I_\nu = \frac{c^2}{(4\pi)^2}\left[\frac{1}{\varepsilon\mu}\left(\frac{\varepsilon E^2 - \mu H^2}{2}\right)^2 + (\vec{E}\cdot\vec{H})^2\right] \geqslant 0.$$

Ferner ist auch die Voraussetzung erfüllt dass aus dem Verschwinden von $I^\nu$ das Verschwinden des Feldes $\vec{E}, \vec{H}$ (und umgekehrt) folgt. Die Gleichungen (9)—(12) sind linear, so dass alle Betrachtungen des 3. Abschnitts auch jetzt gelten.

Wir haben also den Satz, dass durch die Vorgabe von $\vec{E}$ und $\vec{H}$ in $R$, dieses Feld im ganzem Gebiet $\Omega_0^+$ eindeutig bestimmt ist. Wegen $Q \neq 0$ tritt hier eine Umwandlung der elektromagnetischen Energie in Wärme ein, so dass durch das Feld in $R$ das Feld in $R''$ nicht eindeutig bestimmt wird.

5. Procasche Gleichungen. Aus den Gleichungen

$$\text{rot}\,\vec{H} - \frac{1}{c}\frac{\partial \vec{E}}{\partial t} + K_0^2\vec{A} = 0 \qquad (14) \qquad \text{div}\,\vec{E} + K_0^2\varphi = 0 \qquad (16)$$

$$\vec{E} = -\text{grad}\,\varphi - \frac{1}{c}\frac{\partial \vec{A}}{\partial t} \qquad (15) \qquad \vec{H} = \text{rot}\,\vec{A} \qquad (17)$$

folgt der differentielle Energieerhaltungssatz

$$\operatorname{div}\vec{S}+\frac{\partial W}{\partial t}=0, \tag{18}$$

wo $W=\frac{1}{8\pi}[E^2+H^2+K_0^2(\varphi^2+A^2)]$, $\vec{S}=\frac{c}{4\pi}(\vec{E}\times\vec{H}+K_0^2\varphi\vec{A})$.

Wir führen wieder die Bezeichnungen $I^0=cW$, $I^1=S_x$, ... ein; ferner sei der metrische Tensor durch $ds^2=(dx^0)^2-(dx^1)^2-(dx^2)^2-(dx^3)^2$ definiert. Gl. (18) können wir dann in der Gestalt $I^\nu_{,\nu}=0$ schreiben. Wir haben $I^0\geqq 0$, und aus $I^0=0$ ergibt sich das Verschwinden von $\varphi, \vec{A}, \vec{E}, \vec{H}$, und umgekehrt. Wegen[3] $I^\nu I_\nu\geqq 0$ kann man dann auf $I^\nu$ unseren Hilfsatz I anwenden und nach 3. die Eindeutigkeit der Lösungen der Gleichungen (14)—(17) beweisen. Wir haben also den Satz, dass die Werte von $\varphi, \vec{A}, \vec{E}$ und $\vec{H}$ in $R$, eindeutig die Werte dieser Grössen in $\Omega_0^+$ und $\Omega_0^-$ (mit Rücksicht auf $Q=0$) bestimmen[4].

6. Diracsche Gleichungen. Aus der Gleichung

$$\left\{\gamma^\mu\left(\frac{\hbar}{i}\frac{\partial}{\partial x^\mu}+\frac{e}{c}\Phi_\mu\right)-im_0c\right\}|x>=0 \tag{19}$$

folgt für die Wahrscheinlichkeitsstromdichte die Kontinuitätsgleichung $I^\nu_{,\nu}=0$, wo $I^\nu=<x|\alpha^\nu|x>$. Die Komponenten $I^\nu$ lassen sich bekantlich mit Hilfe der Funktionen $\psi_1, \psi_2, \psi_3, \psi_4$ welche $|x>$ darstellen in der folgenden Weise ausdrücken

$$I^0=\psi_1^*\psi_1+\psi_2^*\psi_2+\psi_3^*\psi_3+\psi_4^*\psi_4;\ iI^2=\psi_1^*\psi_4-\psi_2^*\psi_3+\psi_3^*\psi_2-\psi_4^*\psi_1,$$
$$I^1=\psi_1^*\psi_4+\psi_2^*\psi_3+\psi_3^*\psi_2+\psi_4^*\psi_1;\ I^3=\psi_1^*\psi_3-\psi_2^*\psi_4+\psi_3^*\psi_1-\psi_4^*\psi_2.$$

---

[3] $I^\nu I_\nu=\frac{c^2}{(4\pi)^2}\left\{\frac{1}{4}(E^2-H^2)^2+(\vec{E}.\vec{H})^2+\frac{K_0^4}{4}(\varphi^2-A^2)^2+\frac{1}{2}K_0^2\,\omega\right\}$, wo $\omega=$
$(\varphi^2+A^2)(E^2+H^2)-4\varphi\vec{A}(\vec{E}\times\vec{H})\geqq(\varphi^2+A^2)(E^2+H^2)-4|\varphi|.|\vec{A}|.|\vec{E}|.|\vec{H}|\geqq 0$
(wegen $\varphi^2+|\vec{A}|^2\geqq 2|\varphi||\vec{A}|$ und $E^2+H^2\geqq 2|\vec{E}|.|\vec{H}|$).

[4] Streng genommen, kann man die 10 Funktionen $\varphi, \vec{A}, \vec{E}, \vec{H}$ in raumartigen Gebieten $R$ nicht unabhängig von einander vorgeben. Z. B., wird $\sigma$ durch die Hyperebene $t=$ const. gegeben, so genügt es die Funktionen $\varphi, \vec{A}$ und $\frac{\partial\vec{A}}{\partial t}$, also sieben Funktionen von $(x, y, z)$ in $R$ vorzugeben; die Werte von $\vec{E}$ und $\vec{H}$ in $R$ ergeben sich dann aus (15) und (17). Schreiben wir $(A^0, A^1, A^2, A^3)$ statt $(c\varphi, A_x, A_y, A_z)$, so genügt es im allgemeinen auf $R$ sieben Grössen, nämlich diese Grössen sowie die normalen Ableitungen von $A^\nu S_\nu^{(i)}$ vorzugeben, wo die Einheitsvektoren $S_\nu^{(i)}$ zusammen mit der Normale $n_\nu$ (Normale auf $R$) ein Vierbein bilden. Aus diesen 7 Grössen erhalten wir in $R$ stets $\vec{E}$ und $\vec{H}$. (Man darf die normalen Ableitungen von allen $A^\nu$ auf $R$ nicht unabhängig vorgeben wegen der Lorentzschen Bedingung $A^\nu_{,\nu}=0$, die im Falle der Procaschen Gleichungen aus den Feldgleichungen folgt).

Wir sehen also dass wir als das „Feld“ die oben definierten 7 Grössen ansehen mussen; unser Eindeutigkeitsbeweis gilt also eigentlich für diese 7 Grössen.

Wenn man den üblichen metrischen Tensor der Minkowskischen Welt verwendet, kann man leicht zeigen dass

$$I^{\nu}I_{\nu} = \{|\psi_1|^2 + |\psi_2|^2 - |\psi_3|^2 - |\psi_4|^2\}^2 + 4\{Im(\psi_1^*\psi_3 + \psi_2^*\psi_4)\}^2 \geqslant 0.$$

Da selbstverstandlich $I^0 \geqslant 0$, kann man also auf $I^{\nu}$ unseren Hilfsatz anwenden. Da aus $I^0 = 0$ das Verschwinden von $\psi_1, \psi_2, \psi_3, \psi_4$ folgt (und umgekehrt), und da die Diracschen Gleichungen linear sind, gilt nach 3. der folgende Satz: die in $R$ gegebenen $\psi_1, \psi_2, \psi_3, \psi_4$ bestimmen diese Grössen eindeutig in $\Omega_0^+$ und $\Omega_0^-$ (in $\Omega_0^-$ wegen $Q = 0$). Aus diesem Satz folgt: wird die Wahrscheinlichkeitswelle eines Diracschen Elektrons in einem endlichen Gebiet und in einem endlichen Zeitintervall durch die Wechselwirkung mit anderen mechanischen Systemen gestreut, so können sich die durch diese Wechselwirkungen entstandenen Störungen der Wahrscheinlichkeitswelle nur höchstens mit Lichtgeschwindigkeit fortpflanzen.

7. Schlussbemerkungen. Aus diesen Betrachtungen folgt, dass wir immer mittels unserer Hilfsätze die Eindeutigkeit der Lösungen beweisen können, falls aus den in Frage kommenden linearen Differentialgleichungen die Gleichung $I^{\nu}_{,\nu} = -Q$ folgt, wo $Q > 0$ und $I^{\nu}$ die in 3. angegebenen Eigenschaften besitzt. In den den Physiker interessierenden Fällen hat gewöhnlich die angegebenen Eigenschaften der Viervektor des Energiestromes, den man aus dem metrischen Energie-Impulstensor erhalten kann.

In dem Falle der von Bhabha (1949) angegebenen relativistischen Gleichungen für Elementarteilchen mit verschiedenen Spinwerten sind für die Vektoren, auf die unser Hilfsatz anwendbar ist, die Vierervektoren des Wahrscheinlichkeitsstromes zu wählen.

Ich möchte Herrn Prof. Dr A. Rubinowicz meinen verbindlichsten Dank für sein wohlwollendes Interesse an dieser Arbeit aussprechen.

## КРАТКОЕ СОДЕРЖАНИЕ

Г. Плебанский, *О доказательствах однозначности некоторых уравнений физики.*

Продолжая мысль доказательства однозначности для уравнений Максвелла, поданную В. Рубиновичем, которая вязалась с интегрированием дифференциального принципа сохранения энергии по данному пространству четырёх измерений, подана лемма, которая разрешает простым способом доказывать однозначность решений ряда выступающих в физике уравнений полей гиперболического характера.

Эта лемма утверждает, что если векторное поле $I^{\alpha}$ при соответствующем определении метрики $g_{\alpha\beta}$ является временным вектором ($I^{\alpha}I_{\alpha} \geqslant 0$), при чем $I^0 \geqslant 0$, и если $I^{\alpha}_{,\alpha} \leqslant 0$, то если $I^0$ исчезает на известной области трёх измерений R, имеющей пространственный характер, то исчезать также должно $I^{\alpha}$ на трёхмерной области R' более поздней чем R, составляющей общую часть области с четырмя измерениями ограниченной „световыми конусами" растянутыми на берегу R с любой трёхмерной поверхностью пространственного типа.

Применяя эту лемму и пользуясь дифференциальными принципами сохранения, вытекающими из уравнений полей, в ряде случаев можно легко доказать однозначность.

Особенно просто проводятся доказательства в случае уравнений Максвелла для макроскопических тел, для уравнений Прока и уравнений Дирака.

## LITERATURVERZEICHNIS

Bhabha H. J., *Rev. Mod. Phys.*, **21**, 451 (1949).
Friedrichs und Lewy, *Math. Ann.*, **98**, 192 (1927).
Rubinowicz A., *Phys. Z.*, **27**, 707 (1926).

# LABORATORY EQUIPMENT AND TECHNIQUES

## ON THE USE OF $CO_2 + CS_2$ FILLED G. M. COUNTERS FOR AGE DETERMINATION

By W. Mościcki

Department of Experimental Physics, University of Poznań, Poznań*

*(received February 11, 1953)*

Experiments were performed to inquire into the possibility of using $CO_2 + CS_2$ filled G.M. counters for geochronometrical purposes.

A method of determining the absolute age of natural carbon-bearing materials was proposed by Libby and coworkers (1946). For routine $C^{14}$ age measurements the screen wall counter (s.w.c.) (Anderson *et al.* 1947) has been found suitable. Some general conclusions regarding the range of the method, its accuracy and possible sources of error were discussed and compared with analogue conclusions regarding the gas sample counter technique.

Anderson finds (Anderson and Levi 1952), that for counters of a few litres volume the ratio of counting rate of the s.w.c. to that of a gas counter is not much different from unity, but on the basis of the ease of operation (stability, reliability) he finds the s.w.c. technique more advantageous. However, it must be taken into consideration that: (a) The active length of the s.w.c. equals only 1/3 of the total counter length, whilst the counting region of the gas filled counter amounts to about 80 per cent of the total length. (b) The necessity of disassembling the s.w.c. for each sample is a serious drawback of the technique; besides, one has to count both background counts and sample counts separately, thus reducing the effective counting time by 50 per cent. With gas filled counters the total counting time can be utilized for sample counting. (c) The preparation of the $CO_2$ for gas counters takes place within the vacuum system and there is no danger of contamination of the sample during the preparation process. For these and other reasons it seems useful to make a detailed comparison between the s.w.c. technique and the gas filled counter technique.

Let us define the sensitivity $C$ of a technique as the reciprocal value of the activity $L_0$ counts per min. per g at which one is still able to determine $L_0$ within the time $t$ with a statistical standard error

* Now Department of Experimental Physics, Nicholas Copernicus University, Toruń.

$$\Delta L_0 = L_0/k \quad (k = 2, 3, 4 \ldots).$$

If $E_g$, $E_s$ are the effective efficiencies of the gas and screen wall counters respectively, $\sigma$ — the density of carbon in the gas counter, $\varrho$ — the effective surface density of carbon in the „infinitely thick layer" of the s.w.c., $\beta$ — the ratio of counter length to diameter, $s$ — the ratio of the active to the total counter length ($l$), then

$$y = \frac{C\,(\text{gas counter})}{C\,(\text{s. w. c.})} = l.\frac{E_g \sigma . \beta}{2E \varrho . s} . f(l).$$

$f(l)$ is a function depending on $k$ of the order of magnitude of 1. With $k^2/t = 0{,}1$, $E_g = 0{,}65$, $\sigma = 0{,}54$ mg/cm$^3$, $\beta = 0{,}1$, $E_s \varrho = 1{,}1$ mg/cm$^2$, $s = 0{,}3$, one finds $y > 1$ already for $l = 30$ cm.

Anderson has pointed out that a $CO_2$ gas counter requires operation in the proportional region (de Vries H. and Berendsen G.W. 1952) with a filling pressure of 1 atm. This necessitates an operating voltage of the order of 5 kV and detection of pulses of the order of amplitude of millivolts; this means that a proportional $CO_2$ counter is inherently more difficult to operate than a s.w. Geiger counter which gives pulses of several volts at 1 kV.

It was demonstrated, however, that addition of 2—10 mmHg of $CS_2$ makes a good gas mixture for G.M. counters (Brown and Miller 1947). Such counters need external quenching circuits.

In view of the sensitivity, the amount of sample available, the size of counters giving identical results, and other advantages offered by the gas filled counter technique in the "radiocarbon method" of age determination, experiments were performed in this laboratory to inquire into the possibility of using such G.M. counters for geochronometrical purposes. A 15 cm thick lead shield and 21 a.c. G.M. counters were used as a gamma and cosmic-ray shielding. The value of background counts found in course of the experiments (1949—1952) were within 10,5 to 11,2 cpm.

The pressure of $CO_2$ in the counter was limited to 0,5 atm., as the tension which could be got from the voltage stabilizer did not exceed 4500 V. The volume of the counter used in this work was about 400 cm$^3$. In these conditions one can expect about 1,7 cpm more with $CO_2$ filling from a contemporary sample than from a very old one. In the course of the experiments it was found that the $CO_2 + CS_2$ filled G.M. counters need "forming" during which the efficiency of the counters increases from about 70—80 per cent (Miller et al. 1950) to almost 100 per cent. The use of a counter of such a type for geochronometrical purposes is possible, but one has to count separately (a) the background plus sample pulses through an anticoincidence channel, (b) the pulses from the counter (without a.c. channel — L, (c) the pulses from an a.c. shield — N. This allows the elimination of the differences in efficiencies of the counters and of the fluctuations of background in the course of the measurements.

In order to check the reliability of the technique, the countings of three fillings were compared; these $CO_2$ fillings were taken:

(A) from a freshly cut tree,

(B) from anthracite,

(C) from a sample supplied by Muzeum Ziemi (Warsaw). The age of the sample as determined by means of another method was known to lie between 5600 and 7500 years.

The results obtained are collected in table I. ($p$ — pressure of $CO_2$ in mmHg, $t$ — time in min., $L_0$ — effects of $C^{14}$ radiation (Anderson and Libby 1951) without, and $L_e$ — with efficiency correction).

A detailed description of the apparatus as well as of the results obtained, together with a discussion of the advantages and disadvantages of the technique will be published later.

| | p | t | N | L | $L_0$ | $L_e$ |
|---|---|---|---|---|---|---|
| A | 376.5 | 2214 | 583,2 | 76,16 | 1,969 | 1,762 |
| B | 376.0 | 1160 | 573,2 | 71,64 | 0 | 0 |
| C | 372,0 | 2925 | 537,9 | 67,48 | 0,836 | 0,984 |

I would like to thank Professor S. Szczeniowski for helpful discussions and encouragement throughout the course of the work.

## КРАТКОЕ СОДЕРЖАНИЕ

Вл. Мосцицкий. *О употреблении счётчиков Гейгера-Мюллера наполненных $CO_2$+$CS_2$ для определения возраста.*

Были произведены опыты для исследования возможности употребления счётчика Гейгера-Мюллера наполненных $CO_2$ — $CS_2$ в геохронометрических целях

## REFERENCES

Anderson E. C. and Levi H., *Dan. Mat. Fys. Medd.*, **27**, no 6 (1952).

Anderson E. C. and Libby W. F., *Phys. Rev.* **81**, 64 (1951).

Anderson E. C., Libby W. F., Weinhouse S., Reid A. F., Kirschenbaum A. D. and Crosse A. V., *Phys. Rev.* **72**, 931 (1947; *Science*, **105**, 576 (1947); Libby W. F., Anderson E. C. and Arnold I. R., *Science*. **109**, 227 (1949); Libby W. F. and Lee P. D., *Phys. Rev.*, **55**, 245 (1939).

Brown S. C. and Miller W. W., *Rev. Sci. Instrum.*, **18**, 597 (1947).

Libby W. F., *Phys. Rev.* **69**, 671 (1946).

Miller W. W., Ballentine R., Bernstein W., Friedman L., Nier A. O. and Evans R. D., *Phys. Rev.*, **77**, 714 (1950).

De Vries H. and Berendsen G. W., *Physica* **XVIII**, 651 (1952).

# MEASUREMENTS OF THE EXTERNAL PHOTOELECTRIC EFFECT OF POLYCRYSTALLINE LAYERS OF ALKALINE HALIDES BY MEANS OF A G.-M. COUNTER

By B. Sujak

Institute of Experimental Physics, Bolesław Bierut University, Wrocław

*(April 21, 1953)*

It is well known that alkaline halides which possess additional absorption bands in the optical region of the spectrum show there an external photoelectric effect (Lukirsky and al. 1926, Fleischmann 1933, Apker and Taft 1950, 1951) with a weak quantum yield of $10^{-5}$ — $10^{-7}$ electrons per quantum (Fleischmann 1933, Apker and Taft 1950, 1951).

To investigate the photoelectric emissivity of NaCl and KCl layers at different wave lengths of the visible spectrum a cylindrical G. M. photon counter was used. The thickness of the layers, obtained by evaporation of aqueous solutions, did not exceed $10^{-1}$ mm; they were deposited on an inner side of the counter cathode whose opposite side was removed (see Fig. 1). The photoeffect was detected and measured after foregoing sensitization by a continuous discharge in the counter; without such a sensitization the layers did not show any photoelectric emission produced by visible light, which is in agreement with previous observations of other authors (Lukirsky, Gudris and Kulikowa 1926; Fleischmann 1933; Apker and Taft 1951; Kramer 1951). If the measured effect is small (it decreases with prolonged exposure to light, an effect known as photoelectric fatigue), it may be increased by raising the applied voltage so as to produce anew a continuous discharge in the counter.

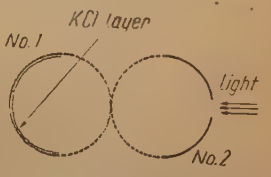


Fig. 1. Cross-section of the counter assembly

Our observations showed also the existence of an influence of the applied voltage across the counter during its normal work on the observed photoelectric emission. To be sure that this effect is not caused by photoluminescence (anti-Stokes radiation: NaCl — 2400 Å, KCl — 2700 Å, see Kac 1948) two counters were mounted in one glass container, the cut out parts of their cathodes facing one another (see Fig. 1). In this assembly counter No. 1 responded strongly to visible light (Fig. 2), whereas counter No. 2 showed no increase of background. This seems to justify the conclusion that the effect produced in counter No. 1 was not due to anti-Stokes radiation in the 2000—3100 Å region. Measurements of the external photoelectric effect from excited NaCl layers showed the existence

of a maximum of photoemission in the neighbourhood of 480 m$\mu$, whereas for KCl this maximum lay in the vicinity of 570 m$\mu$. Fig. 2 shows the spectral distribution of photoemission (curves $a$ and $a'$). On the vertical axis are given the rates of counting in arbitrary units, reduced to equal incident light intensity for different wave lengths and to equal geometries of the assembly. For comparison

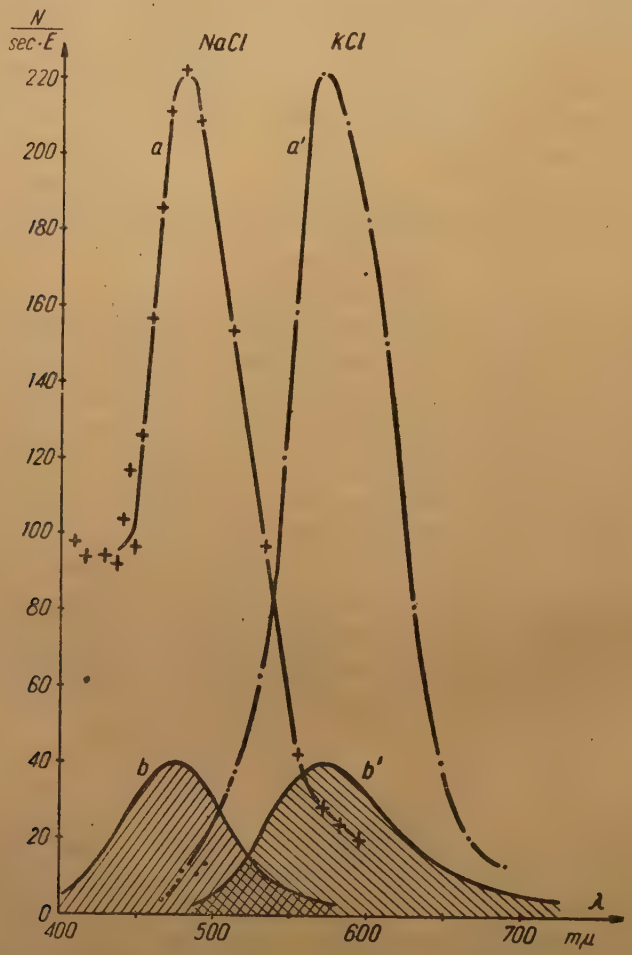


Fig. 2. Spectral distribution of the photoelectric emission of excited layers of NaCl (curve $a$) and KCl (curve $a'$). Curves $b$ and $b'$ — absorption bands of NaCl and KCl in arbitrary units

the maxima of optical absorption for NaCl and KCl containing F-centers (in arbitrary units) are also shown in the diagram (Fig. 2, curves $b$ and $b'$ — see Pohl 1938). Preliminary observations showed a dependence of the heights of the maxima of photoemission on the time of excitation, but no influence of that time on the position of the maxima. The agreement of the shape of the curves and the constancy of the position of the maxima lead us to assume that we have to deal here with an effect connected with the existence of F-centers in the investigated layers. It seems that the smallness of the effect would render its investiga-

tion by other methods rather difficult. The intensities of the photoelectric currents were of the order of $10^2$—$10^3$ electrons per second, corresponding to $10^{-17}$—$10^{-16}$ amperes, in the neighbourhood of the maximum of emission. As source of light it was used a tungsten point-lamp and a double monochromator of Polish make.

Further investigations of the external photoelectric effect of polycrystalline layers as well as monocristals of alkaline halides and other semiconductors are now in progress.

The author wishes to express his gratitude to Professor J. Wesołowski and Professor J. Nikliborc for numerous helpful discussions.

## REFERENCES

Apker L. and Taft E., *Phys. Rev.*, **79** 964 (1950); *Phys. Rev.*, **81**, 698 (1951).
Fleischmann R., *Z. Phys.*, **84**, 717 (1933).
Kac M.L., *Zh. eksper. teor. Fiz.*, **18**, 165 (1948).
Kramer J., *Z. Phys.*, **129**, 34 (1951).
Lukirsky P., Gudris N. and Kulikowa L., *Z. Phys.*, **37**, 308 (1926).
Pohl R. W., *Phys. Z.*, **39**, 36 (1938).

# LETTERS TO THE EDITOR

## ON AN OBSERVATION WITH THE MÜLLER MICROSCOPE

By J. Niklborc

Institute of Experimental Physics, Bolesław Bierut University, Wrocław

*(May 11, 1953)*

During investigations with a Müller microscope (Müller 1937) an image with a characteristic and rather distinct fine structure in the neighbourhood of the fourfold symmetry axes has been obtained (see Fig.); it concerns an incandescent tungsten point ($r = 1\mu$) at a temperature slightly above red heat.

### Interpretation

In its parts surrounding the fourfold symmetry axes the image is probably an adsorption image of oxygen. This may be inferred from the facts that: (1) Previous observations seem to indicate that the image in question represents a last, very stable stage of a cycle of regrouping taking place on the surface of the incandescent point, which is difficult to explain otherwise as by migration of adsorbed atoms. (2) The results of observations of Müller (1937) on the adsorption of oxygen show a strong adsorption in the vicinity of (100). (3) Similar, but less distinct, images were obtained by Sokolskaja (1952) in conditions of poor vacuum; my experiments were also performed in insufficient vacuum (mercury pump and freezing out device). (4) Pictures taken in conditions of ideal vacuum (Becker 1951, Benjamin and Jenkins 1940) evaluated by the authors to about $10^{-13}$ mm Hg, show that in contradistinction to my photograph the neighbourhoods of the fourfold axes for clean points are always very clear, whereas the adsorption of oxygen raised the work function.

In the regions around the fourfold axes the image exhibits subtle bright and dark fringes occuring four times around each axis. The regularity of the adsorption picture points undoubtedly to the regularity of structure of the substratum of the adsorbed systems. I think that this may be explained by the formation of numerous small facets in the vicinity of the fourfold axes. The neighbourhoods of the threefold axes show also some differentiation but there are no sufficient grounds for deciding which rôle is thereby played by adsorption.

## Conclusions

This result is interesting in view of the much discussed and problematic question of the equilibrium figure of crystals (Landau 1950), especially of monocrystalline points in the Müller tube (Smirnov and Shuppe 1952). In their review article Herring and Nichols (1949), referring to observations with the electron microscope (Haefer 1940), assume that after full annealing the point takes the form of a surface of revolution; they consider this as rather enigmatic. If my interpretation is correct, it means that in my case the point of the annealed monocrystal assumed the form of a polyhedron possessing in some parts at least a multitude of small facets. This was inferred mainly from the adsorption. A difficulty of this interpretation consists in the fact that these facets ought to have high Miller indices; unfortunately the evaluation of these indices would exceed the accuracy of my observations. It must be kept in mind, however, that the conditions of growth of macroscopic crystals (Buckley 1951) are quite different from those of the microcrystalline point, under the influence of an intense electric field at a high temperature. It may be also mentioned here that Becker (1951) states that "careful inspection of the negatives" points to the existence of "submicroscopic facets on the paraboloidal surfaces".

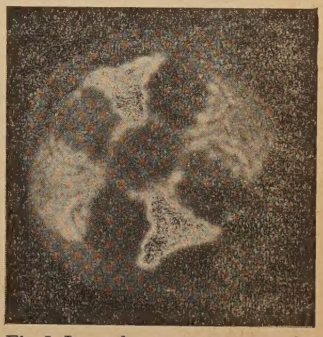

Fig. 1. Incandescent tungsten point at a temperature slightly above red glow, partially covered with adsorbed gas

Further investigations are needed for complete elucidation of this question. I take the opportunity to thank Mr. J. Raułuszkiewicz, Mr. J. Mycielski, and Mr. W. Giriat for assistance in this work.

Note added in proof: After submission of this letter for publikation a paper has veen published of Kirchner F., Z. angew. Phys. 5,281 (1953), who obtained similar pictures in the case of adsorption of oxygen on tungsten.

## REFERENCES


Becker J. A., *Bell Syst. tech. J.*, **30,** 907 (1951).
Benjamin M. and Jenkins R. O., *Proc. Roy. Soc.* A, **176,** 262 (1940).
Buckley H. E., *Crystal Growth*, (1951).
Haefer R., Z. *Phys.*, **116,** 604 (1940).
Herring C. and Nichols M. H., *Rev. Mod. Phys.*, **21,** 185 (1949).
Landan L. D. Seventieth' Aniversary Volume Dedicated to A. F. Joffe, 44 (1950).
Müller E. W., Z. Phys., **106.** 541 (1937)
Smirnov B. N. and Shuppe G. N., *Zh. tekh. Fiz.*, **22,** 973 (1952).
Sokolskaja I. L., *Zh. tekh. Fiz.*, **22,** 1301 (1952).

# ERRATA

*Acta Physica Polonica*, **12**, 14 (1953).

Conservation Laws in Non-Local Field Theories by J. Rzewuski. On page 14, read (received June 1, 1952) instead of (recived June 1, 1953).

*Acta Physica Polonica*, **12**, 77 (1953).

Relativistic Quantum Dynamics of a System of Interacting Particles by J. Rzewuski. On page 77, read (received November 18, 1952) instead of (received November 18, 1953).

Czasopismo ukazuje się corocznie w jednym tomie złożonym z czterech kwartalnych zeszytów.

Maszynopisy prac w 2 egzemplarzach w językach rosyjskim, angielskim, francuskim lub niemieckim, zaopatrzone w krótkie streszczenia w języku pracy oraz rosyjskim należy nadsyłać pod adresem redakcji niżej podanym. Wszystkie ryciny powinny być zaopatrzone w krótkie objaśnienia jako podpisy do klisz. Autorzy otrzymują 25 odbitek swych prac bezpłatnie.

---

Журнал издаваемый ежегодно в одном томе состоящем из четырех выпусков.

The periodical appears yearly in one volume of four quarterly issues.

Le périodique paraît dans un volume par an en quatre fascicules trimestriels.

Die Zeitschrift erscheint in einem Bande von vier Heften jährlich.

---

Adres redakcji — Адрес Редакции — Adresse de la Rédaction:
Kraków 2, al. Słowackiego 15 m. 9

Adres wydawnictwa: Warszawa 1, Krakowskie Przedmieście 79, skrytka pocztowa 455

---

Cena zeszytu pojedynczego wynosi 12 zł, prenumerata roczna 48 zł, półroczna 24 zł

Wszelkie wpłaty za rocznik 1953 należy przekazywać na konto Państwowego Wydawnictwa Naukowego w PKO: Warszawa Nr 1-110-28504

Cena zł 12.—